

INTERIM REPORT

Accession No. \_\_\_\_\_

Contract Program or Project Title: PWR Blowdown/ECC  
Subject of this Document: Program Progress  
Type of Document: Monthly Letter  
Author(s): G. W. Burnette  
Date of Document: May 1980  
Responsible NRC Individual and NRC Office or Division: W. D. Beckner

This document was prepared primarily for preliminary or internal use. It has not received full review and approval. Since there may be substantive changes, this document should not be considered final.

Prepared for  
U.S. Nuclear Regulatory Commission  
Washington, D.C. 20555

INTERIM REPORT

THIS DOCUMENT CONTAINS  
POOR QUALITY PAGES

NRC Research and Technical  
Assistance Report

8007150 407

# GENERAL ELECTRIC

GENERAL ELECTRIC COMPANY, 175 CURTNER AVE., SAN JOSE, CALIFORNIA 95125

NUCLEAR ENERGY

ENGINEERING

DIVISION  
Mail Code 583

June 23, 1980

TO: Edward L. Halman, Director  
Division of Contracts  
U.S. Nuclear Regulatory Commission  
Washington, D.C. 20555

Dr. P. Kalra  
Safety & Analysis Department  
Electric Power Research Institute  
P.O. Box 10412

SUBJECT: BWR Blowdown/ECC Program  
Contract No. NRC-04-76-215  
Informal Monthly Progress Report for May 1980

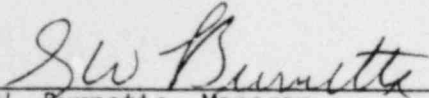
Gentlemen:

The following summarizes the subject matter covered in the attached report:

Additional detail is being developed at PMG request on a single channel upgrade of TLTA. The modified system for direct measurement of blowdown flow has been installed and appears to work well. A series of separate effects, boiloff tests has been completed and the data are being evaluated. Data packages are included for the BD/ECC 1A reference test (large break) and for the second small break test.

Distribution of this report is being made in accordance with the "Monthly Distribution List" provided with W.D. Beckner's letter of September 6, 1979.

Very truly yours,

  
\_\_\_\_\_  
G.W. Burnette, Manager  
External Programs (408) 925-5375

/fs: enclosures

cc: R.G. Bock

NRC Research and Technical  
Assistance Report

BWR BD/ECC PROGRAM  
FIFTY-FIFTH MONTHLY PROGRESS REPORT  
MAY 1980

Prepared for:

Division of Reactor Safety Research  
U.S. Nuclear Regulatory Commission  
Washington, D.C. 20555  
NRC-FIN. NO. B3014

and:

Electric Power Research Institute  
3412 Hillview Avenue  
Palo Alto, California 94303  
EPRI Project NO. RP-495-1

and

General Electric Company  
175 Curtner Avenue  
San Jose, California 95125

BY

General Electric Company

UNDER

Contract No. NRC-04-76-215

NRC Research and Technical  
Assistance Report

## BD/ECC PROGRAM

### FIFTY - FIFTH MONTHLY REPORT

MAY 1980

#### Summary

Additional detail is being developed at PMG request on a single channel upgrade of TLTA. The modified system for direct measurement of blowdown flow has been installed and appears to work well. A series of separate effects, boiloff tests has been completed and the data are being evaluated. Data packages are included for the BD/ECC 1A reference test (large break) and for the second small break test.

#### Task AA - Program Planning and Administration

At the April 1980 PMG meeting, the PMG requested development of additional details and further cost and schedule information for a single channel upgrade of the TLTA.

A significant milestone will be met by July or early August: completion of the BD/ECC 1A large break test series. The TLTA configuration for BD/ECC 1B has not been agreed upon, as yet, so additional experimental work cannot be planned pending this important decision by the program sponsors.

#### Task CC - Test Facility Preparation

The modified turbine meters and drag discs for use in the large break blowdown lines were installed. These units have been modified by Measurements Incorporated to include:

- new turbine rotors for different ranges;
- increased target sizes on both drag discs;
- new RF - type turbine meter sensors and preamplifier electronics;
- modified readouts for the turbine meters

Some shakedown tests were conducted to confirm the operation of these devices. All units operated satisfactorily in a test in which the system depressurized from full pressure and temperature conditions, but with low bundle power ( $\sim 300$  kw). Output from the turbine meters was not affected by SCR noise associated with bundle power supply, so apparently this problem has also been solved.

#### Task FF - Testing

The planned series of five boiloff tests was successfully completed in the TLTA. The objective of these separate effects tests was to evaluate bundle heatup at constant power and system pressure as the mixture level slowly uncovered the bundle.

The system pressure and power levels for each test were steady, but varied from test to test. Evaluation of preliminary results indicates that the test conditions were satisfactorily met. Data evaluation is continuing.

#### Task GG - Analysis

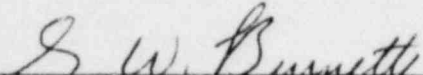
##### Large Break Test Results

The data report for the reference, large break test in TLTA 5A (6422 Run 3) is included in Appendix A.

An analytical effort is underway to evaluate bundle heat transfer coefficients and local conditions in the 8x8 bundle, based on available BD/ECC 1A test results. The scope of this effort is summarized in Appendix B.

##### Small Break Test Results

The data report for the second small break test (6432 Run 1) is included in Appendix C.

  
\_\_\_\_\_  
GW Burnette, Manager  
External Programs, (408) 925-5375

/fs: attachments

## APPENDIX A

### BD/ECC 1A

#### DATA REPORT FOR TLTA-5A REFERENCE TEST (6422 RUN 3, Average Power, Average ECC Rates)

L.S. Lee, May 1980

#### SYNOPSIS

The reference test data along with discussion of results are included in this report. Also included is a recapitulation of simulation improvements made to TLTA that render configuration 5A (TLTA-5A) even more representative of a BWR system.

As a result of the realistic bundle power decay and bundle to bypass flow coupling, the bundle was reflooded completely at ~140 seconds and the peak cladding temperature was below 700°F.

#### BACKGROUND

Improvements to TLTA for additional testing were deemed desirable by the PMG in January 1979<sup>1</sup> after the PMG members had reviewed results from the scoping series<sup>2</sup> of BD/ECC1A tests. The scoping series of tests, conducted in TLTA 5, was selected from the test plan<sup>3</sup> by PMG following the March 1978 meeting. The intent of the scoping series was to obtain a data base from which to guide further testing.

The balance of BD/ECC 1A tests, conducted in the improved TLTA, was finalized with input from PMG members after the March 1979 PMG meeting. Included were five large break (DBA) tests, and a small break scoping test.<sup>4</sup>

TLTA improvements, including hardware modifications and instrumentation changes, have been documented and issued.<sup>4</sup> Significant modifications included: realistic bundle power decay, improved simulation of bypass leakage path, and improved simulation of systems inventory. The resulting configuration was designated TLTA 5A (Figure 1).

In TLTA 5A two core-leakage flow paths were included (Fig 2). These paths simulate the leakage flow through the fuel support/lower tie plate (paths 4 to 7, Fig. 2), finger springs (path 3, Fig 2) and holes in the lower tie plate (path 2 Fig 2). In all previous TLTA configurations, only the leakage path from the lower plenum to the guide tube was simulated.

#### RESULTS

##### System Thermal-Hydraulic Response

The test conditions for this reference test are summarized in Table 1. The bundle power decay for the test (Fig. 3) was based on ANS-5 for a central-average BWR/6 bundle and included the effect of decay heat and stored heat.

The system pressure response as measured at three locations is presented in Figure 4. The pressure differences between plena are initially due to the flow and hydrostatic head differences in the system. After the recirculation pumps are tripped and blowdown begins, these pressure differences become small and the three pressures are seen to be nearly identical. Later in the transient as the system refills, the hydrostatic head difference becomes discernible (see Figure 4).

The ECC injection rates (Figures 5 through 8) are governed by the system pressure as the pumps characteristics were designed<sup>6</sup> to simulated those of a LWR. Injection commences at 27 sec. for HPCS (Fig 5), 63 Sec. for LPCS (fig 6), and 71 sec. for LPCI (Fig 7). The total amount of ECC injected at any time is included in Fig 8.

An overview of the system response is presented in Figures 9 and 10. The initial system response is similar to the previous scoping test series<sup>2</sup>. Following the onset of lower plenum flashing the steam generation in the lower plenum holds up inventory in the bundle because of counter current flow limiting (CCFL) at the side entry orifice (SEO) below the bundle. Similarly, CCFL at the upper tie plate and the bypass outlet holds up inventory in the upper plenum. As the blowdown continues, the mixture level in the lower plenum recedes, reaching the jet pump exit plane at ~34 seconds. An alternative path becomes available for the lower plenum vapor to escape, and therefore less vapor vents through the SEO to the bundle. The liquid continuum previously maintained in the bundle by the vapor updraft is now lost and bulk heat-up within the bundle begins. During this period, the inventory in the upper plenum remains fairly constant (Figures 9 and 10), with drainage into the bundle being replenished by continued core spray.

The guide tube/bypass region begins to refill (Fig 10) shortly after the onset of LPCI injection (~90 sec). The subcooled LPCI fluid condenses steam in the bypass region and eliminates CCFL at the top of the bypass. This partially drains the upper plenum as the bypass is refilled (Fig 10.)

The bundle refloods concomitantly with bypass refill for these reasons:  
1) increased hydrostatic head in the bypass region produces increased leakage flow into the bundle and 2) continuing CCFL at the SEO prevents complete drainage of the bundle inventory into the lower plenum. As the bundle refloods, the hydrostatic head increases and the leakage flow from the bypass diminishes. The subcooled LPCI that was flowing downward through the bypass region is then forced to flow upward into the upper plenum. This LPCI fluid combines with other subcooled liquid being sprayed into the upper plenum and leads to CCFL breakdown at the top of the bundle. As a result, the bundle reflood is accelerated and the upper plenum inventory completely drained. The upper plenum remains drained for the balance of the test (Fig. 9).

The filling of the bundle produces a hydrostatic head on the lower plenum fluid and increases the pressure drop across the jet pumps. The pressure drop is sufficient to carry the ECC fluid, which is now draining through the bypass and bundle, out of the lower plenum and into the downcomer region (see Figure 11). The hydrostatic head of the bundle, therefore, prevents the lower plenum from completely refilling. The system achieves pseudo steady state for the remainder of the transient except, as discussed below for two short periods of vapor venting through the bypass region.

Plots of regional mass are included (Figures 12 through 17). From these plots the timing and extent of mass transfer from one region to another can be determined.

A schematic of the TLTA bundle showing pressure tap elevation is included in Fig. 18 for reference. Nodal differential pressures along the bundle are shown in Figures 19-22. Bundle reflood from the bottom and final reflooding from the top can be observed from these measurements. Nodal differential pressure along the guide tube and bypass are shown in Figures 23 and 24.

#### Bundle Heat Up Response

The thermal response of the bundle is marked by: 1) low peak cladding temperatures below 700°F (Fig 25), 2) well cooled bundle ( $\sim T_{sat}$ ) after 150 seconds, and 3) eventual subcooling of bundle (below  $T_{sat}$ ).

Temperature measurement locations are shown in Fig 18. Peak cladding temperature is presented in Fig 25, while temperature measurements at different locations are included in Figures 26 through 47.

Some dryouts at  $\sim 20$  seconds are seen at certain locations (Figures 32, 34, 35, 37, 38, 40) as lower plenum flashing subsides. However, these dryouts are all rewetted at approximately the time of HPCS flow inception. As the elapse times between the HPCS inception and rod rewetting are rather short, rewet of the dryout rods are attributed to fallback cooling from the inventory in the upper plenum.

Bulk dryout of the bundle occurs at approximately 34 seconds when the liquid continuum in the bundle is lost following jet pump exit uncover in the lower plenum. The bundle heatup is, nevertheless, limited to  $\sim 700^\circ\text{F}$  due to the effectiveness of the HPCS which penetrates the upper region of the bundle and rewets many of the rods. The maximum cladding temperature reached the peak value before LPCS injection begins (Fig 25).

The upper half of the bundle becomes further cooled (Fig 35 through 47) following LPCS injection, which begins at 63 seconds. This causes the remaining dried out rods in the upper bundle to be rewetted and the thermocouple measurements to indicate saturation temperature.

The lower half of the bundle, by contrast, continues to show local dryout



even after the heat up rate and cladding temperatures have peaked. The region becomes well cooled when the bundle refloods between 110 seconds and 140 seconds (Fig 10, Figs 25 through 34).

With the bundle completely reflooded and with the continuous injection of subcooled ECC, the fluid inventory within the bundle becomes subcooled. This is evident in Figures 26 to 47 where it is seen that after about 150 seconds the cladding temperatures in the bundle show values below the saturation temperature for the system pressure.

#### Further Evaluations of Bundle Heat Up Response

Heat up rate within the bundle is being evaluated by deriving heat transfer coefficients (HTC) with HCODE from thermocouple measurements. Preliminary results indicate that during the spray cooling period, prior to bundle reflood, the HTC on the peak rod at peak power plane is  $\sim 16 \text{ Btu}/^\circ\text{F HrFt}^2$ . This HTC value is consistent with that required to maintain the PCT at  $\sim 700^\circ$  at the decay heat level for this test. The bundle inlet flow during this period is very low and is counter current, therefore, no direct flow rate measurements are available. The vapor upflow from the lower plenum to the bundle, however, has been estimated from mass and energy balance in the lower plenum. The upper bound value of steam flow to the bundle is  $\sim 0.1 \text{ lbm/sec}$ . The corresponding single phase HTC (from Dittus-Boelter) for this vapor flow is  $\sim 6 \text{ Btu}/^\circ\text{F HrFt}^2$ . The effectiveness of the spray cooling is evidently accounting for the higher heat transfer rate observed in the test.

The bundle thermal response can be summarized as follows:

- CCFL at the SEO delays bulk heat up until  $\sim 34$  seconds into transient.
- Realistic bundle power simulation contributes to lower PCT beyonds 50 seconds (compared to earlier TLTA 5 results).
- ECCS contributes significantly to bundle heat removal and therefore lower PCT
- Improved simulation of leakage path in TLTA contributes to completely reflooding the bundle (even with the short jet pump) and further lowers the bundle temperatures.

BD/ECC 1A TL, A 5A REFERENCE TEST 6422 RUN 3.

INITIAL CONDITIONS

Bundle power	5.05 .03 MW
Steam dome pressure	1035 $\pm$ 5 psia
Lower plenum pressure	1062 $\pm$ 5 psia
Lower plenum enthalpy	524 $\pm$ 5 Btw/lbm
Initial water level	124 $\pm$ 6" Elevation
Feed water enthalpy	41 $\pm$ 2 Btw/lbm
Bundle inlet to outlet	17 $\pm$ $\frac{1}{2}$ psi
Steam flow	6 + 1 lbm/sec
Feed Water flow	1.6 $\pm$ .3 lbm/sec
Drive pump #1 flow	8.7 $\pm$ 1 lbm/sec
Drive pump #2 flow	8.5 $\pm$ 1.0 lbm/sec
Jet pump #1 flow	20. $\pm$ 2 lbm/sec
Jet pump #2 flow	21 $\pm$ 2 lbm/sec
Bundle inlet flow	35. $\pm$ 5 lbm/sec

TIMINGS

Blowdown valves opening	0.00 $\pm$ .02 sec.
Power decay	0.40 $\pm$ 0.05 sec.
HDCS actuated	27 sec
HPCS flow begins	27 sec $\pm$ !
LPCS activated	37 sec
EPCI flow begins	63 $\pm$ 7 sec
Bundle power tripped	37 sec
Blowdown valves closed	71 $\pm$ 2 sec
	328 $\pm$ sec
ECCS temperature	120 $\pm$ 15 °F

All uncertainty bands are judged from the maximum of data fluctuation and/or absolute uncertainties of the measurements.

LSL  
4/17/80

### Vapor Venting in Guide Tube/Bypass Region

Vapor venting in the guide tube/bypass region is primarily due to rapid filling of the bypass region with two-phase mixture coupled with inequality of fluid density in the two parallel columns (bundle and bypass).

The region refills in 30 seconds (from ~100 to ~130 seconds as shown in Fig. 9). The mass of the guide tube increases from 60 to 90 lb, the bypass from ~0 to ~65 lb (Figures 15 & 16). Of this increase of ~95 lb mass, the one LPCI system accounts for ~25 lb, the balance comes from the two phase fluid in the upper plenum.

When the bypass refills at ~100 sec. the bundle begins to reflood slowly. The hydrostatic head across the bypass is seen in Fig. A1 to be higher than that across the bundle. The difference in hydrostatic heads, shown in Fig. A2, causes the bypass fluid to flow into the bundle and the guide tube fluid into the lower plenum. This leakage flow from the bypass to the bundle contributes to bundle reflood; that from the guide tube contributes additional vapor to the lower plenum. The combined effects of flashing in the lower plenum and the added vapor flow from the guide tube render the counter current flow condition at the SEO to prevent liquid drainage from the bundle (Fig. A3a)

The reversed leakage flow from the bypass is accompanied by the down flow of LPCI. The subcooled LPCI fluid condenses vapor generated in the bypass and the guide tube. The reversed leakage flow as well as the downward LPCI flow diminishes as the bundle refloods and the hydrostatic heads difference decreases. On the other hand, the vapor updraft from the guide tube into the bypass increases as the leakage flow into the lower plenum decreases. The combined effect of decreased subcooled LPCI downflow and increased guide tube vapor upflow is that the vapor travels higher up into the bypass before mixing with the subcooled LPCI fluid. This decreases the bypass fluid density, hence the hydrostatic head, and further reduces the hydrostatic heads difference.

The hydrostatic head difference is also diminished by the bundle fluid density increase. This comes about when the bundle begins reflooding and cools the lower bundle. Then, as the lower bundle becomes well cooled, less vapor is generated and hence more liquid drains into the bundle from the upper plenum. Finally, as the bypass flow decreases, more subcooled ECC fluid becomes available to flow into the bundle (Figure A 3b).

The hydrostatic heads become equal at  $\sim 200$  seconds and the bypass flow becomes zero (Fig A2). The LPCI fluid can no longer flow downward and is forced into the upper plenum where it combines with the subcooled sprays and flows into the bundle. This renders the bundle hydrostatic head higher relative to the bypass and the leakage flow reverts to the forward direction, i.e. fluid flows from bundle to bypass and from lower plenum to guide tube.

The forward leakage flow facilitates the vapor to escape from the bypass region. As both the liquid and the vapor continue to flow upward, the liquid continuum is pushed into the upper plenum (Fig 24,  $\sim 210$  sec). The vapor continuum is condensed as it comes into direct contact with either the subcooled LPCI at the top of the bypass or the subcooled spray in the upper plenum. Following this, the vapor flow diminishes, and the upper part of the bypass is clear of liquid continuum (Fig A3C). The LPCI fluid flows downward again to fill the bypass. At the same time, the hydrostatic head of the bypass region has been reduced farther and allows more bundle fluid to drain into and refill the region. As the bypass refills, the hydrostatic head difference decreases and with it the forward leakage flow.

The forward leakage flow also allows the lower plenum vapor to escape through the guide tube/bypass region. Consequently, the vapor upflow at the SEO decreases, which allows more liquid downflow from the bundle to the lower plenum. As the bundle drains partially and the hydrostatic head decreases, the jet pump path pressure drop correspondently decreases. This results in a simultaneous increase of mass influx to and decrease of mass outflux from the lower plenum. Therefore mass inventory in the lower plenum increases (Fig A4.)

The forward leakage flow to the bypass reverses later (Fig A2) when partial loss of inventory in the bundle coupled with refilling<sup>of</sup> bypass leads to reversal of the hydrostatic head difference. This allows the restoration of the pseudo steady state conditions that precedes the vapor venting from the guide tube. For, as the guide tube flow is reversed into the lower plenum, the combined vapor flow is forced through the SEO. The increase in the vapor flow causes the SEO to reduce the liquid drain from bundle and allows the bundle to accumulate inventory once again. At the same time, as the hydrostatic head of the bundle increases, the pressure drop across the jet pumps increases correspondingly (Fig A2). This results in a simultaneous decrease of mass influx to and an increase of mass outflux from the lower plenum. Therefore mass in the lower plenum decreases until the mixture level returns to that of the jet pump exit plane. With the mixture reaching that level, a pseudo steady state is momentarily restored, (see Figures 9 and 3d)

This process repeats itself later in the transient. However, after this last refill, a sufficient amount of subcooled liquid enters the guide tube and bypass regions. This, in conjunction with decreased flashing due to decreased depressurization rate, diminishes the vapor up flow, and subsides further vapor venting.

This venting process in the bypass region of TLTA is believed to be influenced by the one dimensional configuration of the TLTA geometry and may not be representative of a BWR. In TLTA, the bypass region volume is mocked up by four parallel tubes which communicate from the guide tube to the upper plenum. LPCI is injected equally into each tube. In the BWR the bypass is a more open, three-dimensional region with LPCI injection at the core shroud wall. Communication between the bypass and guide tube, and bypass and bundle are less influential as the bypass region has a large, plenum effect. Therefore, the venting process observed in TLTA is not expected in a BWR.

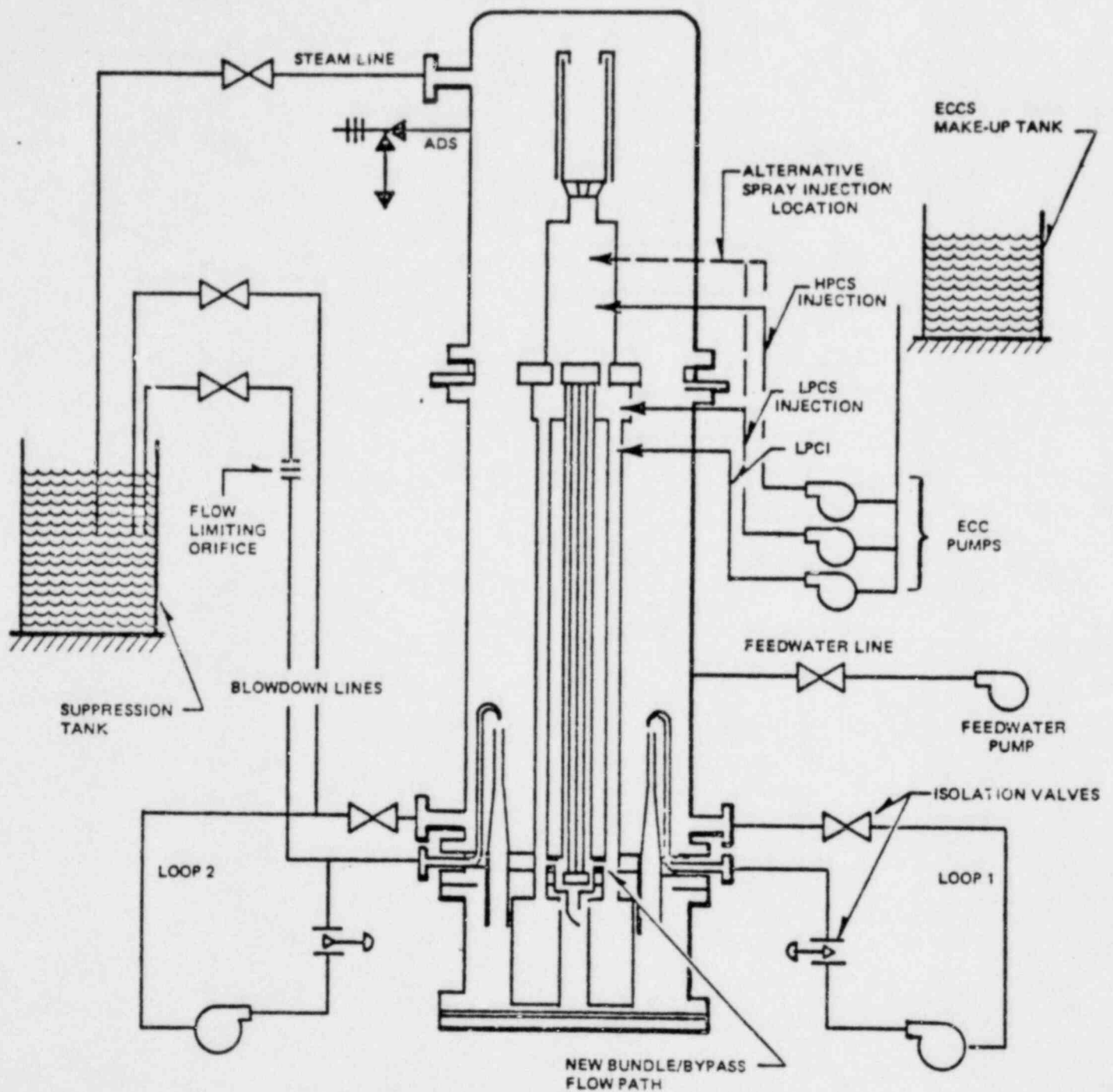


Figure 1. Two-Loop Test Apparatus Configuration 5A (TLTA-5A) with Emergency Core Cooling Systems

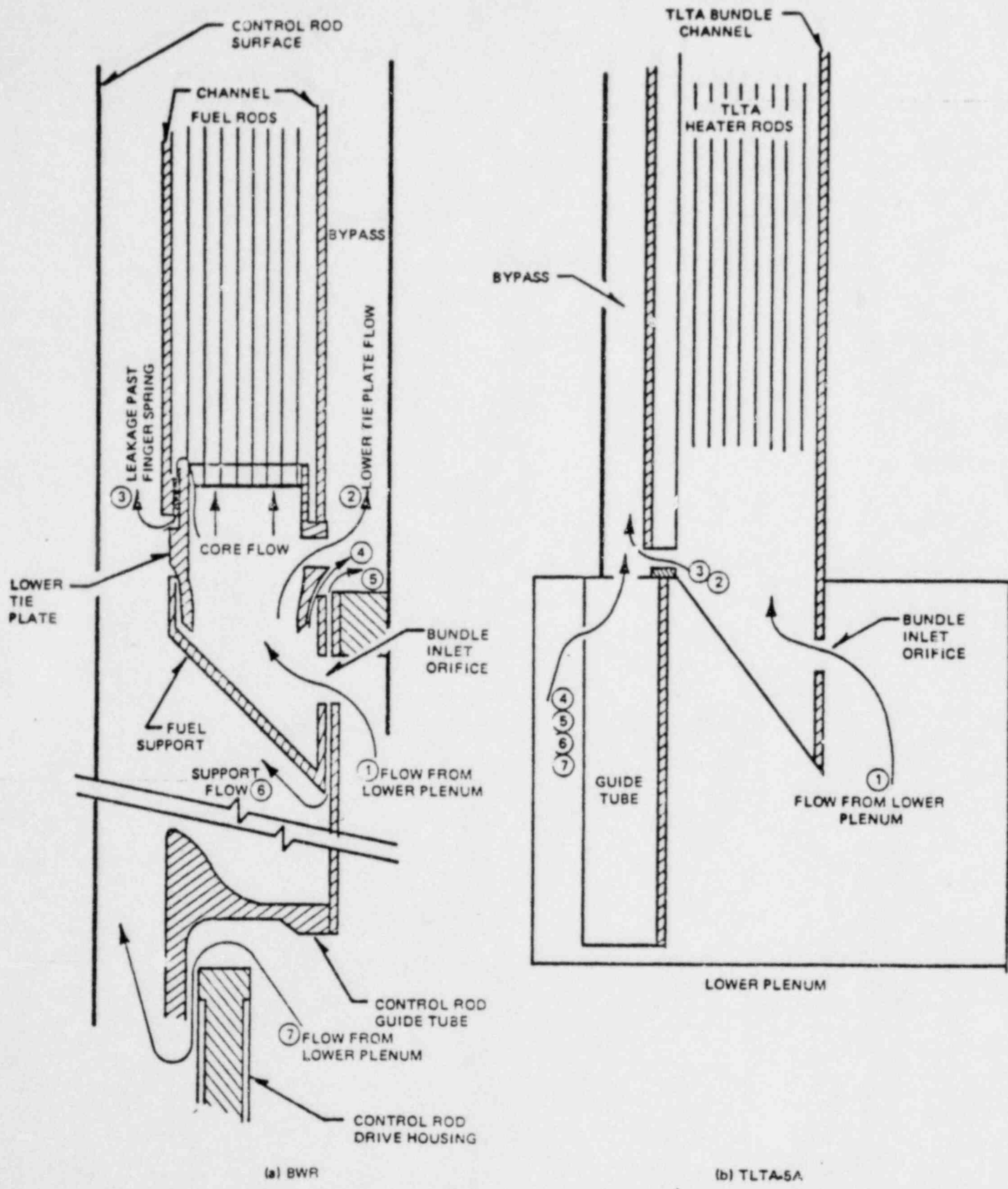


Figure -2. Flow Paths at Inlet Region of a BWR Fuel Bundle and the TLTA Simulation

BD/ECC1A 5.05MW TLTASA

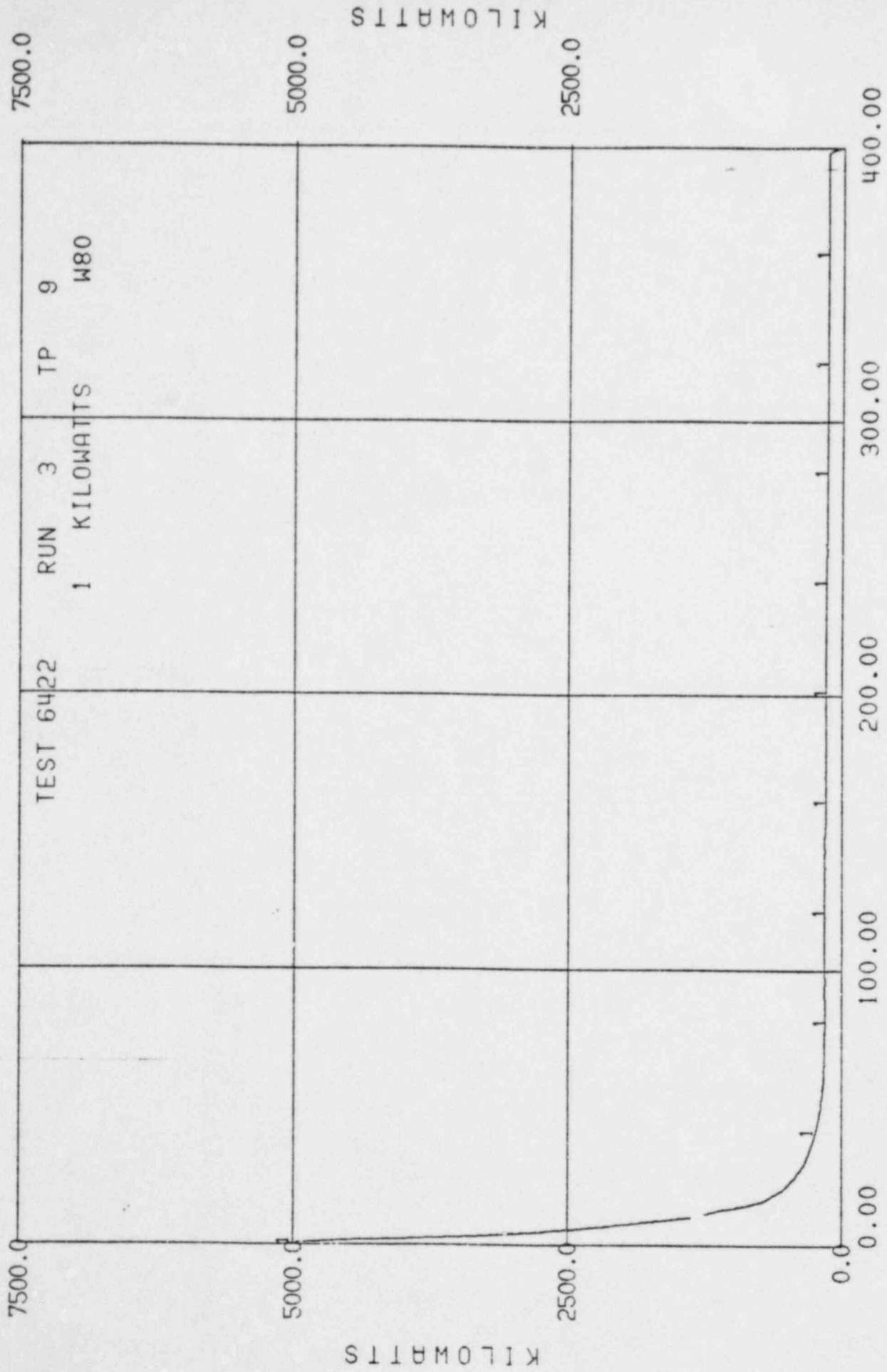


Figure 3, Bundle Power Decay



BD/ECC1A 5.05MW TLTA5A

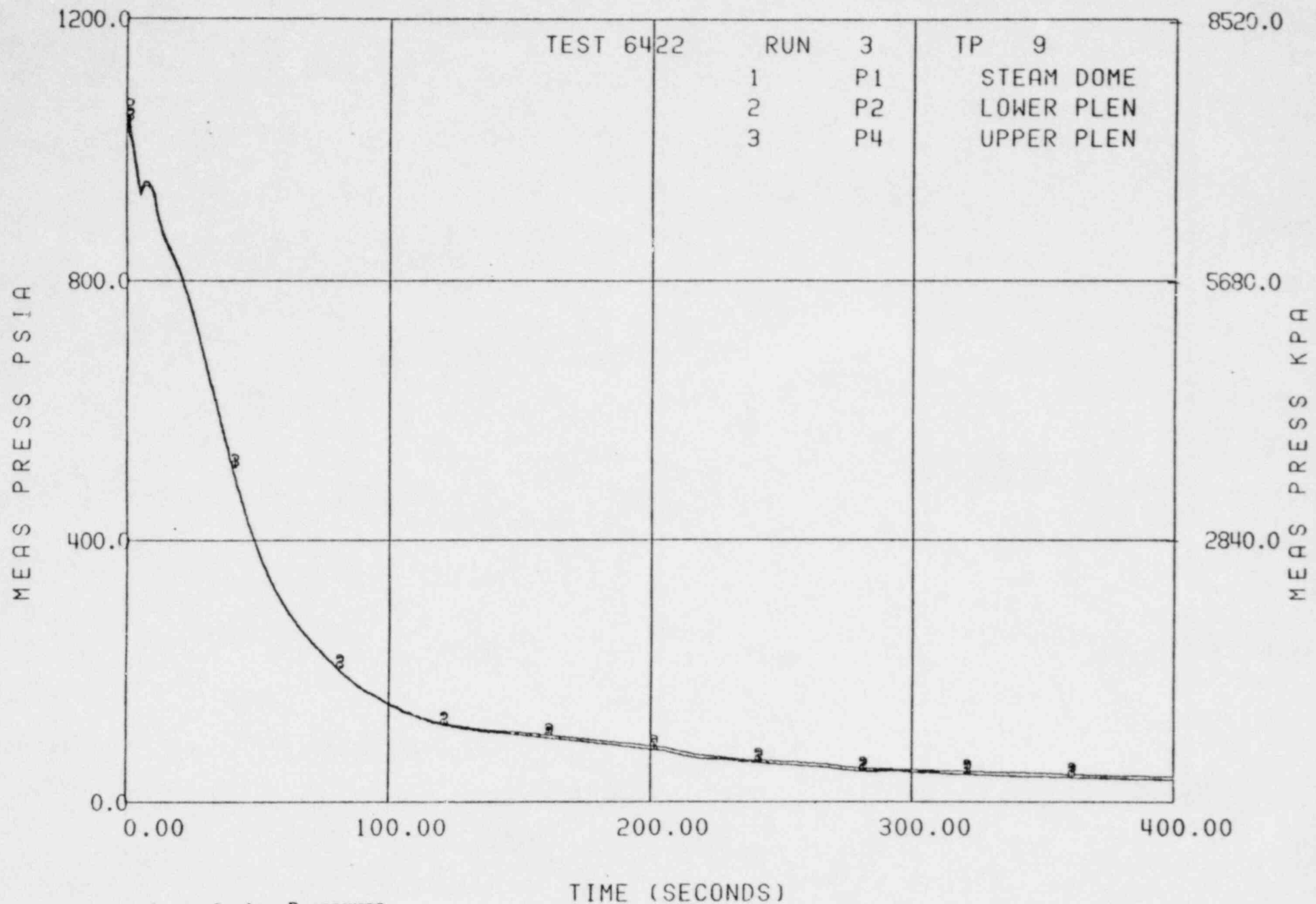


Figure 4, System Pressures

BD/ECC1A 5.05MW TLTA5A

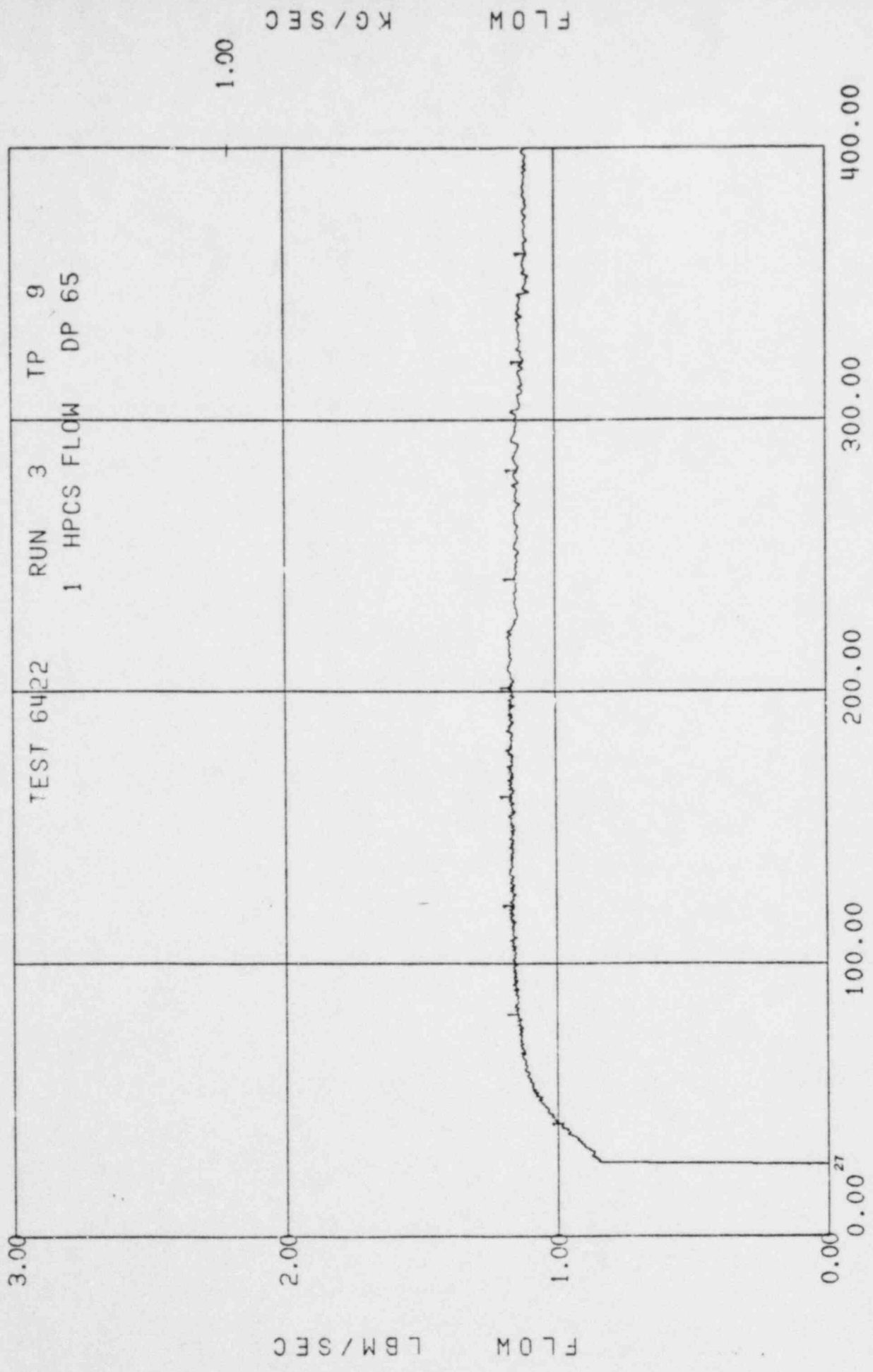


Figure 5, HPCS Injection Rate

BD/ECC1A 5.05MW TL1A5A

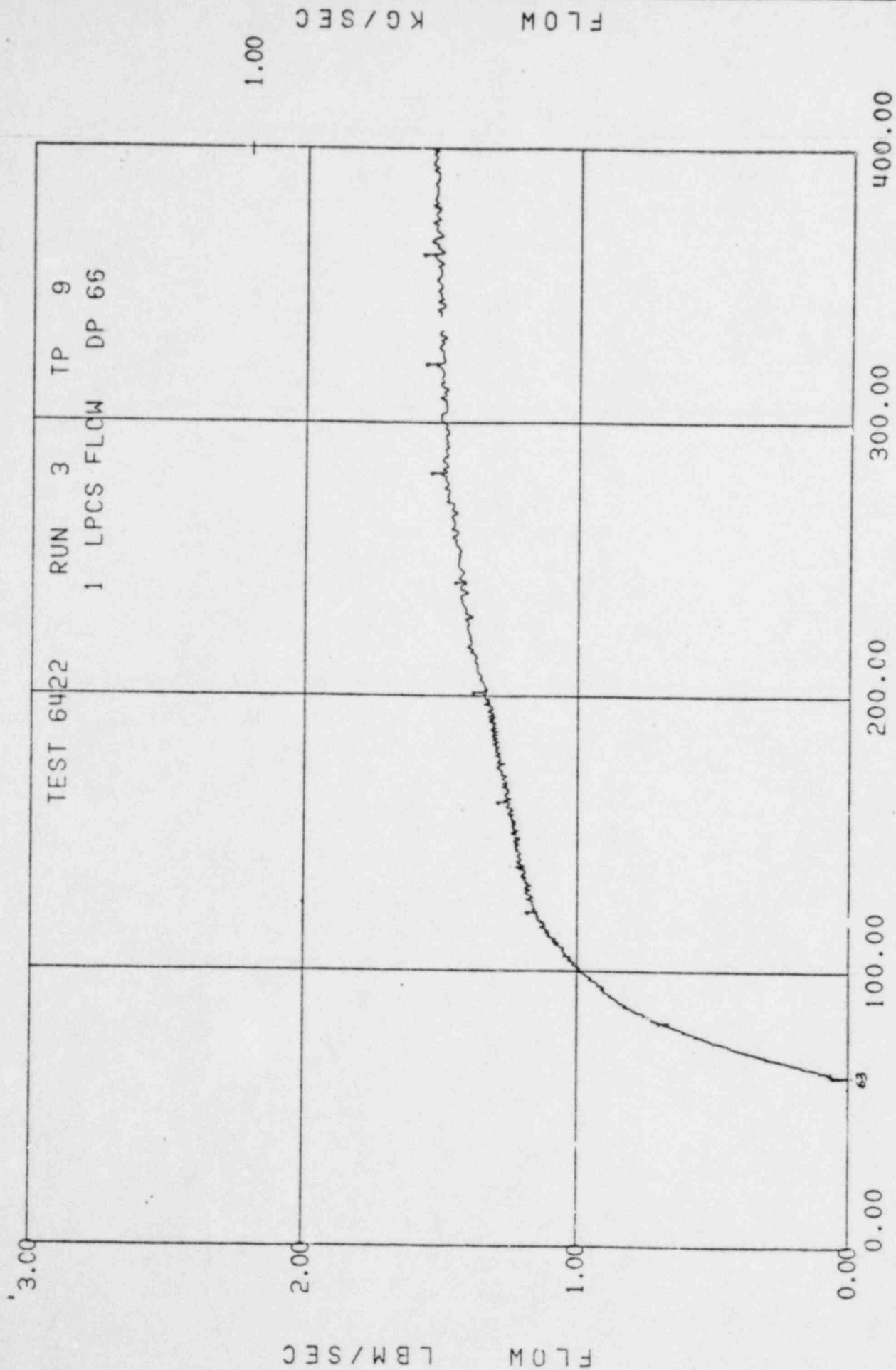


Figure 6, LPCI Injection Rate

BD/ECCIA 5.05MW TLTASA

TEST 6422 RUN 3 TP 9  
1 LPCI FLOW DP 63

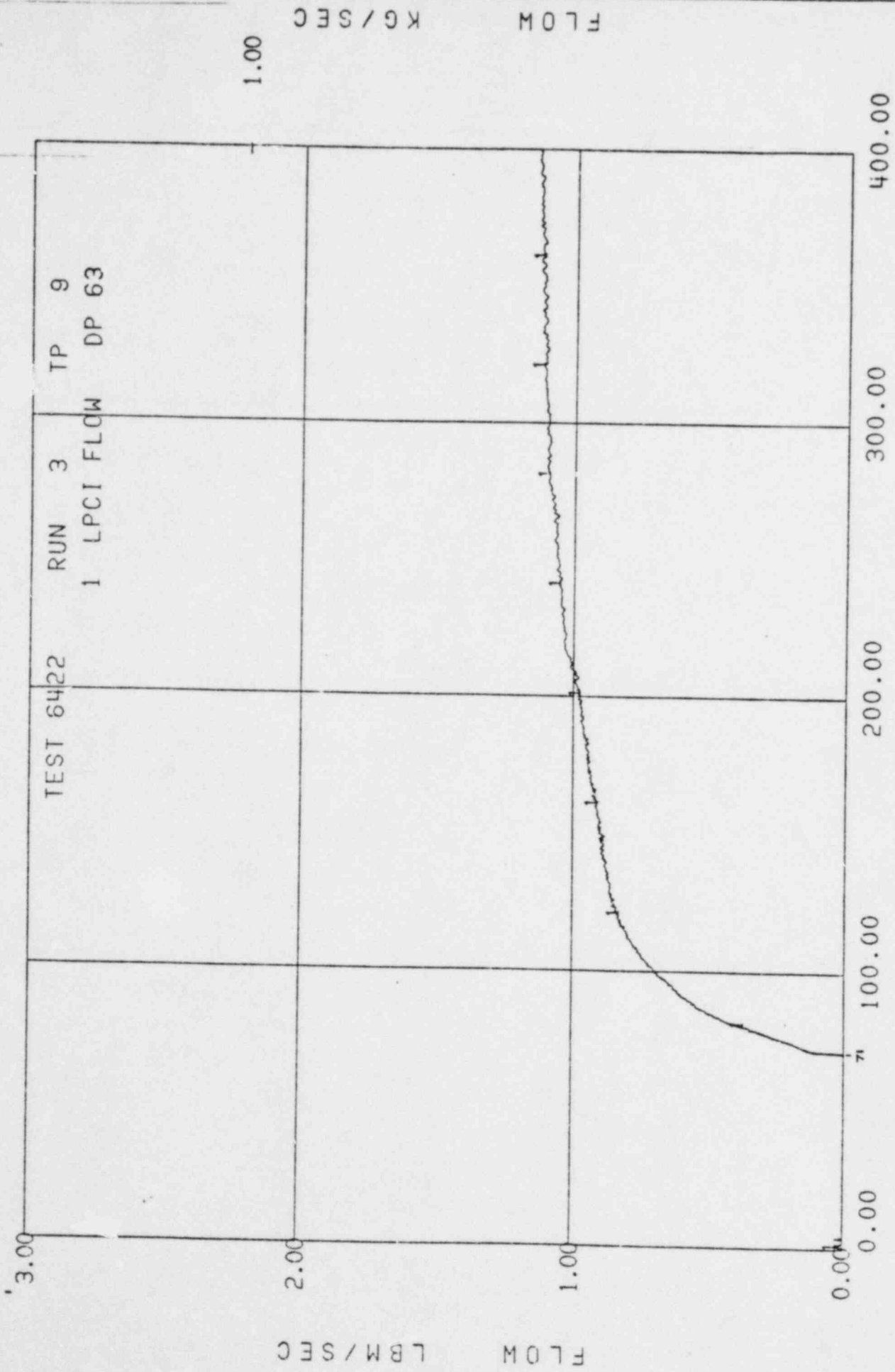


Figure 7, LPCI Injection Rate

BD/ECC1A 5.05MW TLTA5A

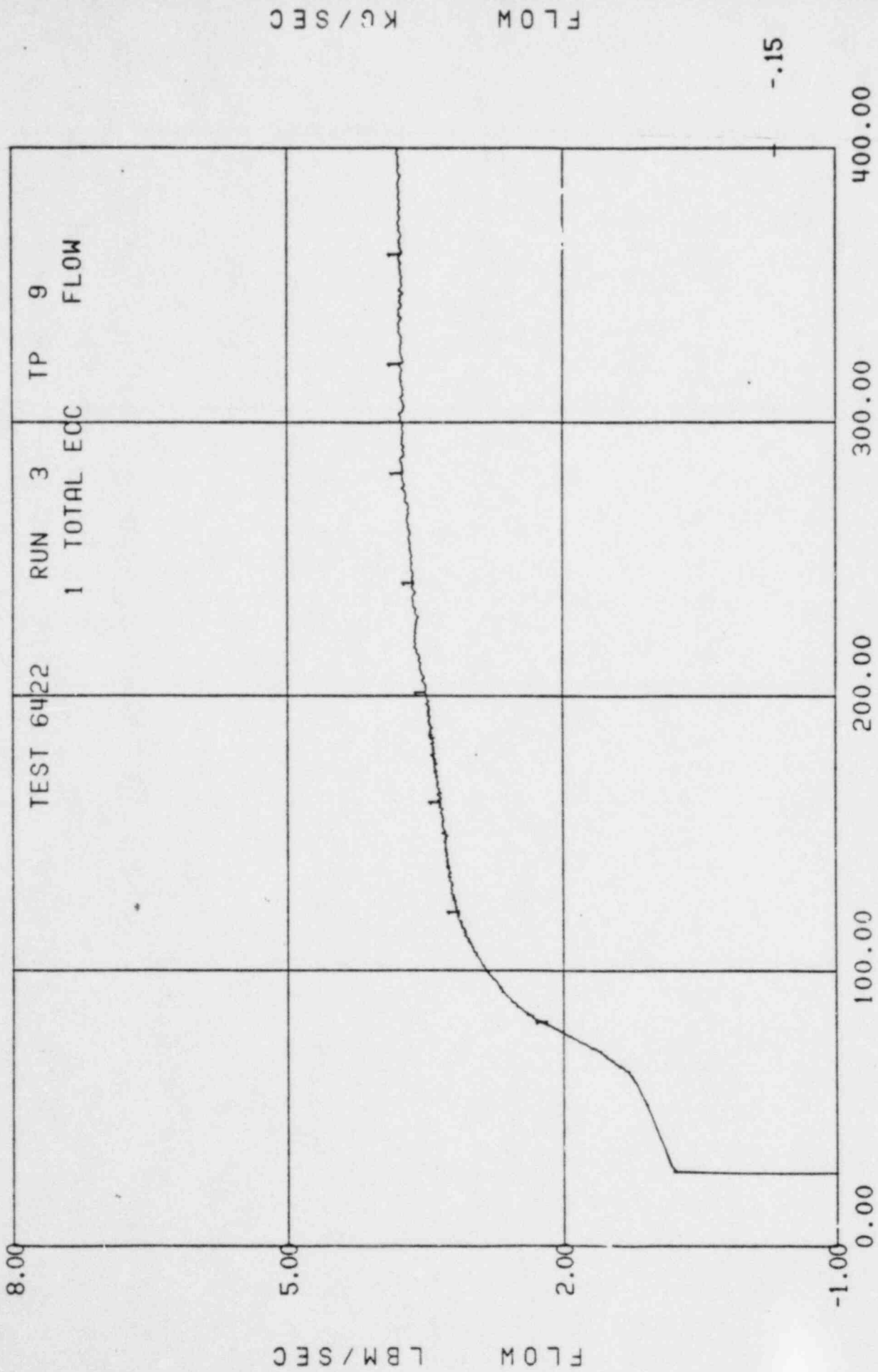


Figure 8, Total ECC Injection Rate

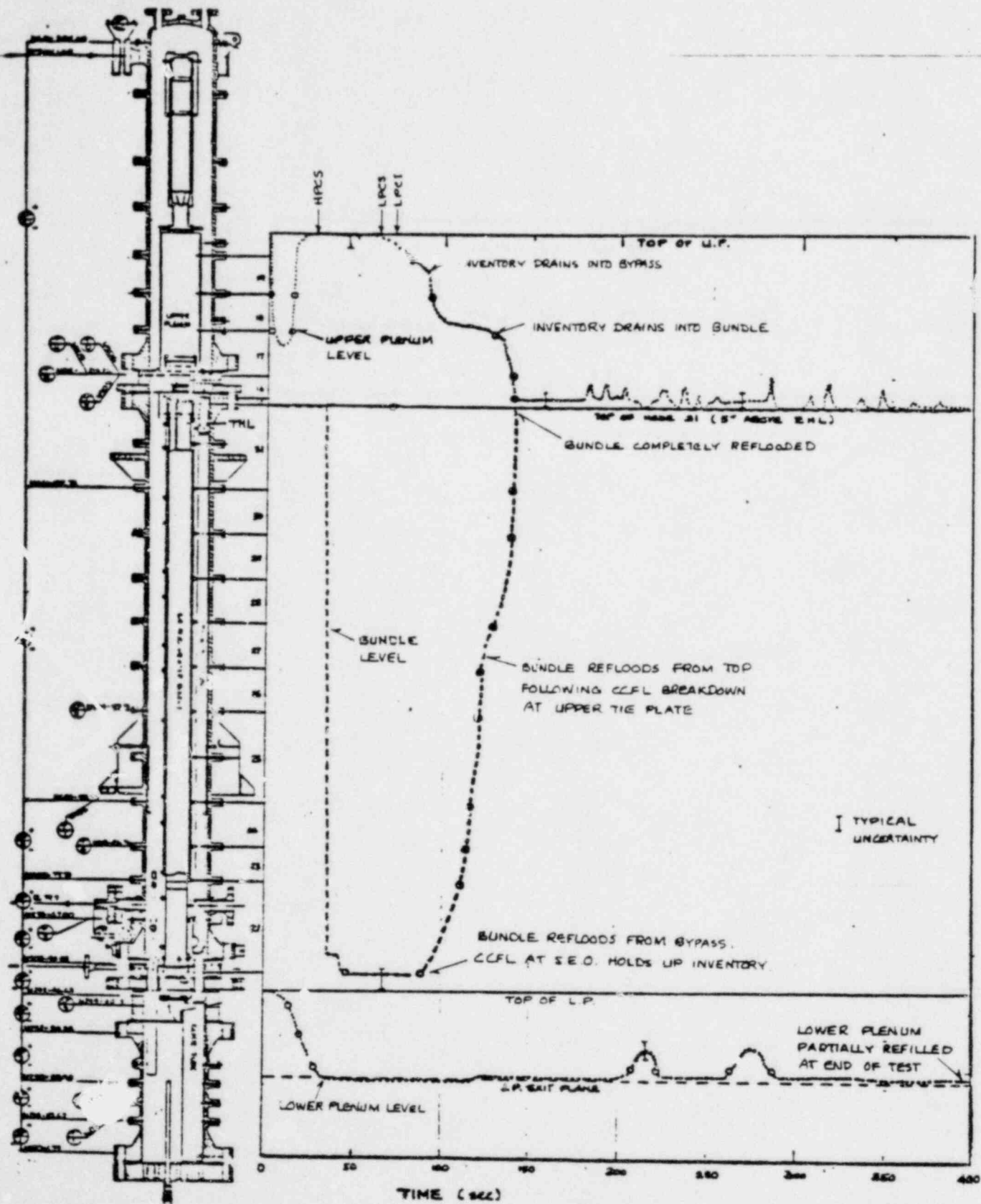


Figure 9, Mixture levels along the bundle path; TLTA 5A Reference Test (6422 Run 3, Average Power, Average ECC rates)

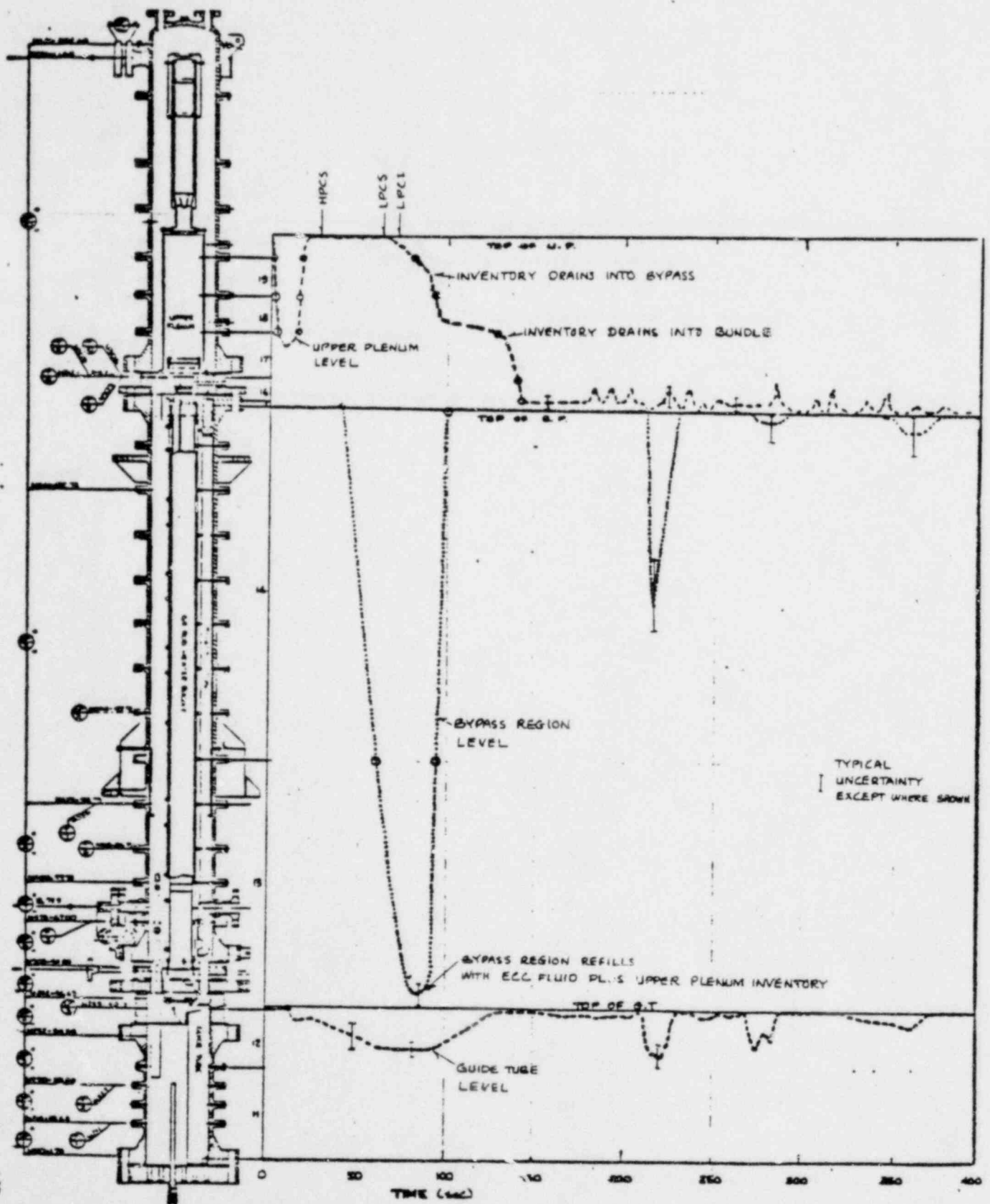


Figure 1C, Mixture level along the bypass path; TLTA 5A Reference Test (6422 Run 3, Average Power; Average ECC rates)

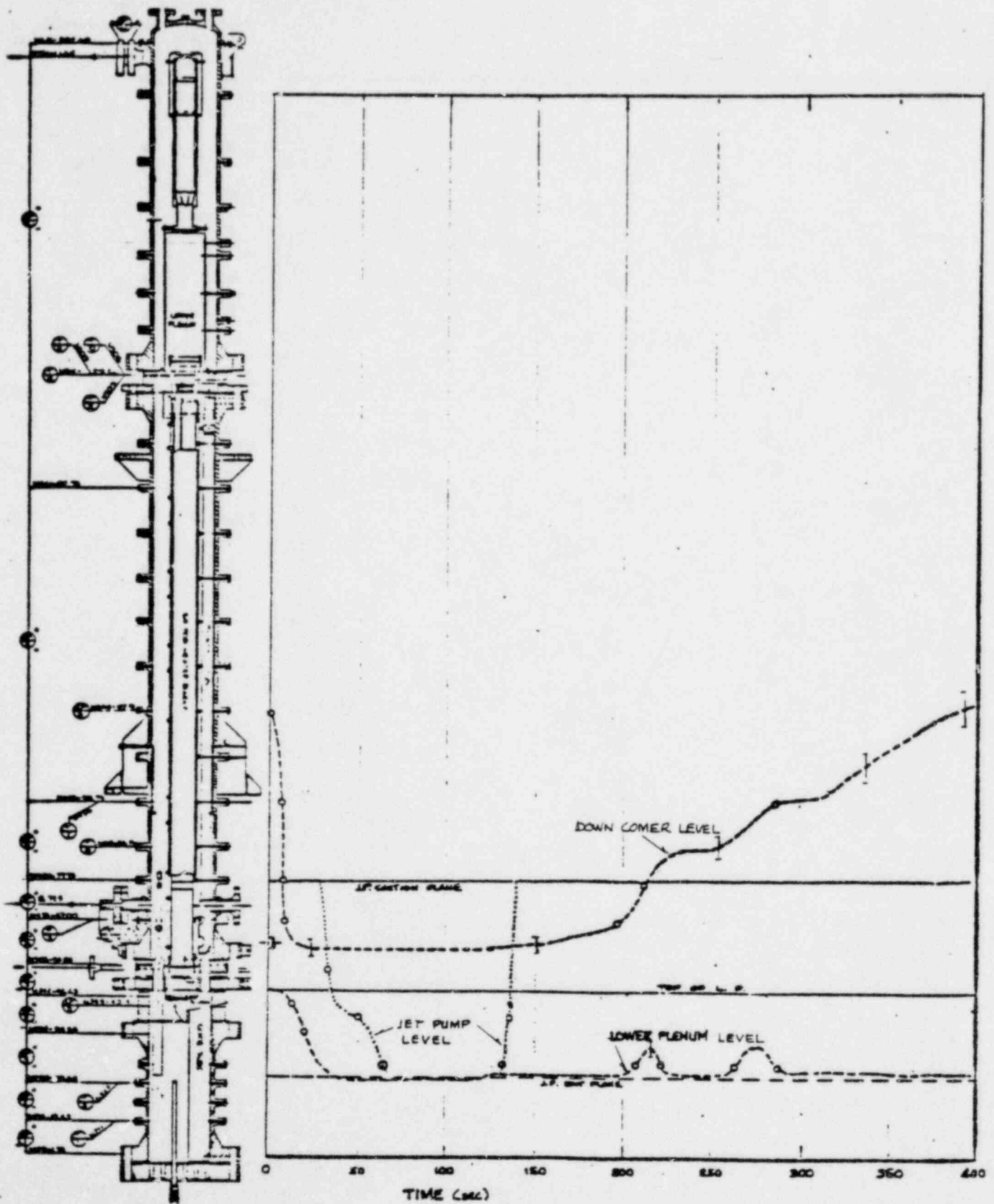


Figure 11, mixture levels along the jet pump path; TLTA 5A Reference Test (6422 Run 3, Average Power, Average ECC rates)



BD/ECC1A 5.05MW TLTASA

IF FULL OF  
SAT. LIQUID

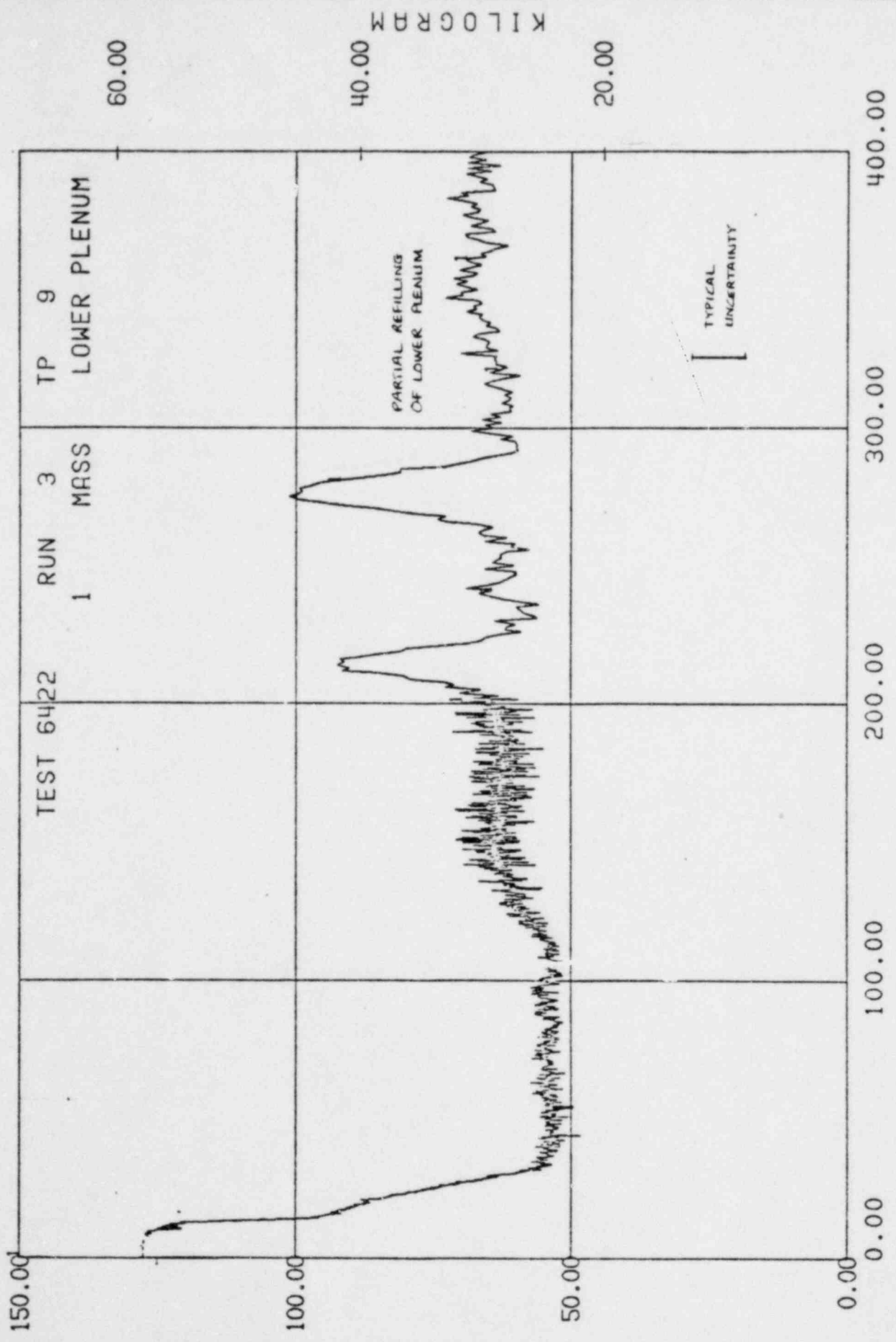


Figure 12, Lower Plenum Mass

BD/ECC1A 5.05MW TLTA5A

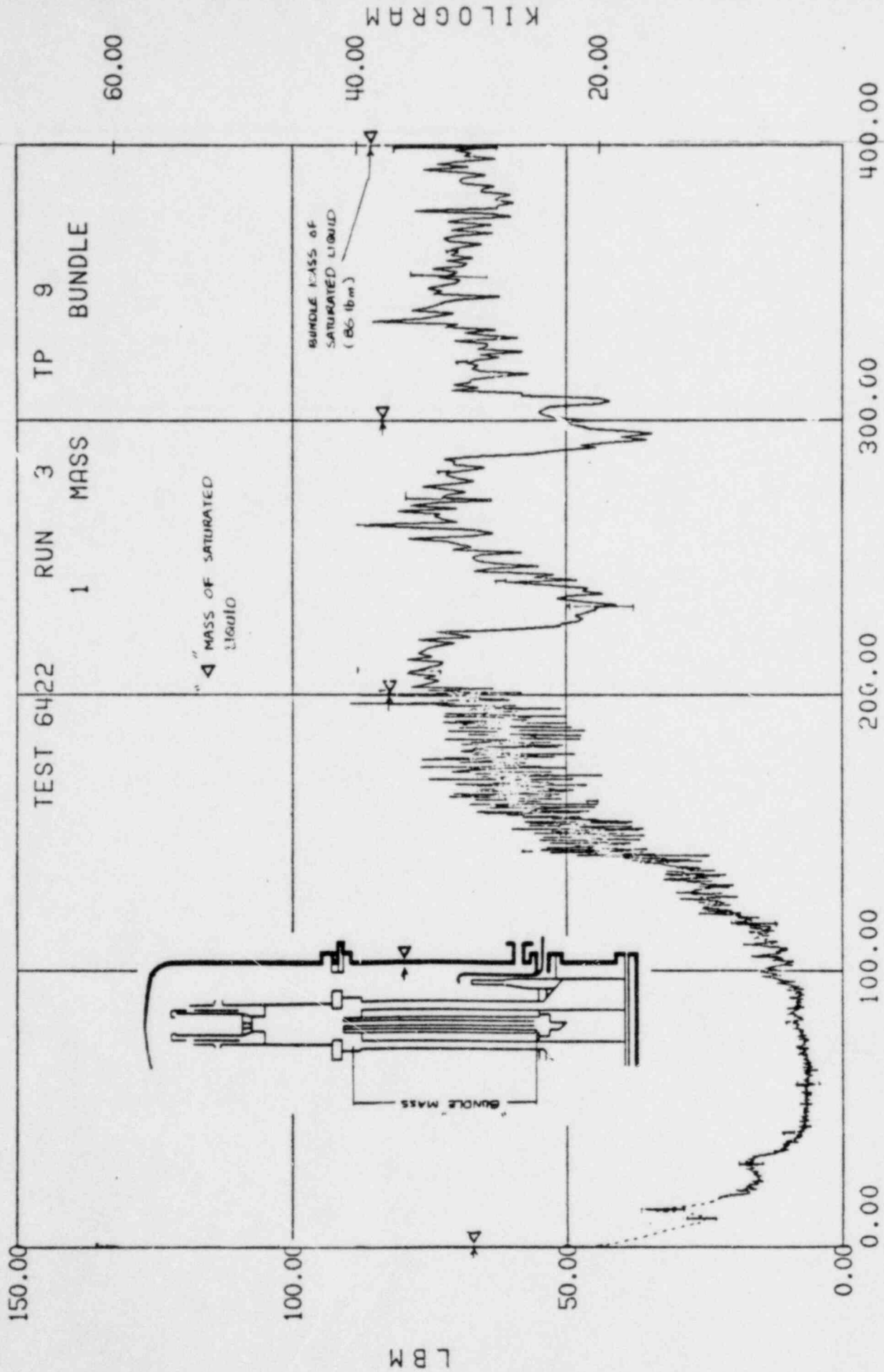


Figure: 12A Bundle Mass

TIME (SECONDS)

BD/ECC1A 5.05MW TLTA5A

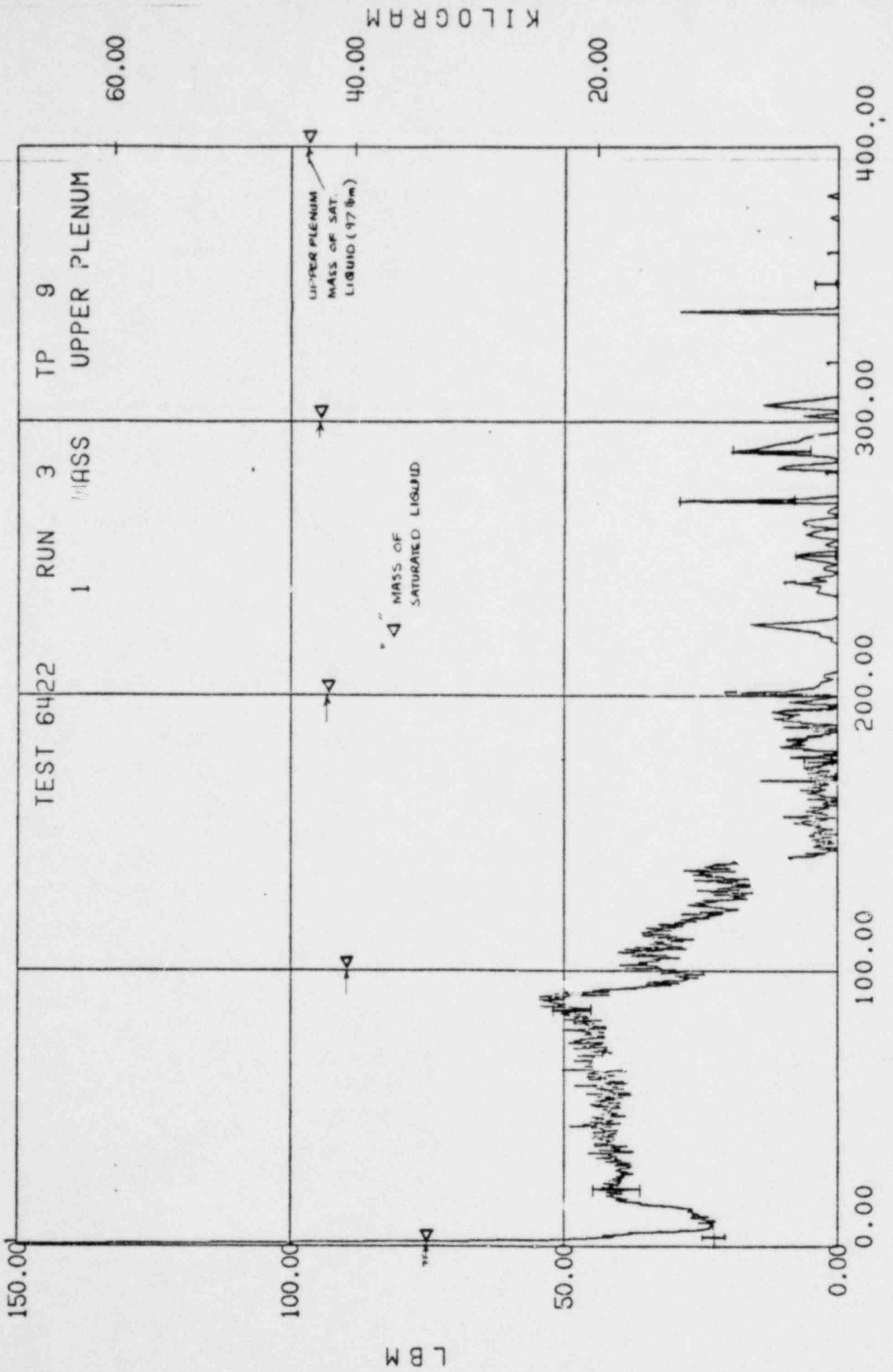


Figure 13, Upper Plenum Mass

TIME (SECONDS)

BD/ECC1A 5.05MW TLTASA

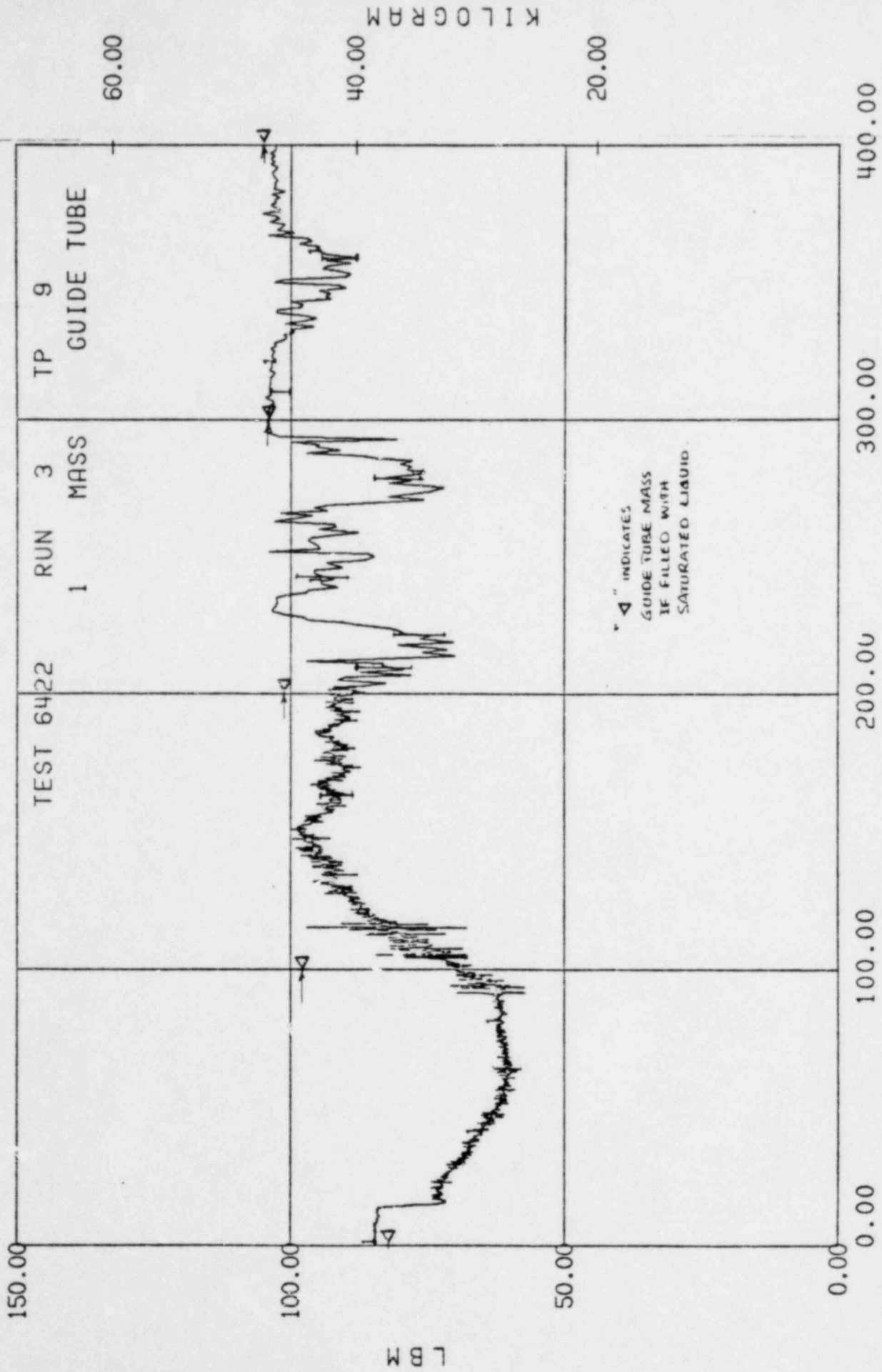


Figure 14, Guide Tube Mass

BD/ECC1A 5.05MW TLTASA

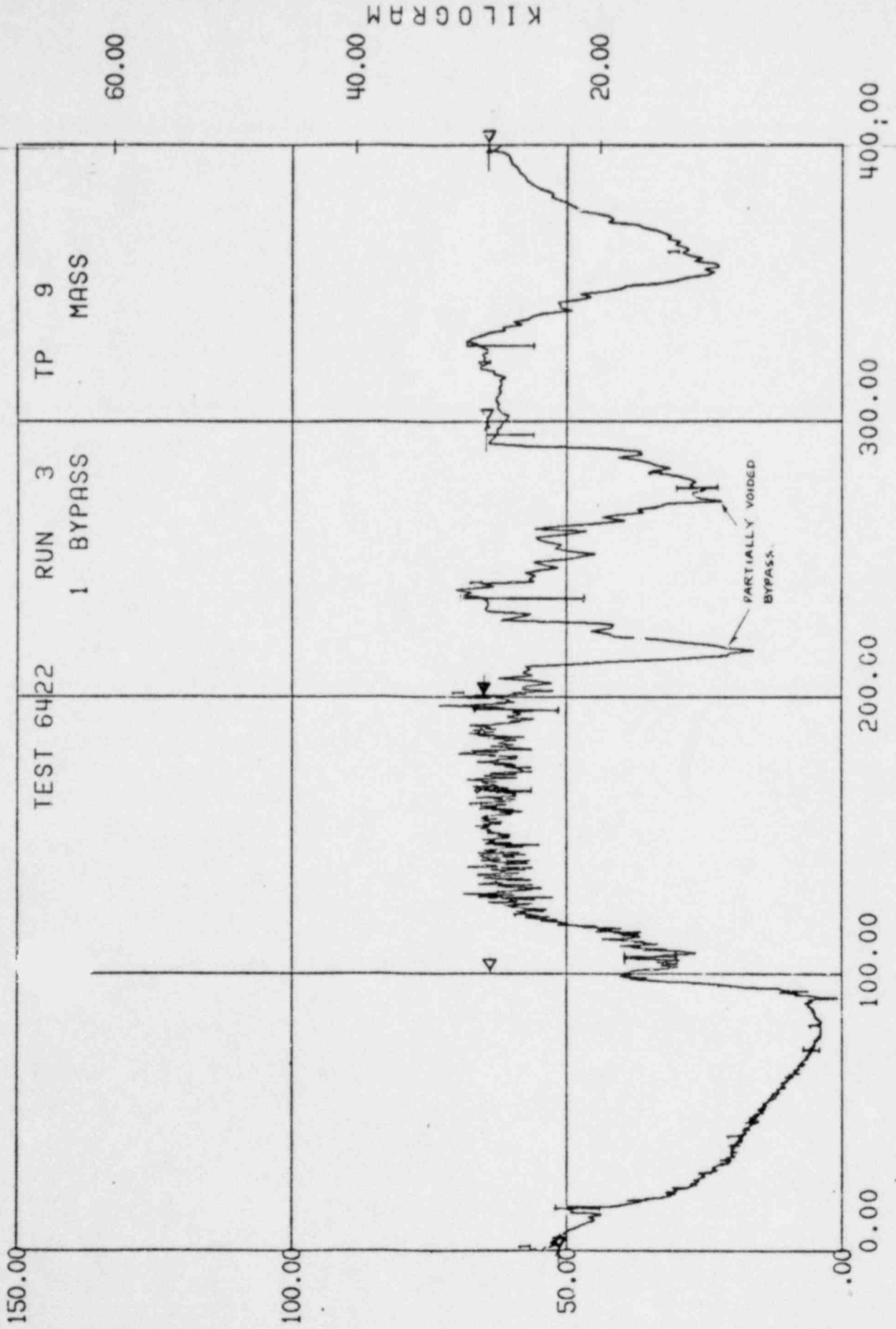


Figure 15, Bypass Mass

BD/ECC1A 5.05MW TLTA5A

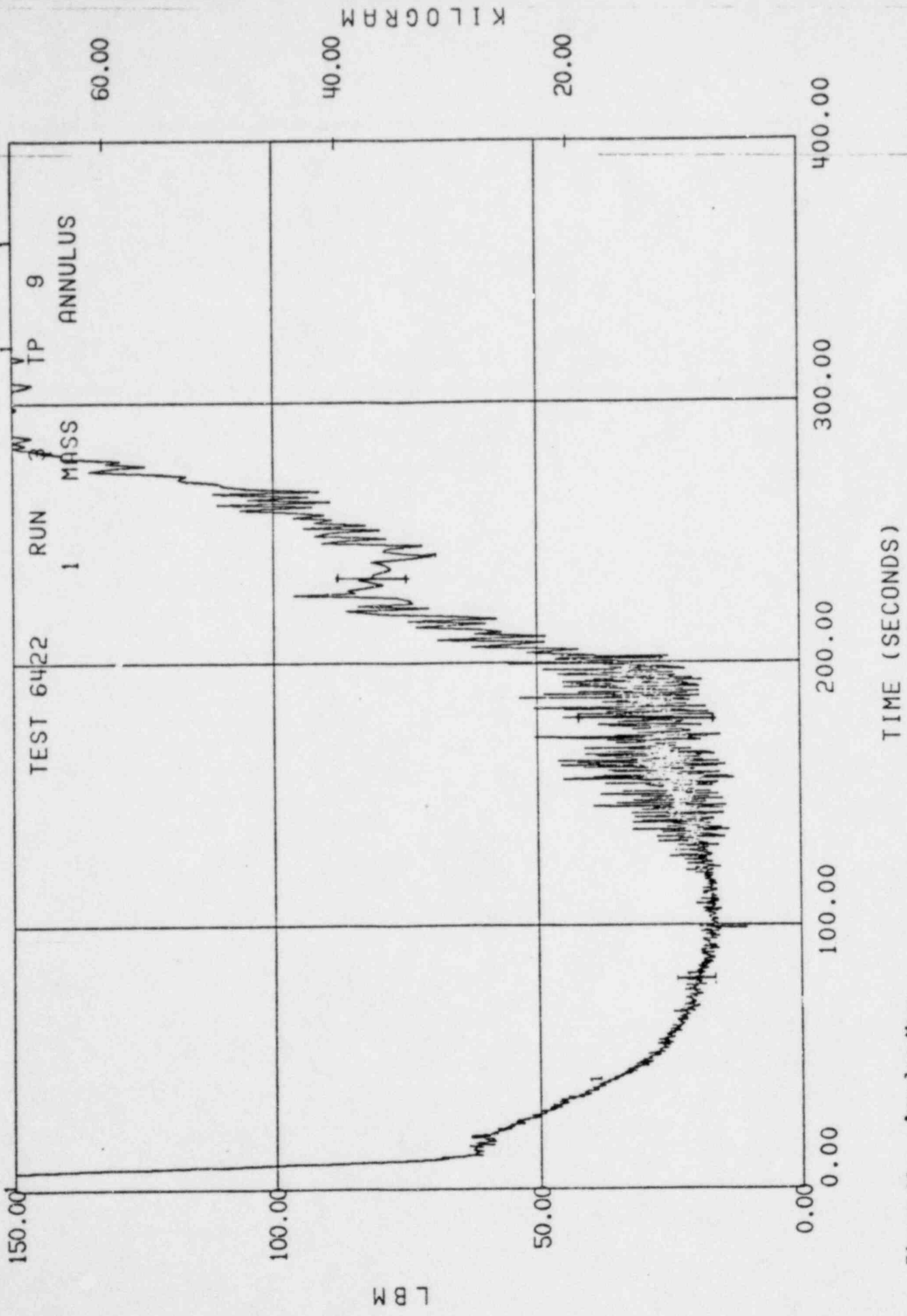


Figure 16, Annulus Mass

BD/ECC1A 5.05MW TLTA5A

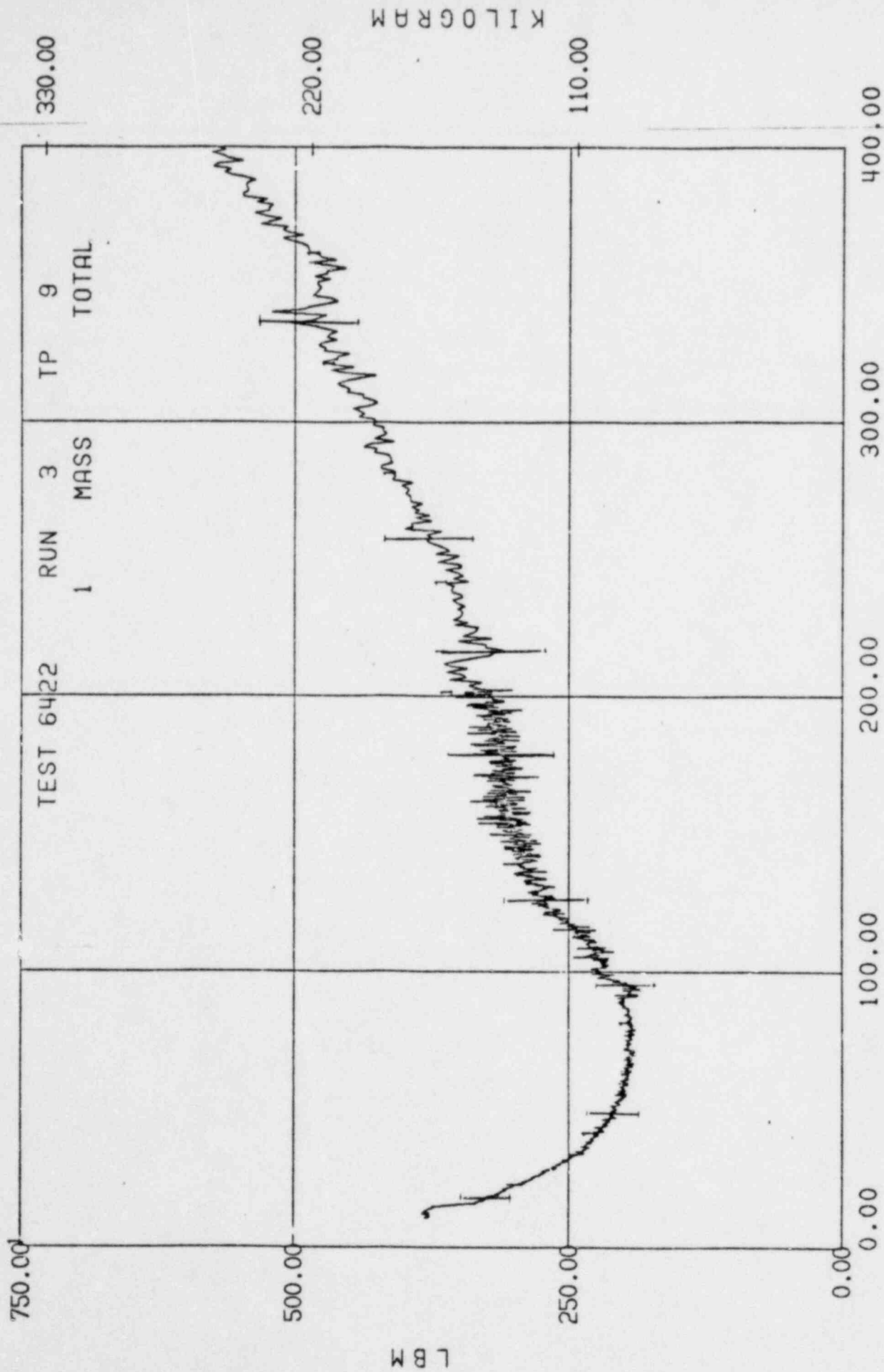
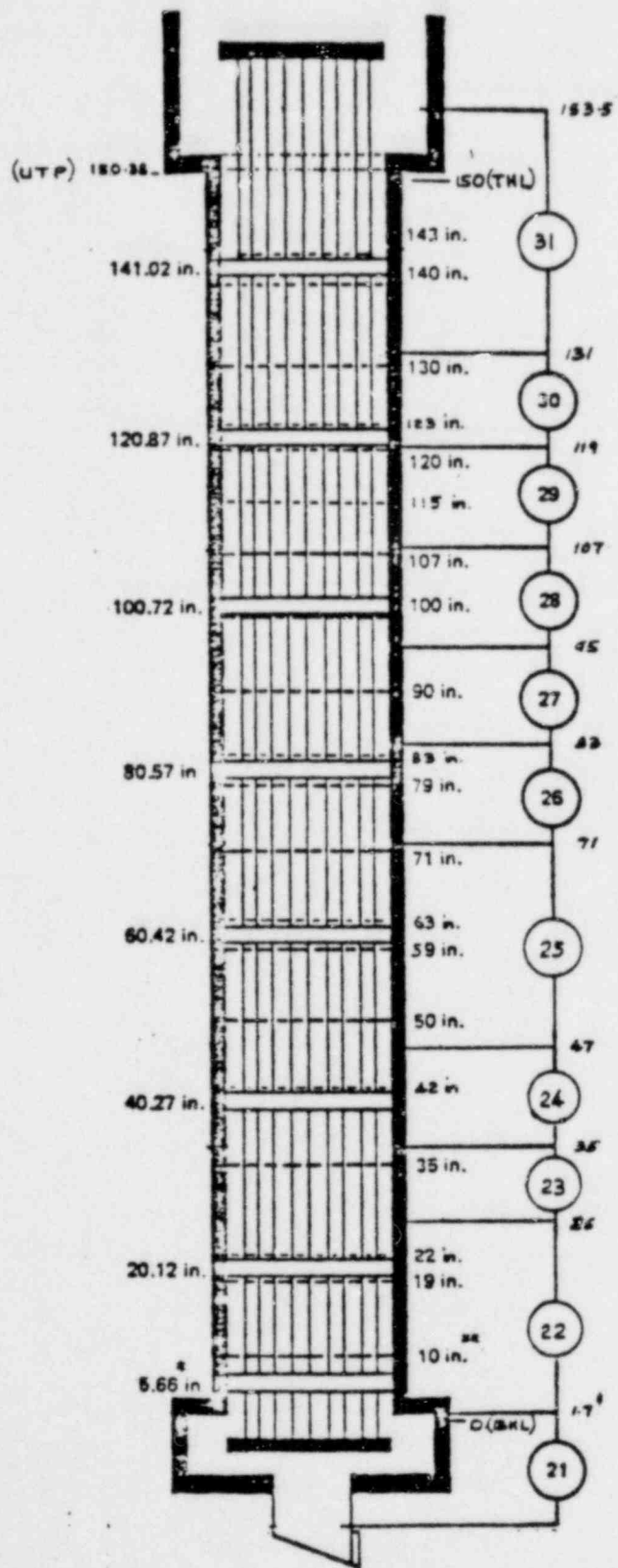


Figure 17, Total Mass



NOTE: \* ELEVATION OF GRID SPACER  
 BOTTOM RE. BOTTOM OF HEATED  
 LENGTH (TLTA EL 51.7 in.)

\*\* ELEVATION OF TEMPERATURE  
 MEASUREMENT RE. BHL

† ELEVATION OF PRESSURE  
 TRANSDUCER TAPS RE. BHL

Fig. 18, TEMPERATURE AND DIFFERENTIAL PRESSURE MEASUREMENTS IN TLTA 5A



BD/ECC1A 5.05MW TLTASA

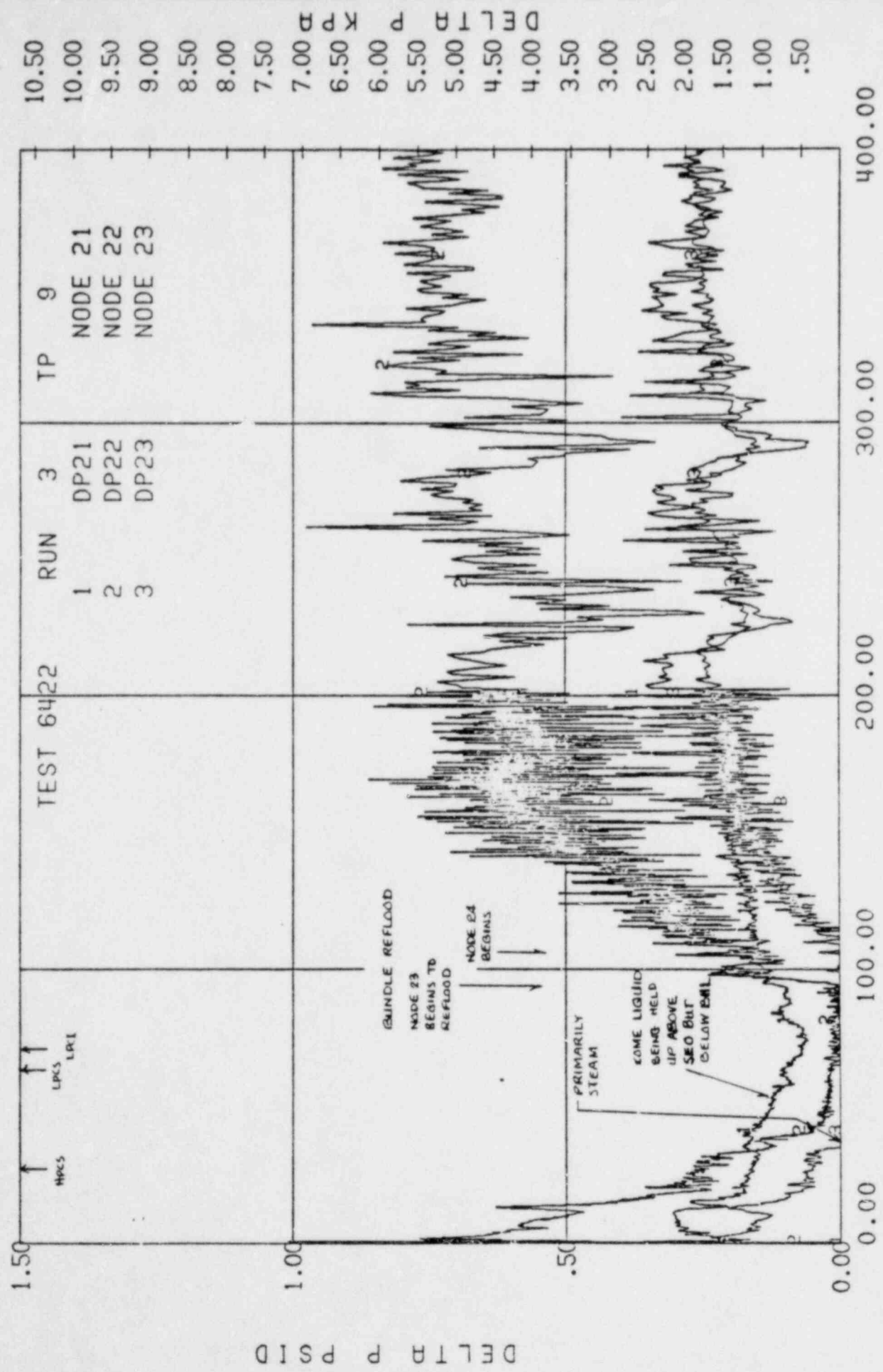


Figure 19, Bundle DP's bottom nodes

BD/ECC1A 5.05MW TLT5A

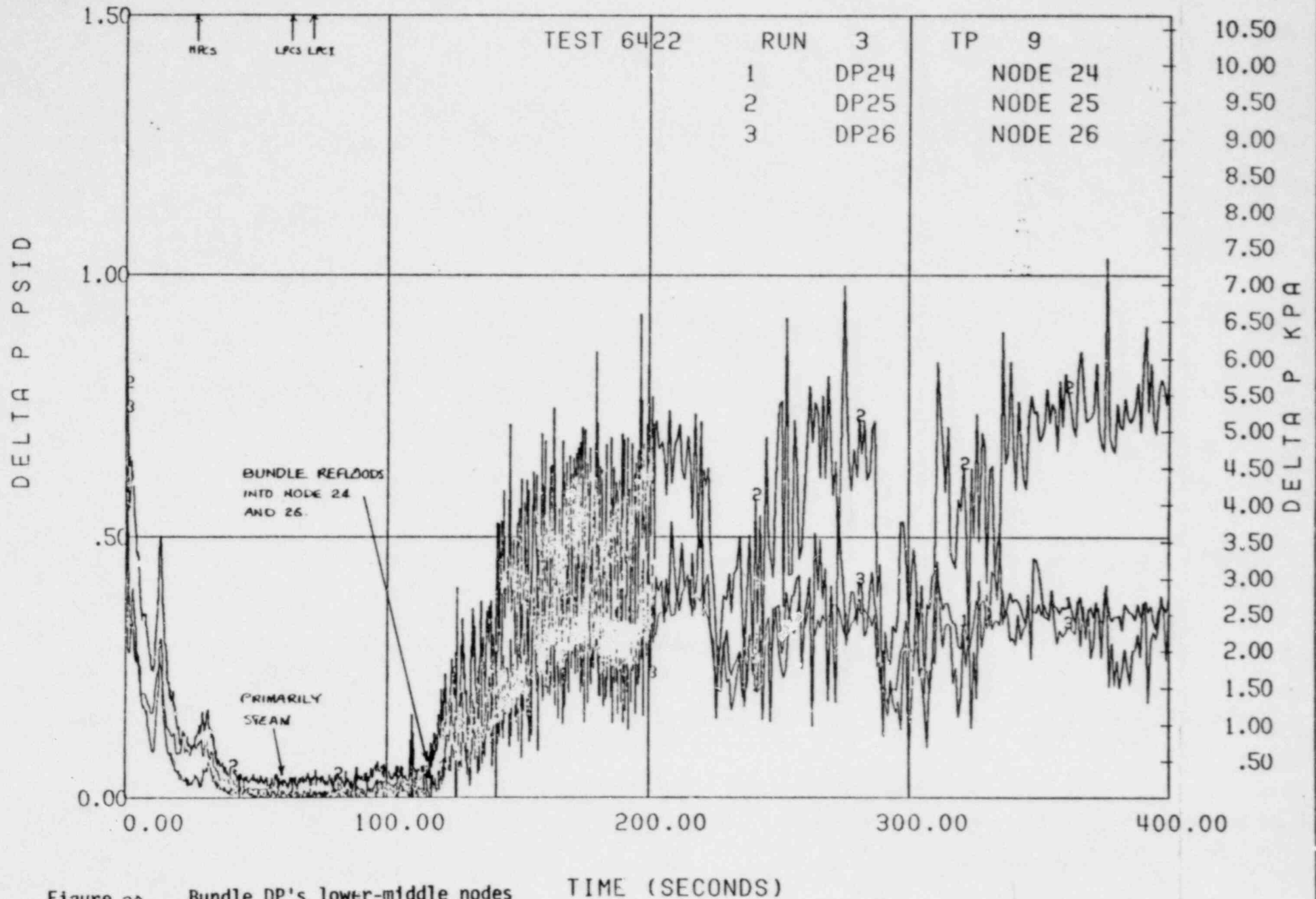


Figure 20, Bundle DP's lower-middle nodes

BD/ECC1A 5.05MW TLT5A

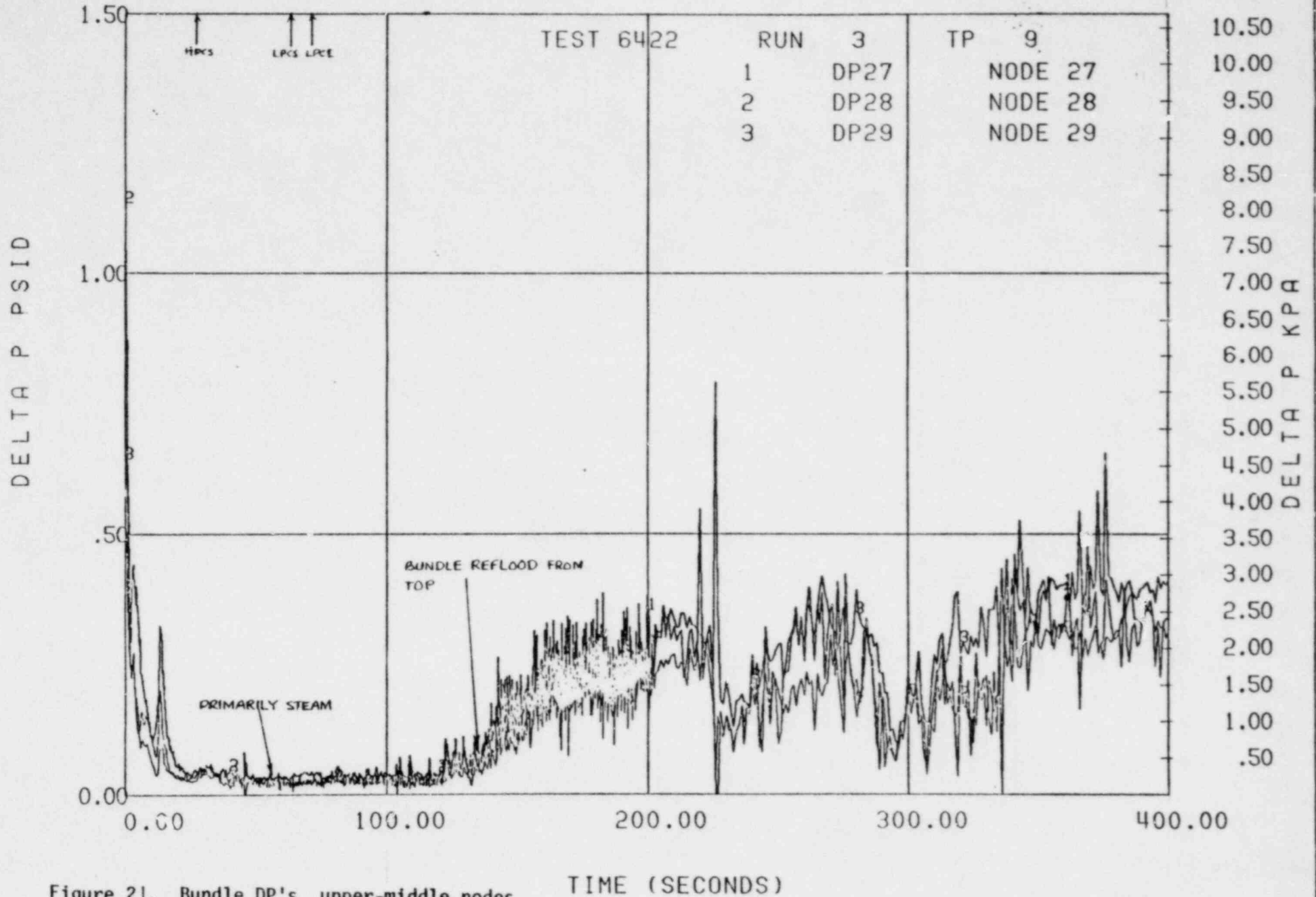


Figure 21, Bundle DP's upper-middle nodes

BD/ECC1A 5.05MW TLTA5A

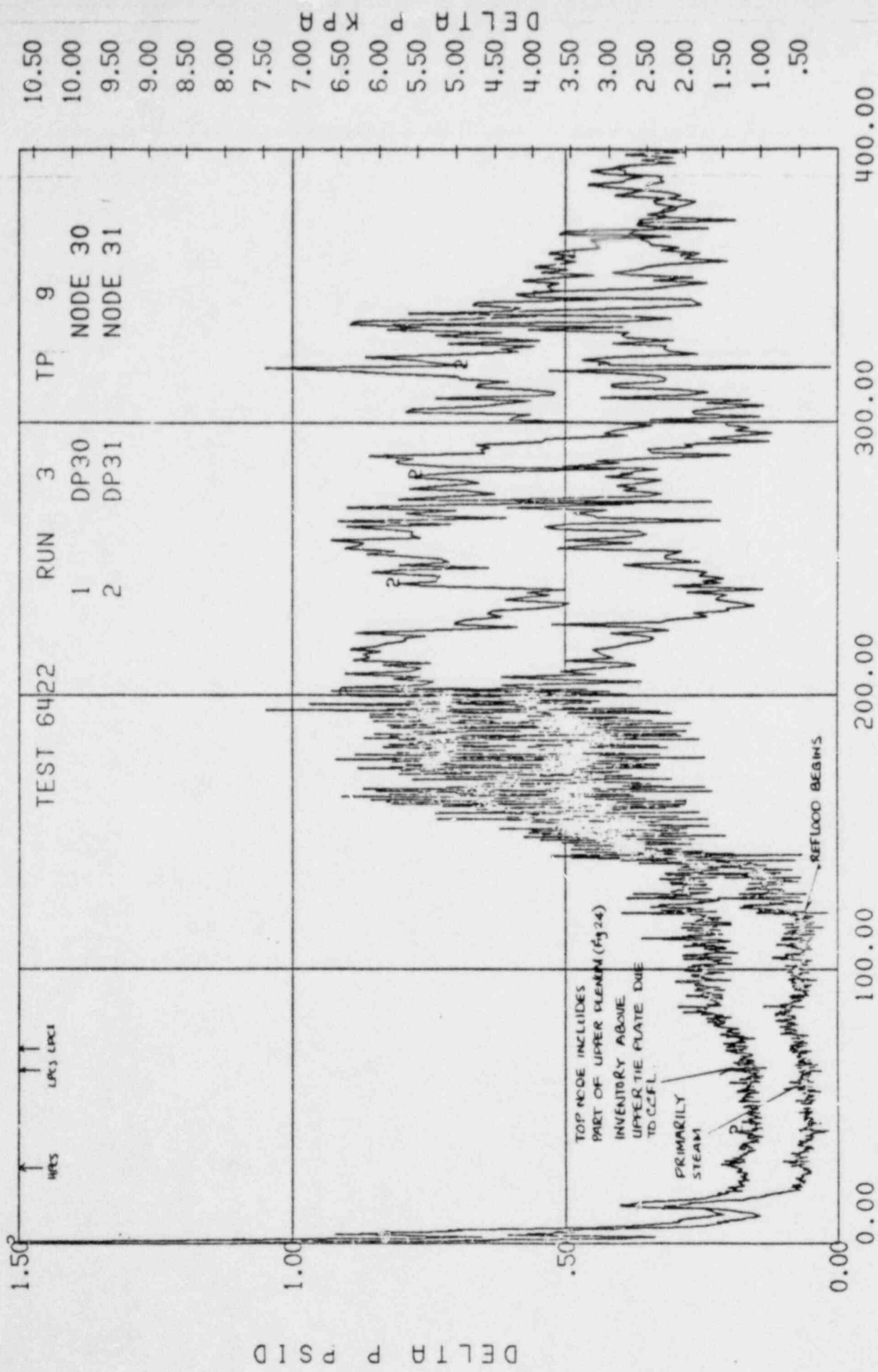


Figure 22, Bundle DP's top nodes

BD/ECC1A 5.05MW TLTA5A

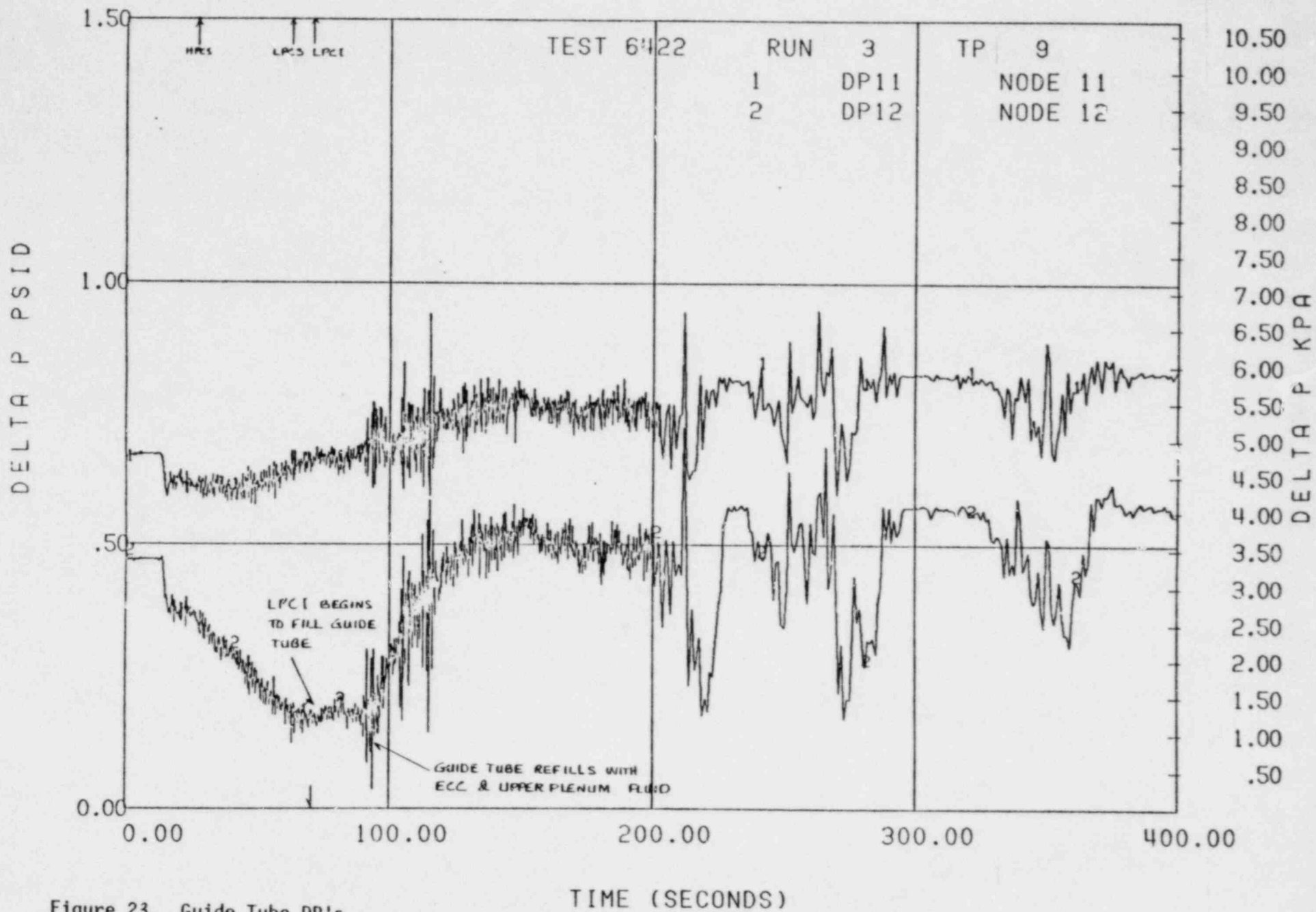


Figure 23, Guide Tube DP's

BD/ECC1A 5.05MW TLTA5A

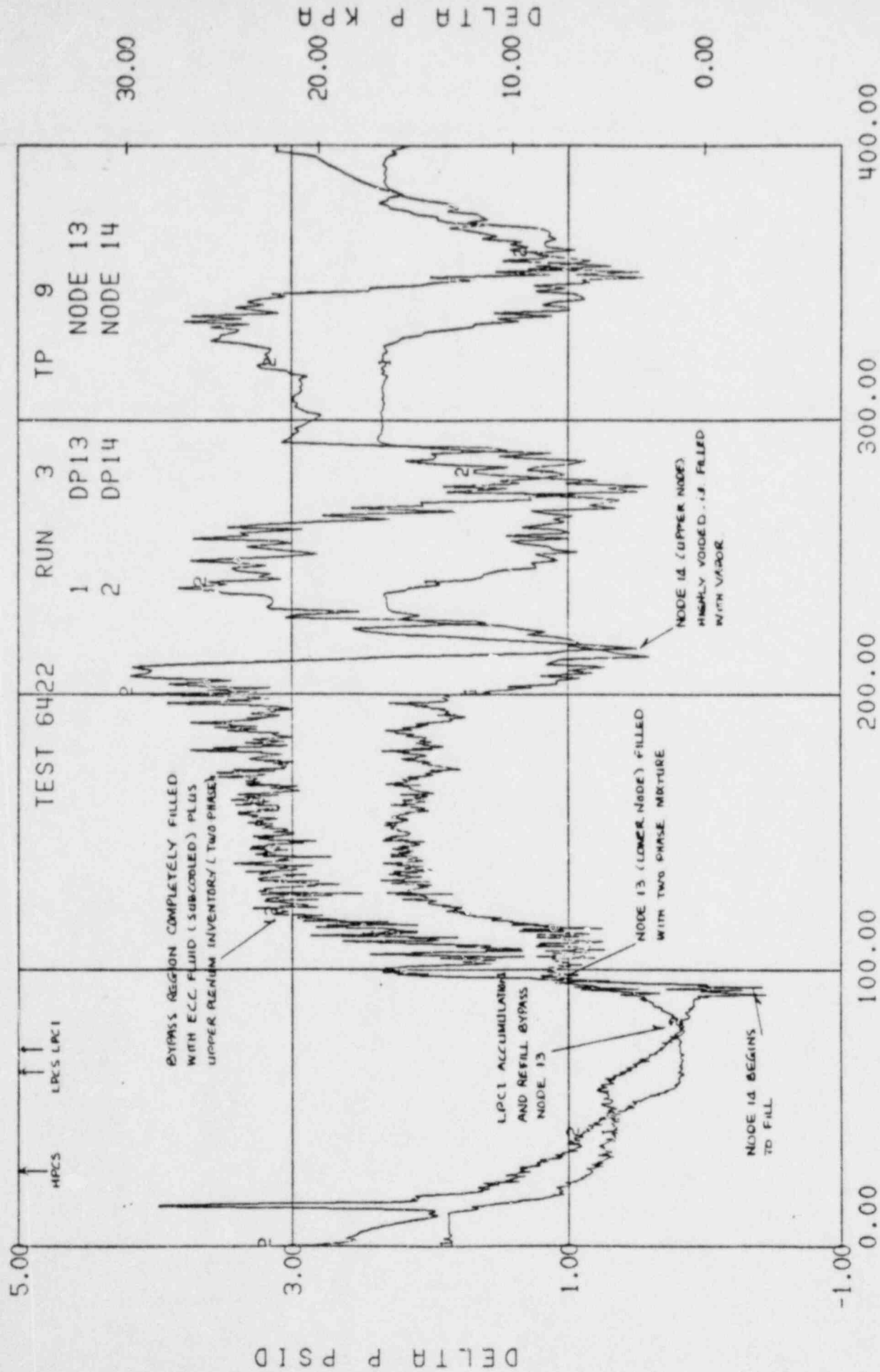


Figure 24. Bypass Region DP's

BD/ECC1A 5.05MW TLTA5A

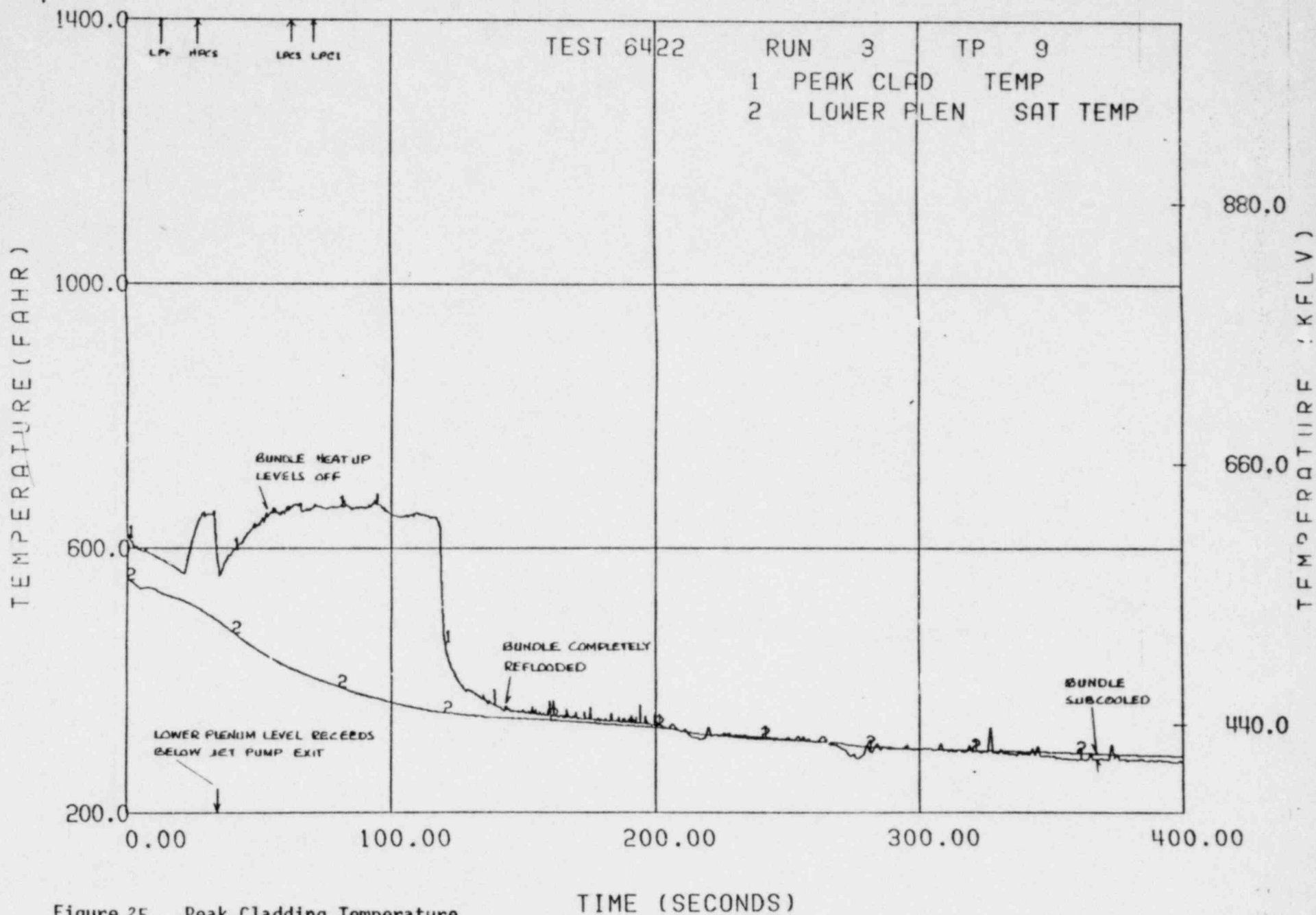


Figure 25, Peak Cladding Temperature

BD/ECC1A 5.05MW TLTA5A

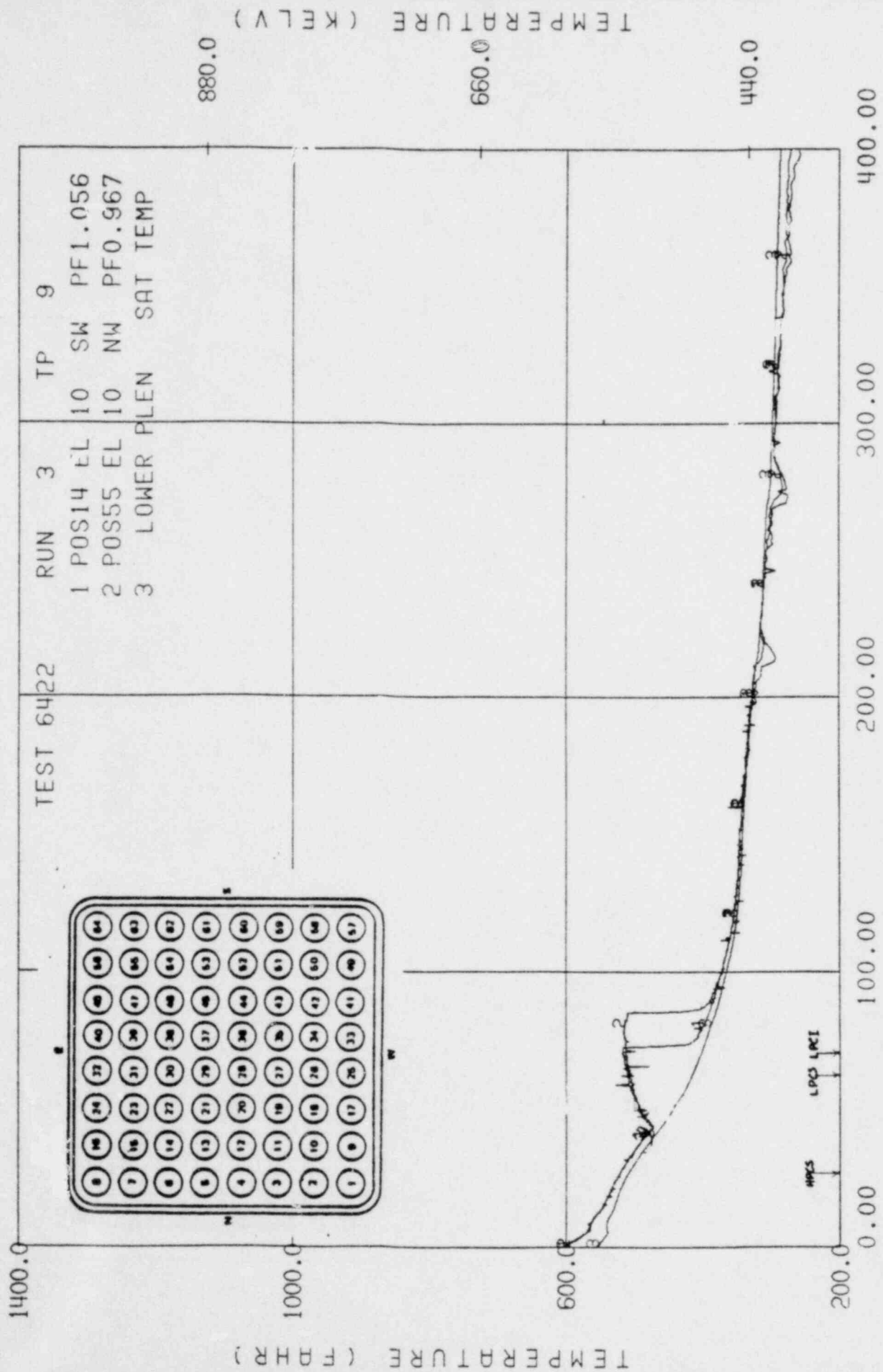
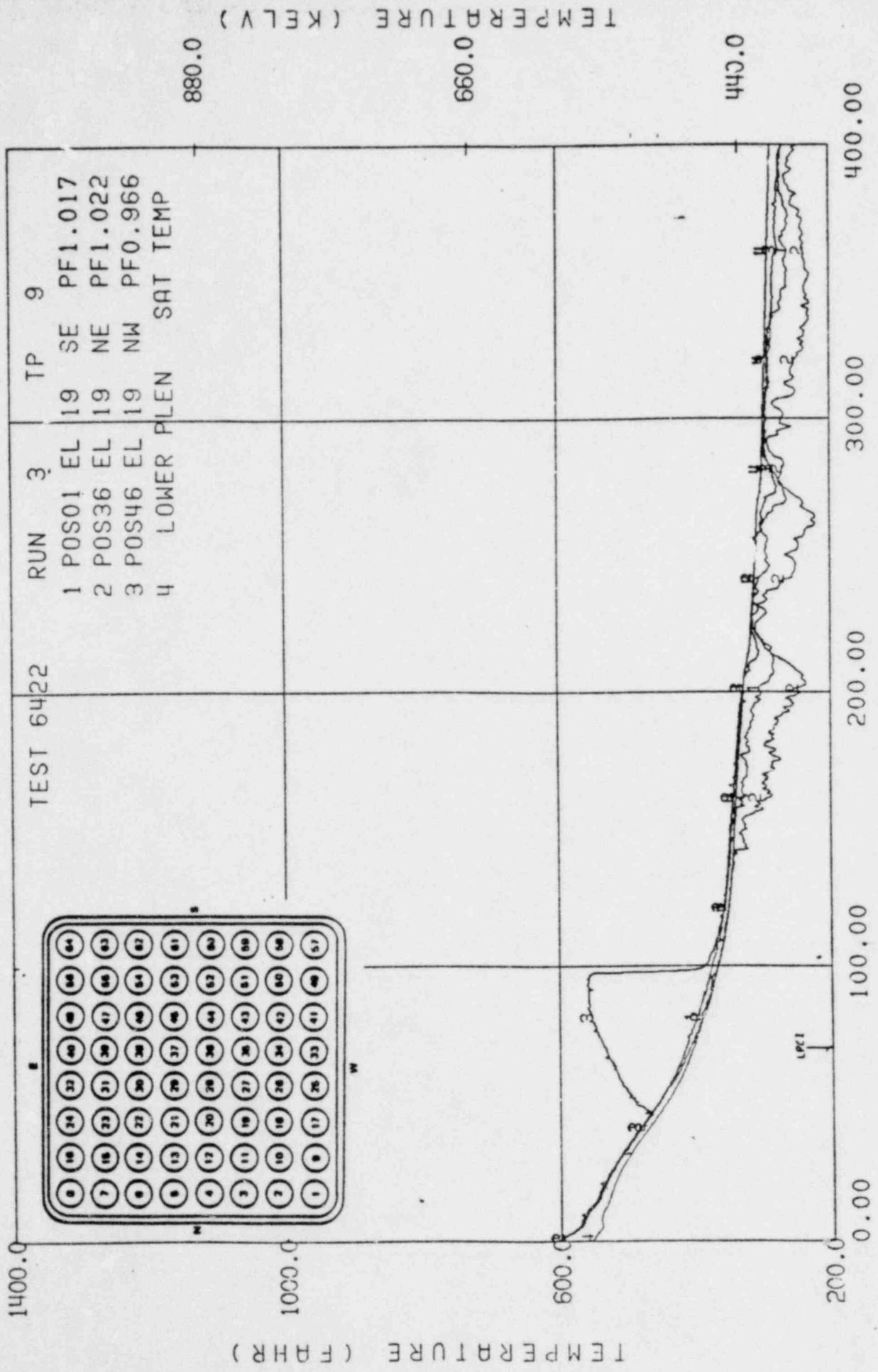


Figure 26



BD/ECC1A 5.05MW TLTASA



TIME (SECONDS)

Figure 27

BD/ECC1A 5.05MW TLTASA

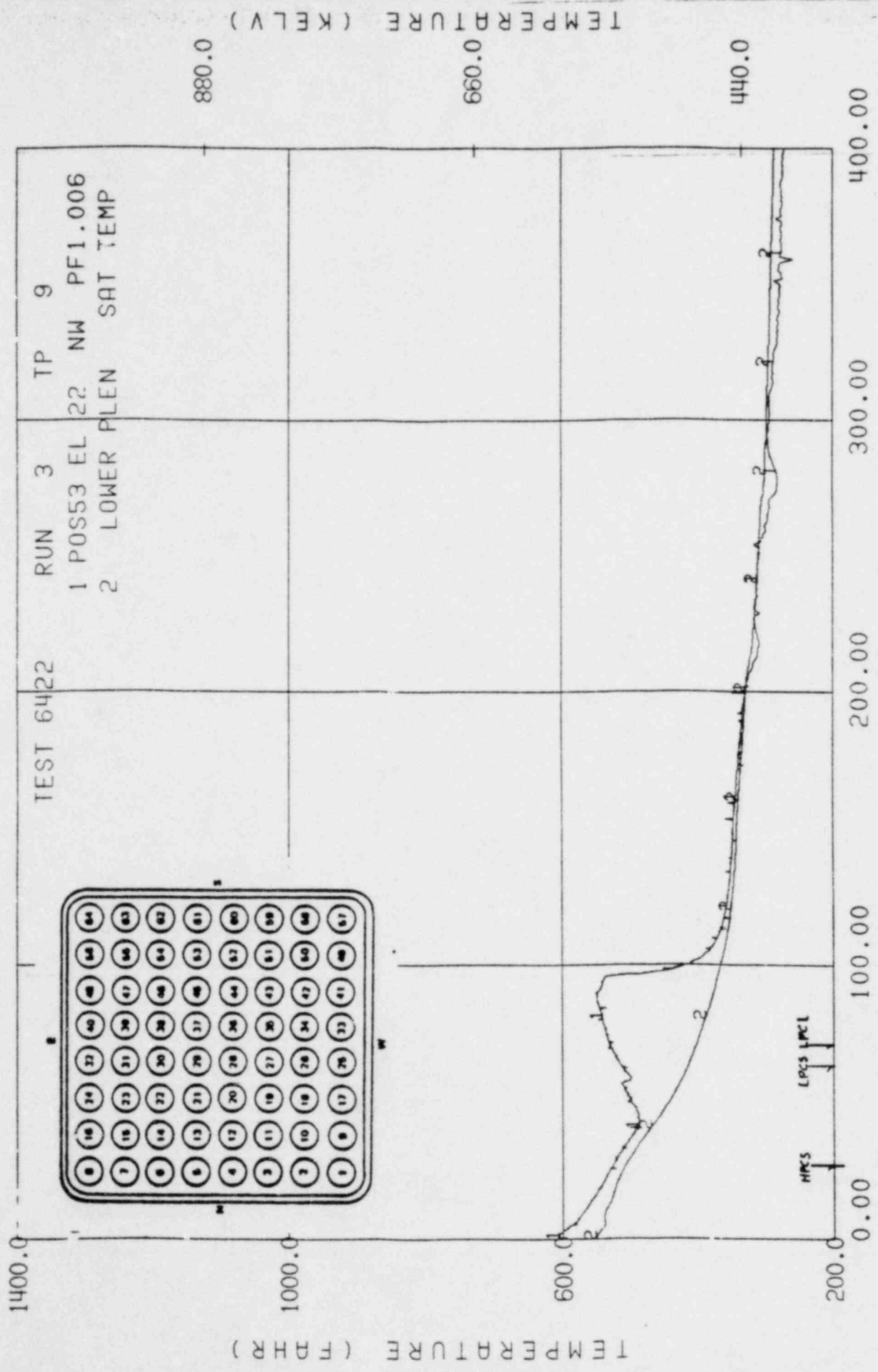


Figure 28

BD/ECC1A 5.05MW TLTA5A

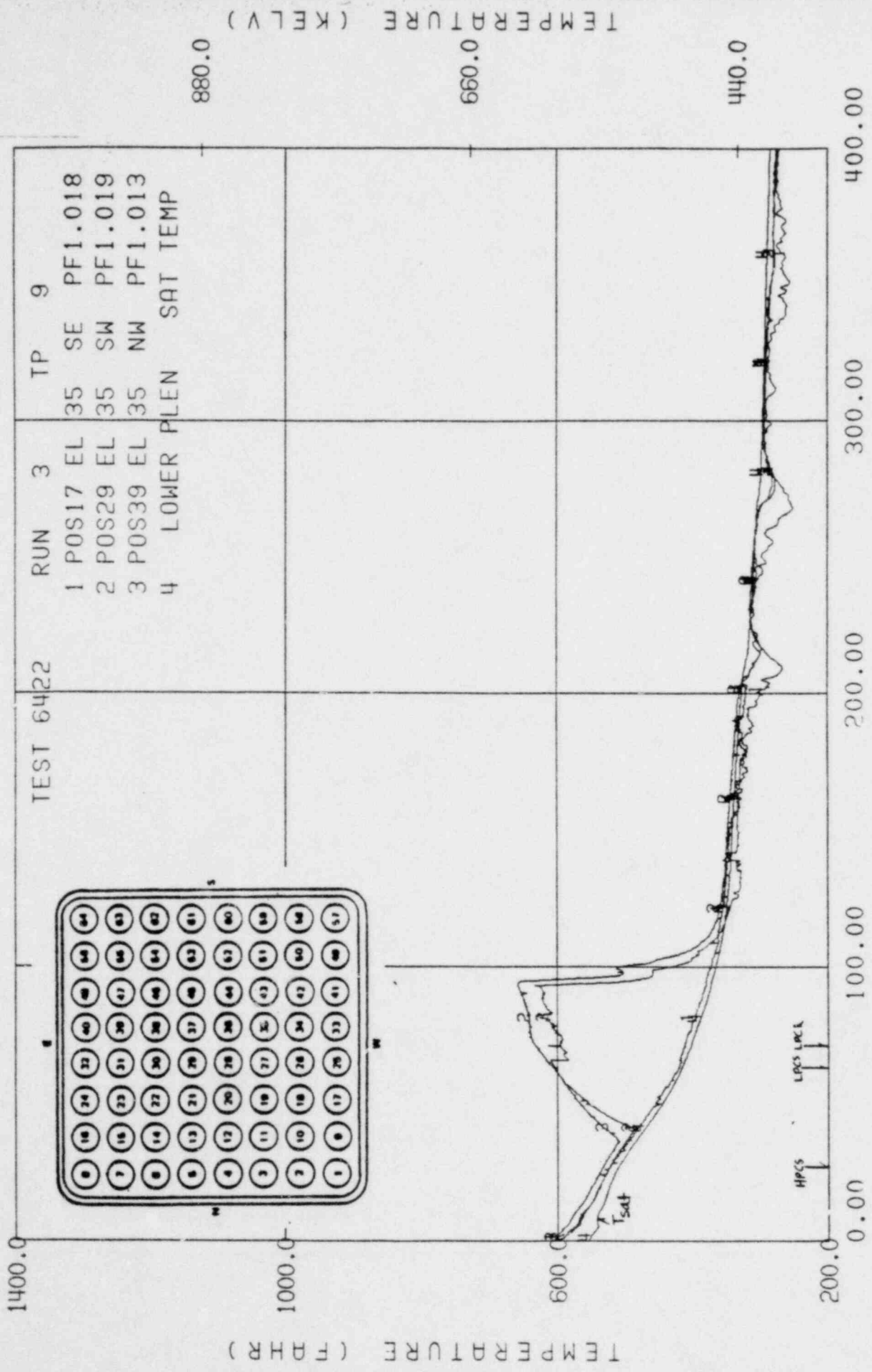


Figure 29

BD/ECC1A 5.05MW TLTA5A

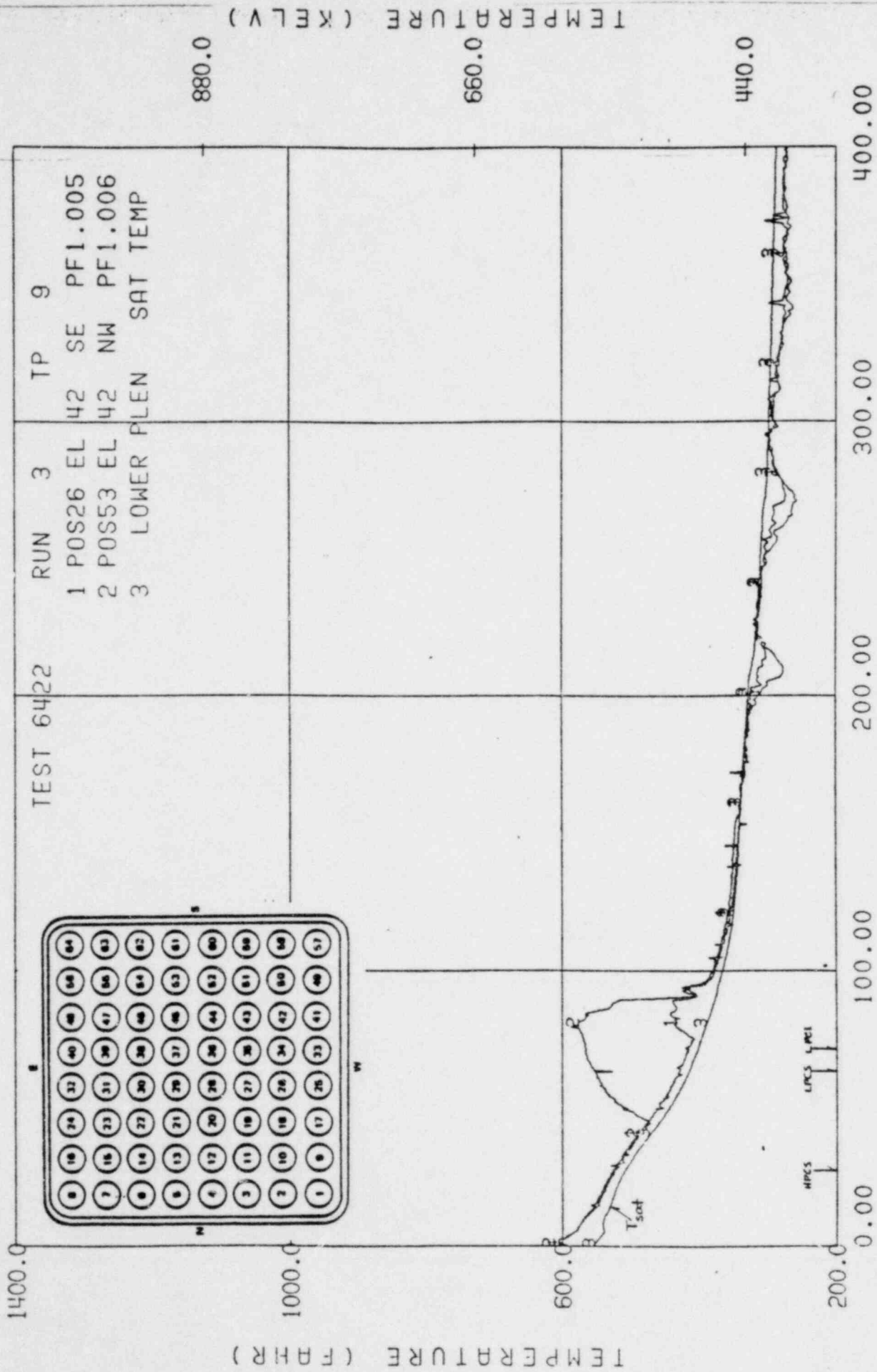


Figure 30

BD/ECC1A 5.05MW TLTAS5A

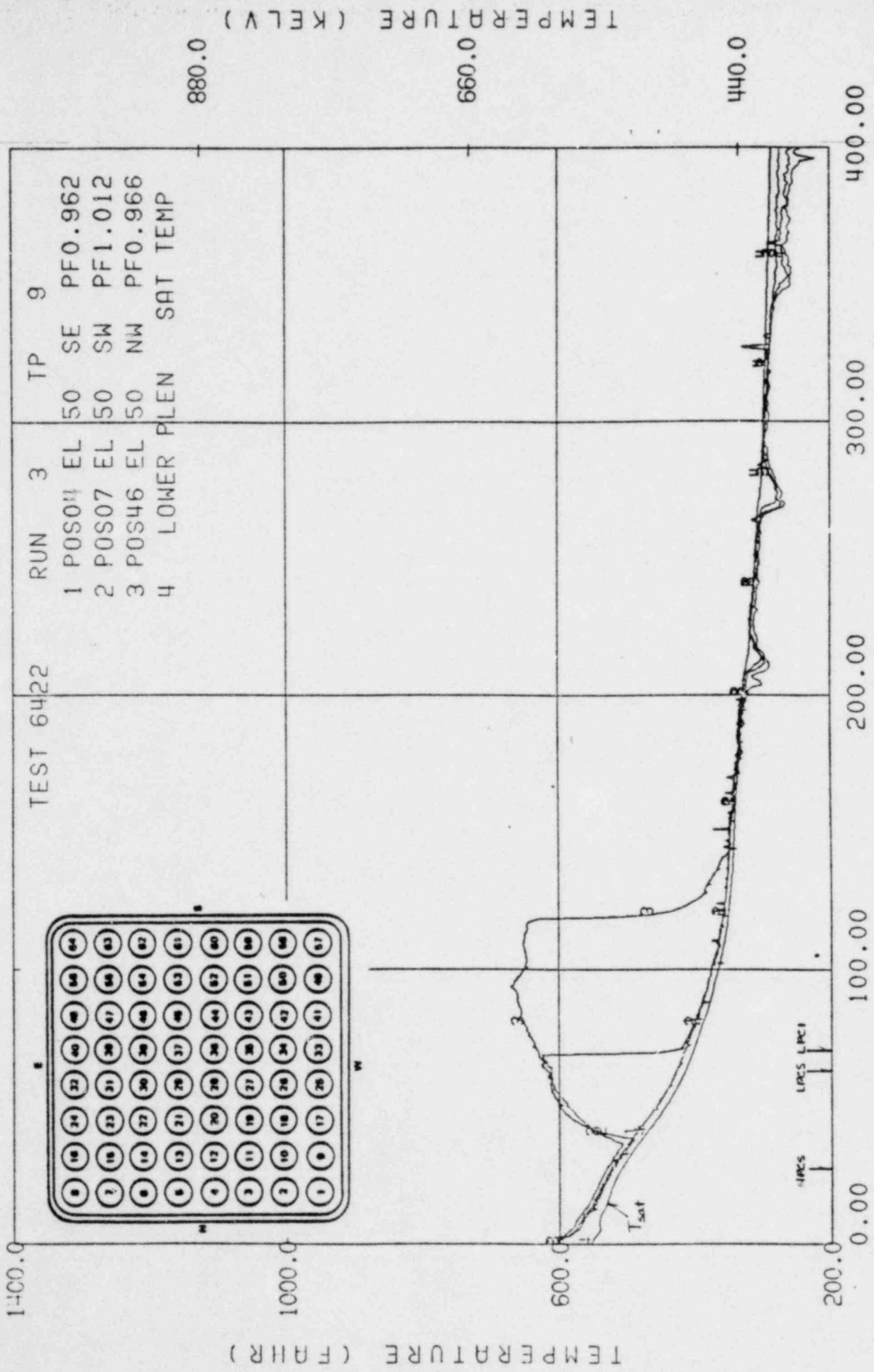
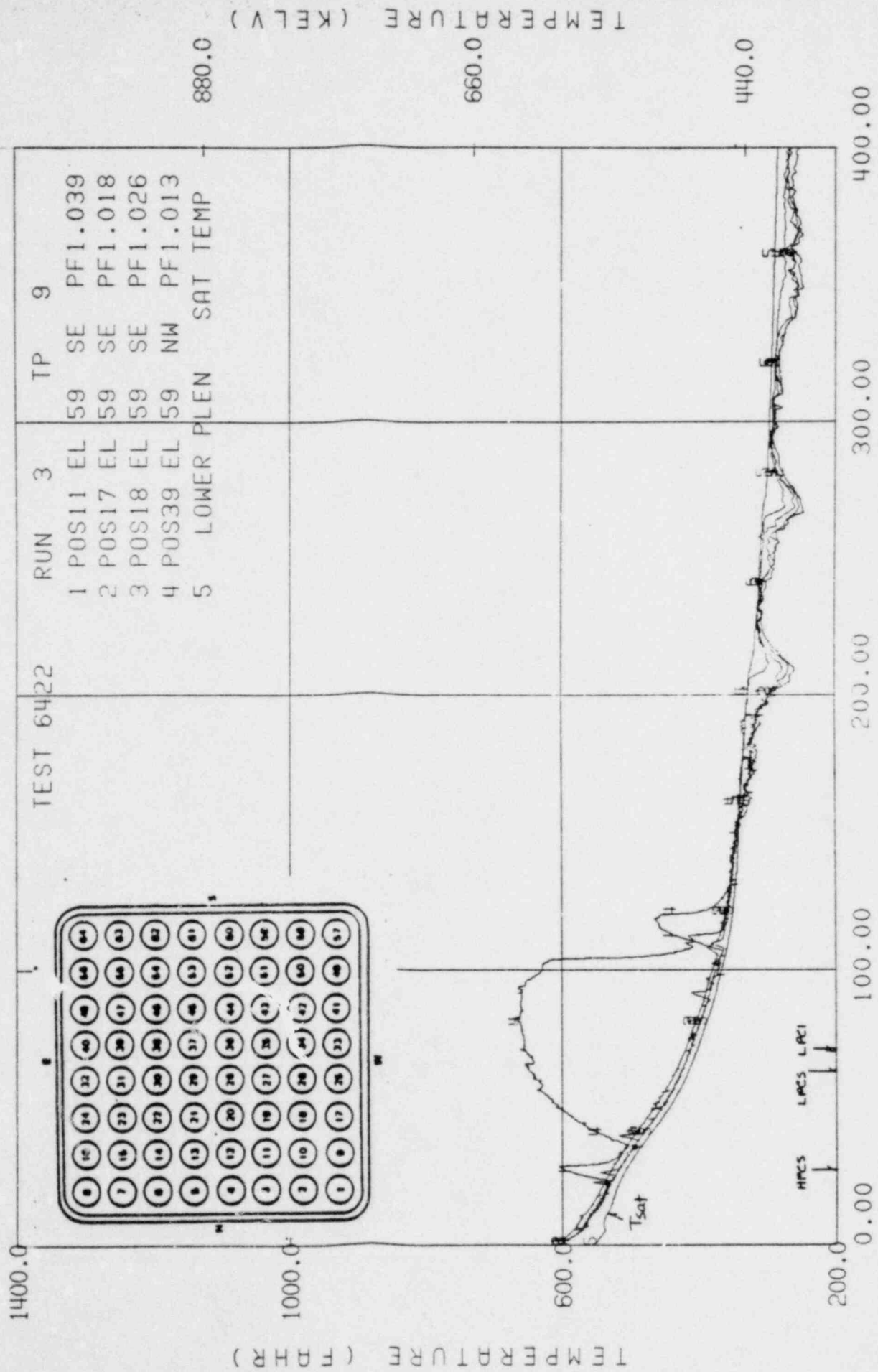


Figure 31

BD/ECC1A 5.05MW T1A5A



TIME (SECONDS)

Figure 32

BD/ECC1A 5.05MW TLTA5A

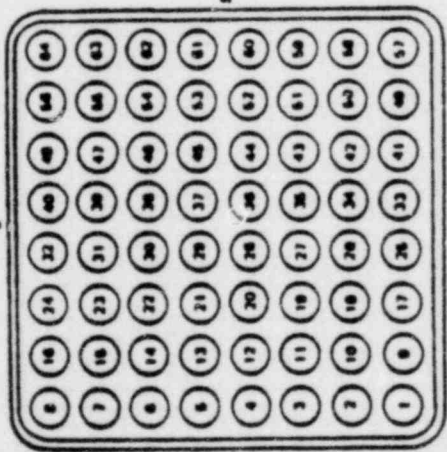
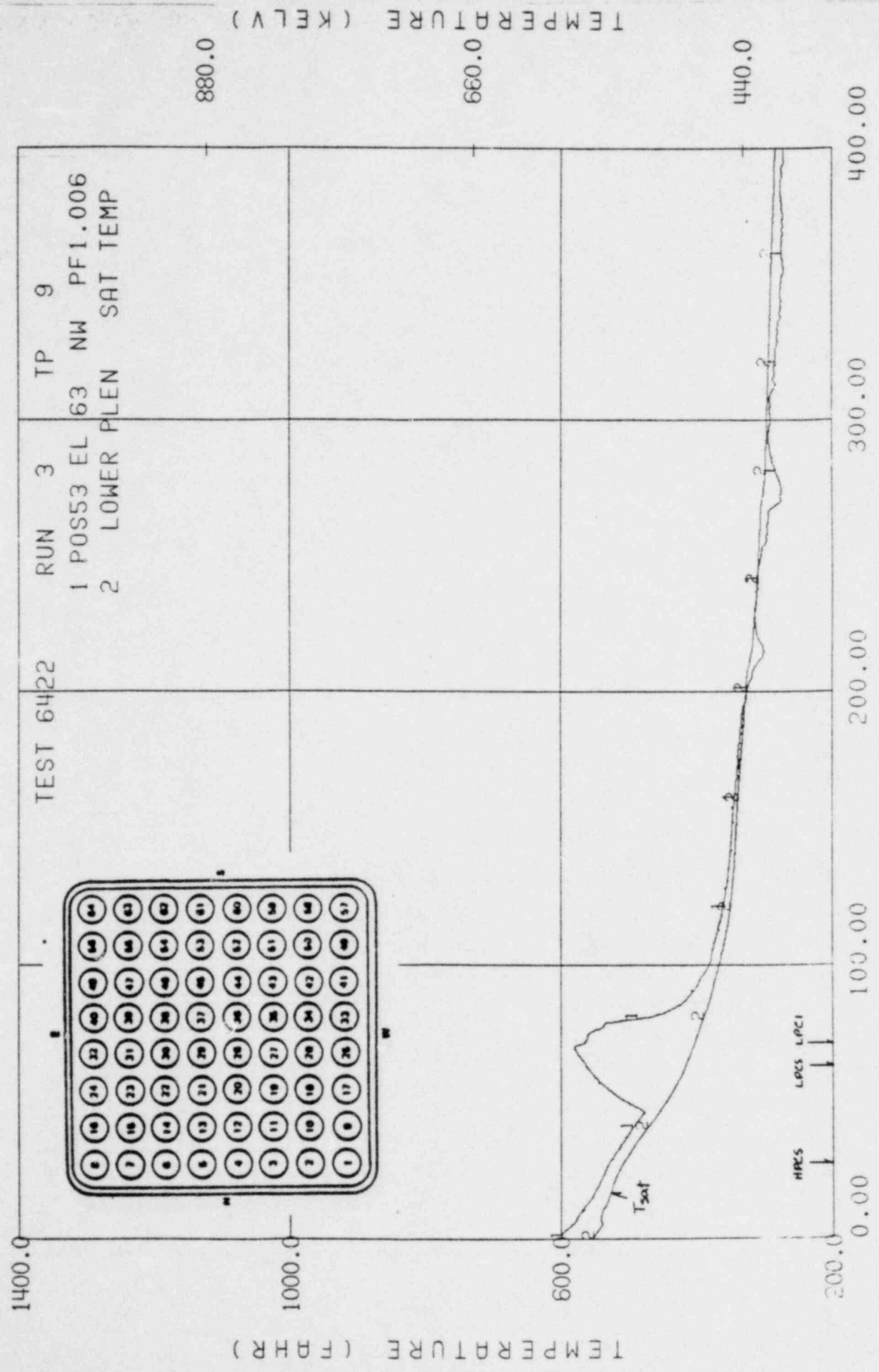
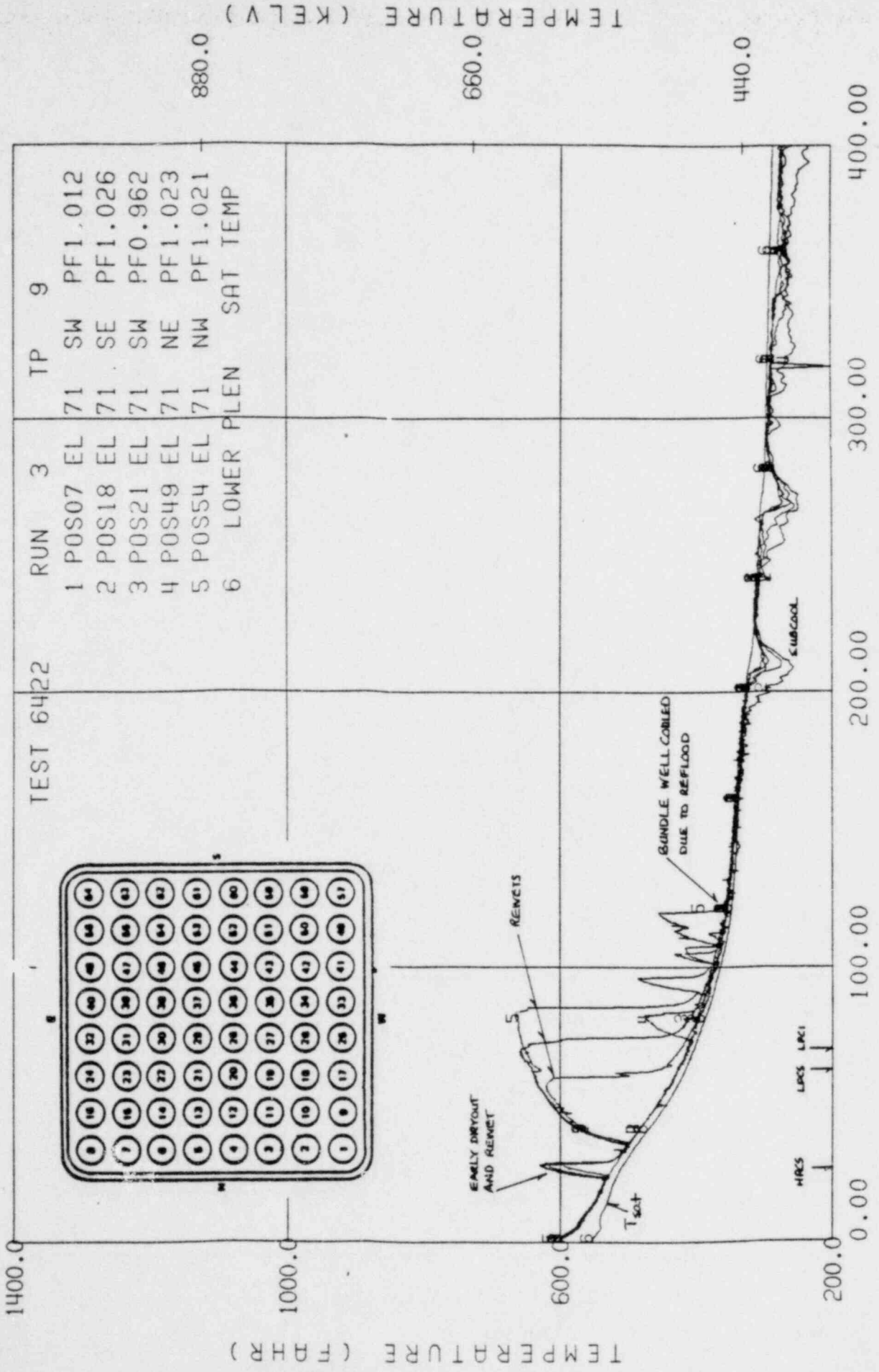


Figure 33

BD/ECC1A 5.05MW TLTA5A

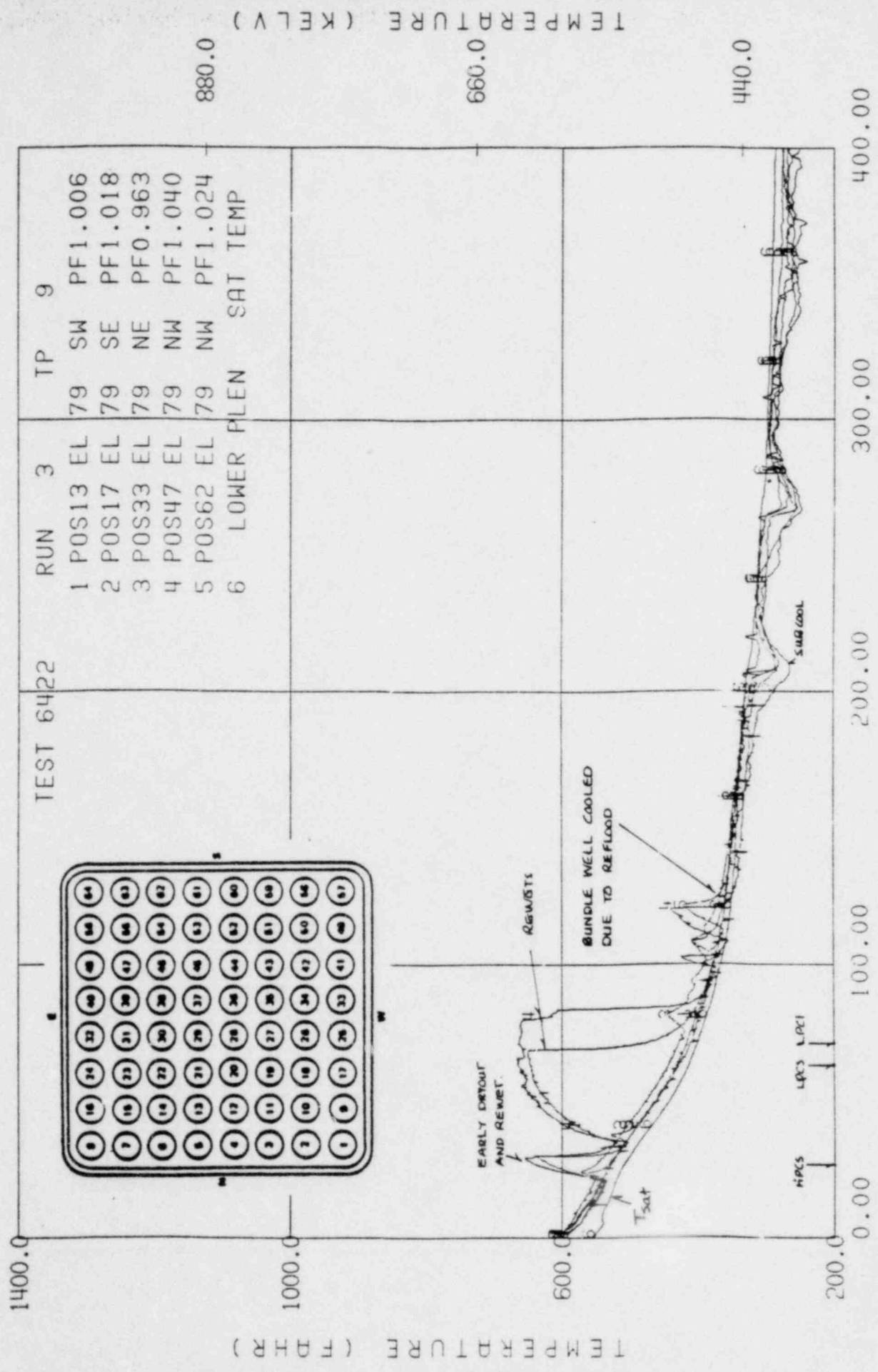


TIME (SECONDS)

Figure 34



BD/ECC1A 5.05MW TLTASA



TIME (SECONDS)

Figure 35

BD/ECC1A 5.05MW TLTA5A

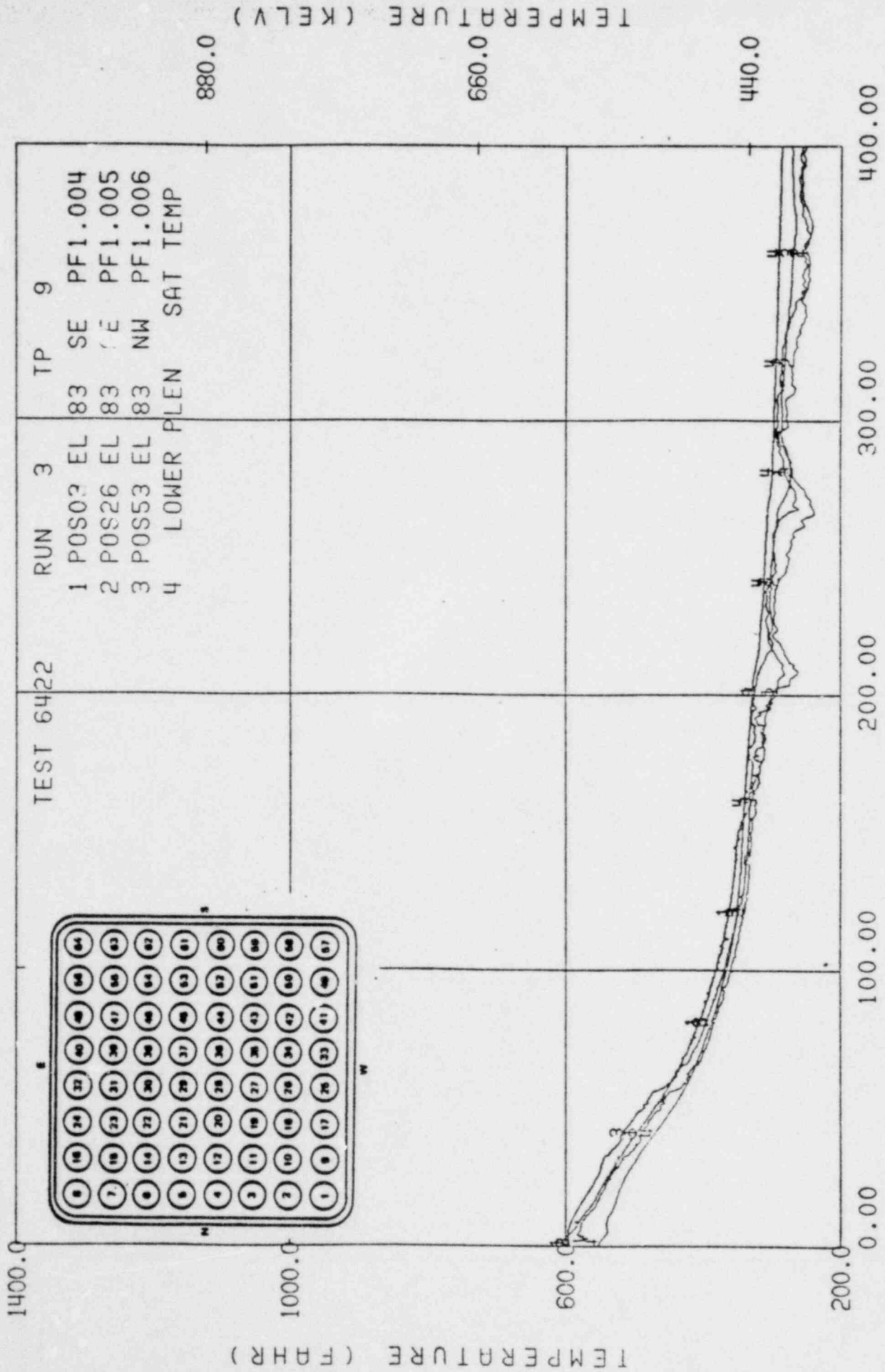
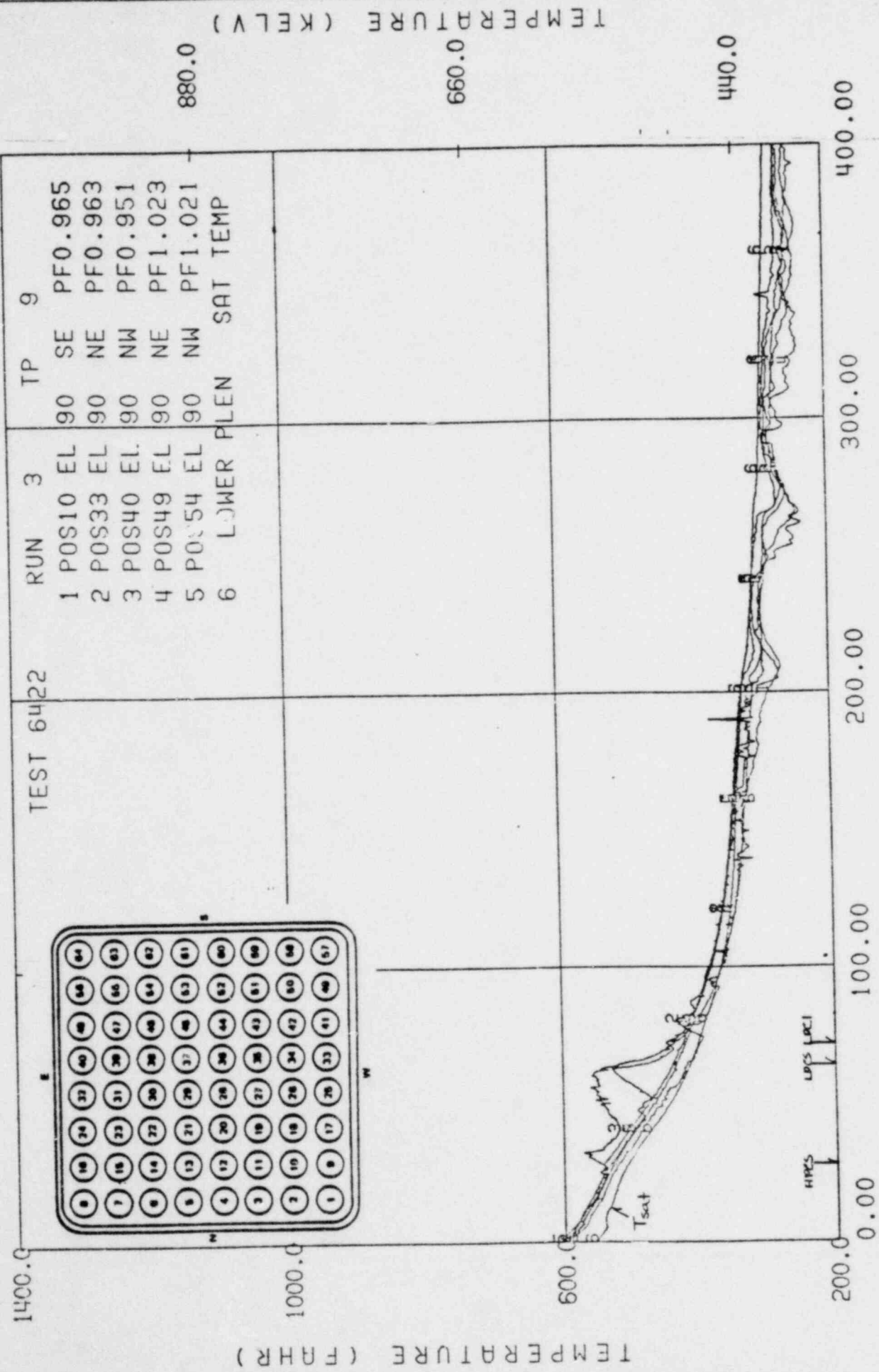


Figure 36

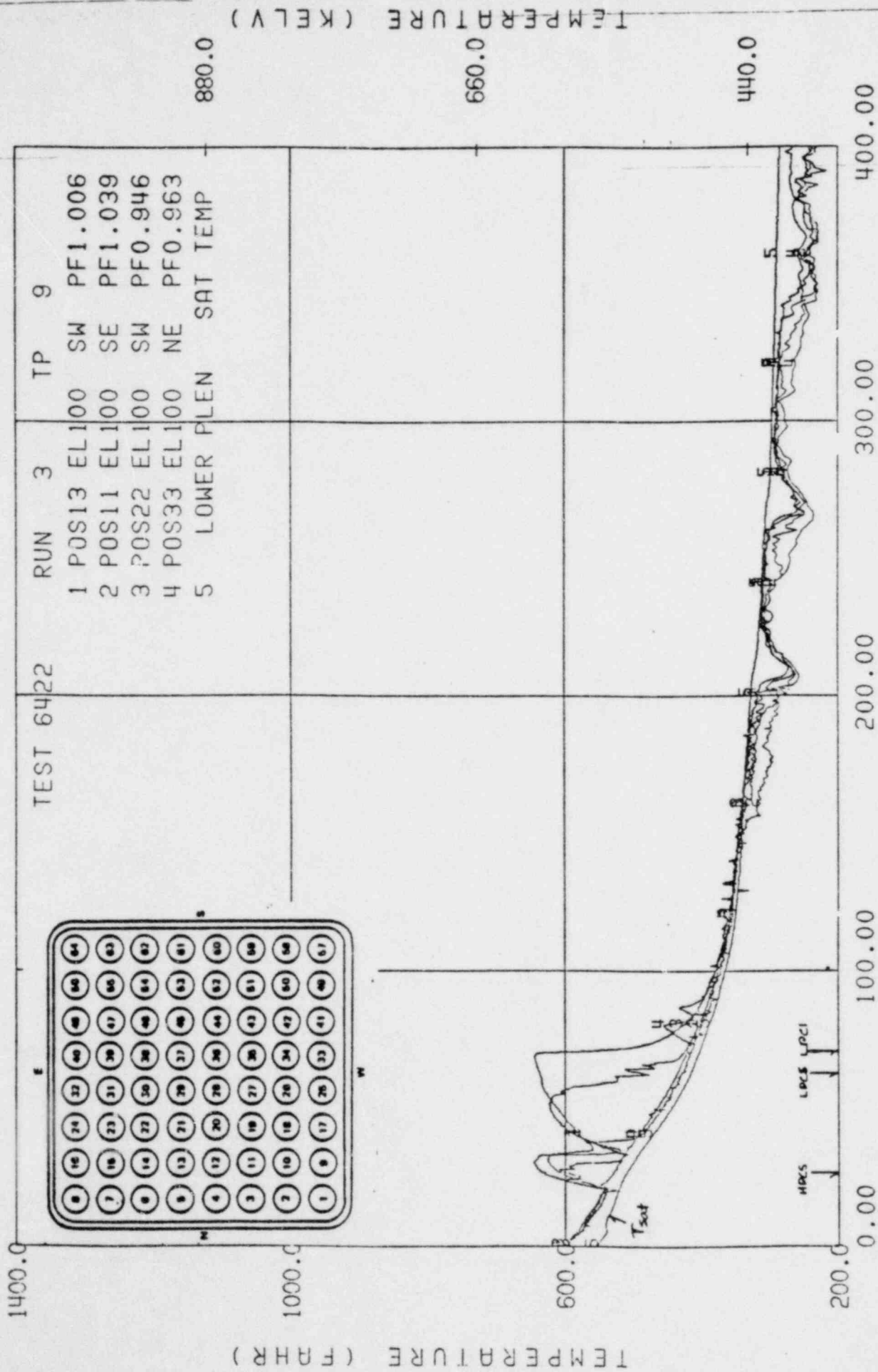
BD/ECCIA 5.05MW TLTA5A



TIME (SECONDS)

Figure 37

BD/ECC1A 5.05MW TLTA5A

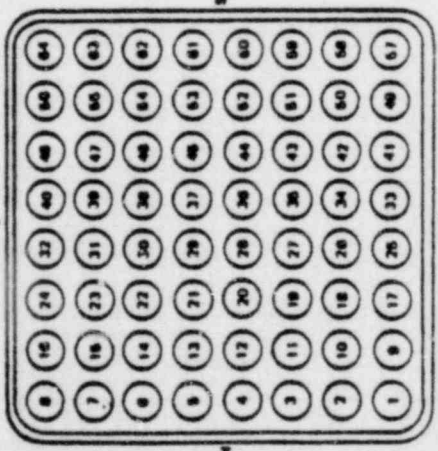


TEST 6422

RUN 3

TP 9

- 1 POS13 EL100 SW PF1.006
- 2 POS11 EL100 SE PF1.039
- 3 POS22 EL100 SW PF0.946
- 4 POS33 EL100 NE PF0.963
- 5 LOWER PLEN SAT TEMP



TIME (SECONDS)

Figure 38

BD/ECC1A 5.05MW TLTASA

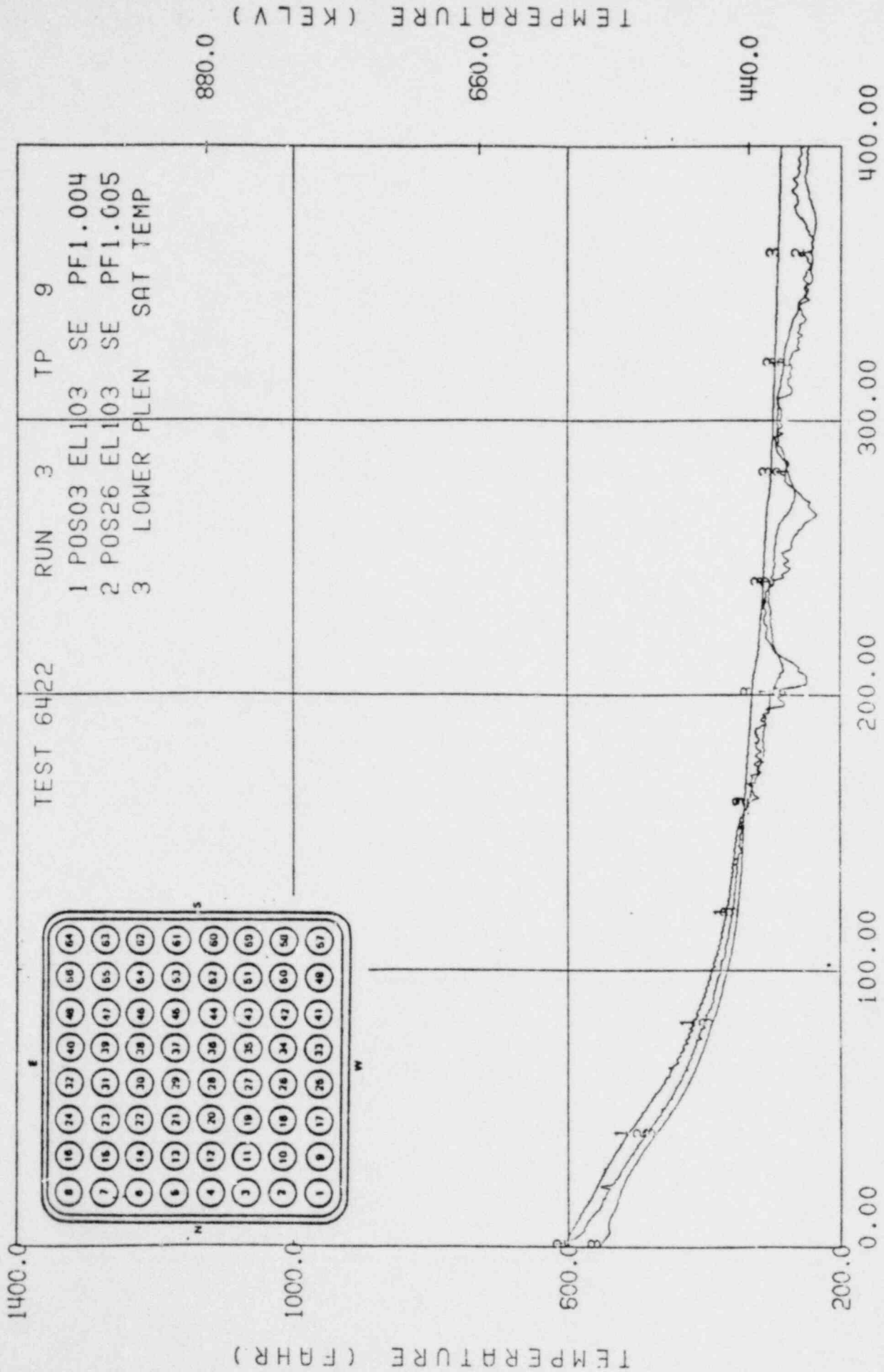


Figure 39

BD/ECC1A 5.05MW TLTA5A

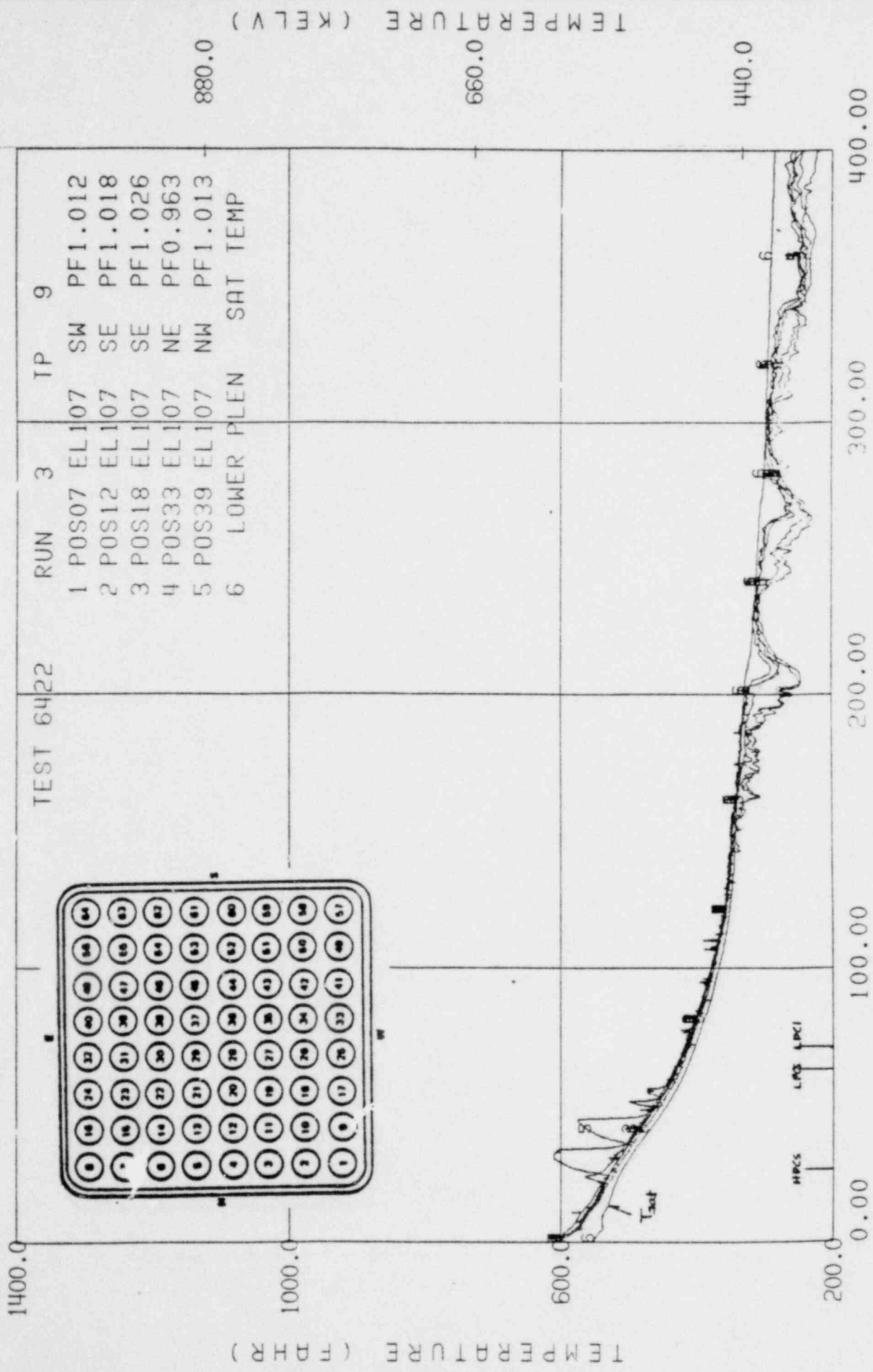


Figure 40

BD/ECC1A 5.05MW TLTAS5A

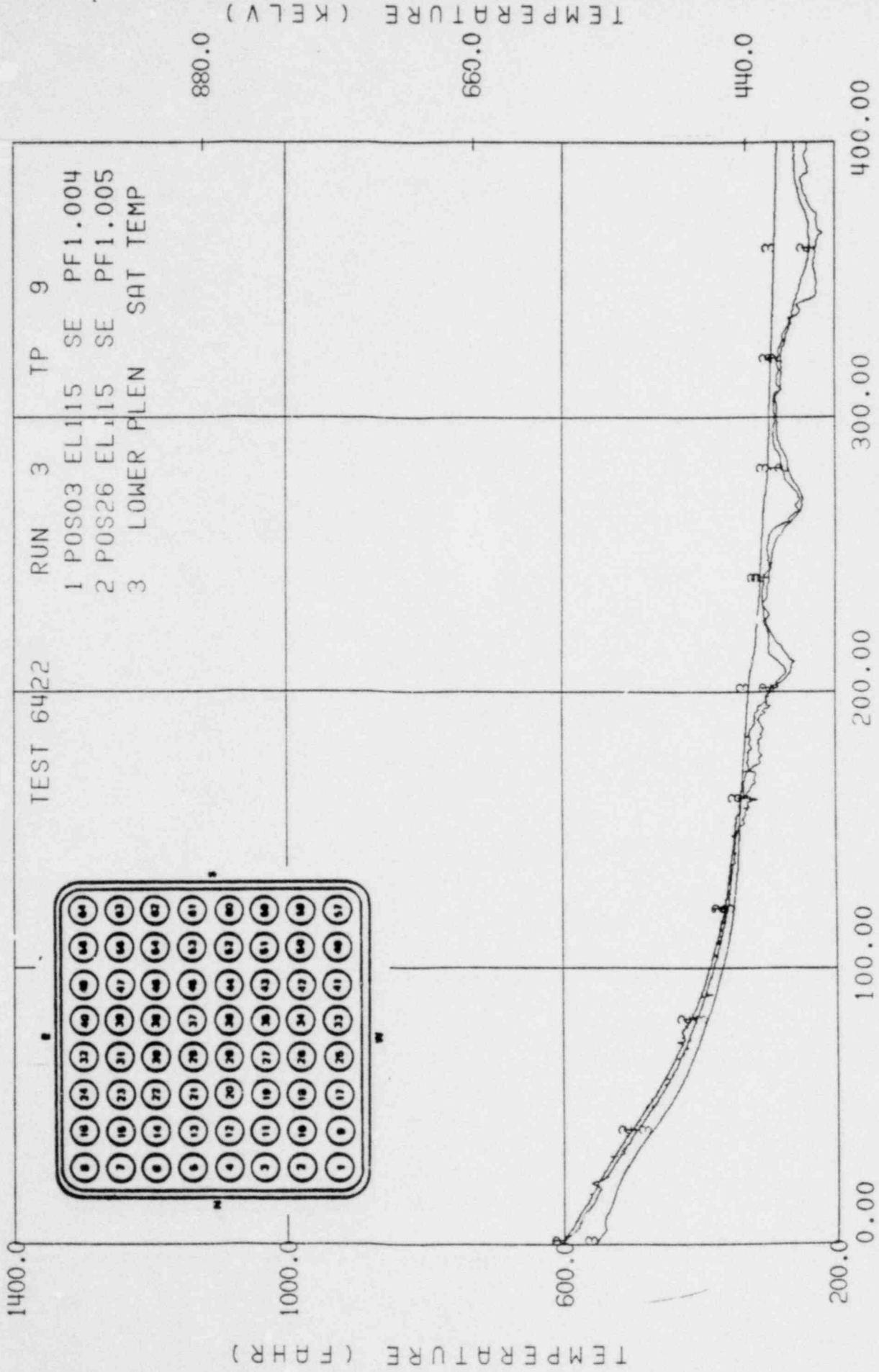
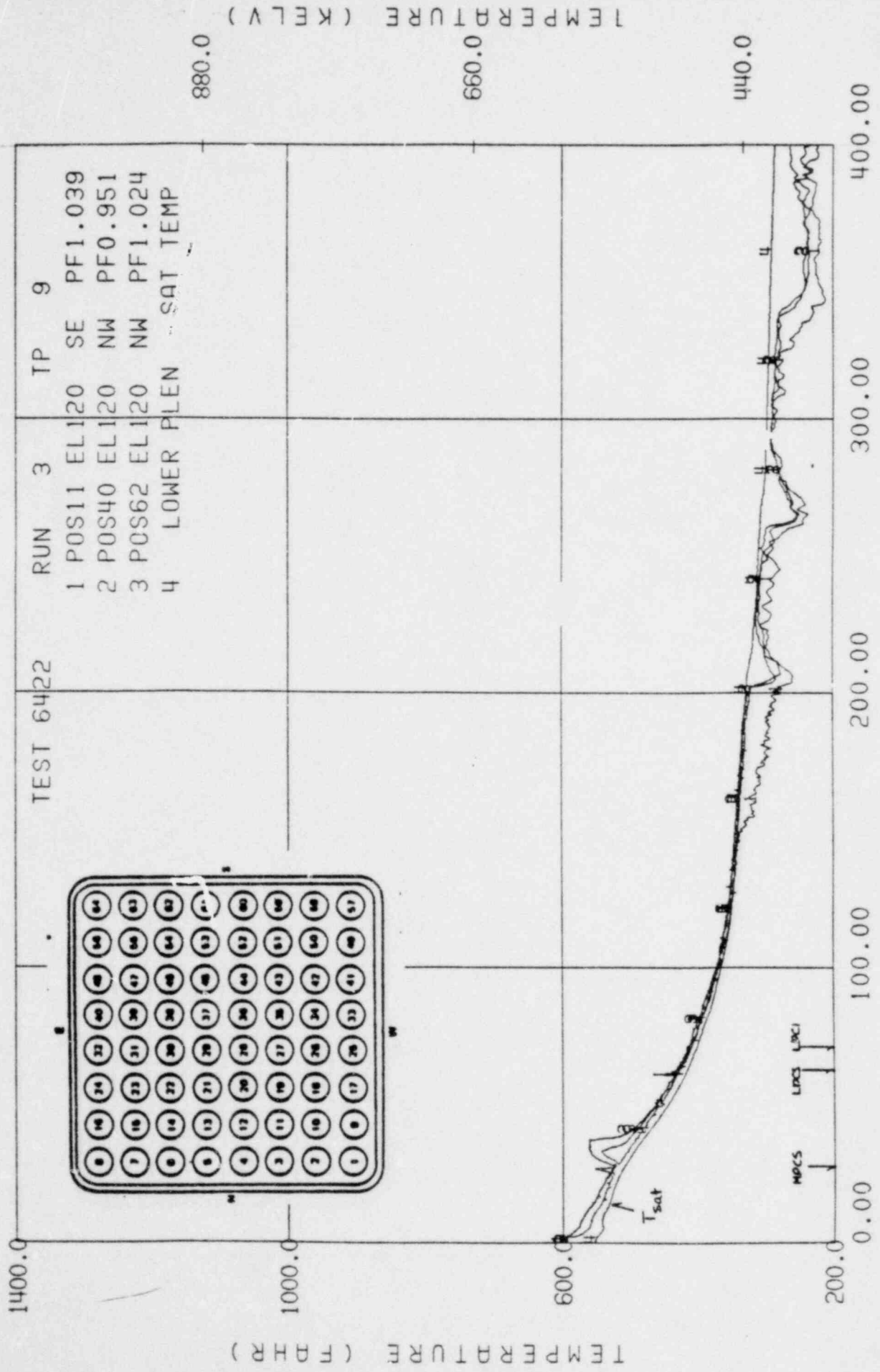


Figure 41

BD/ECC1A 5.05MW TLTASA

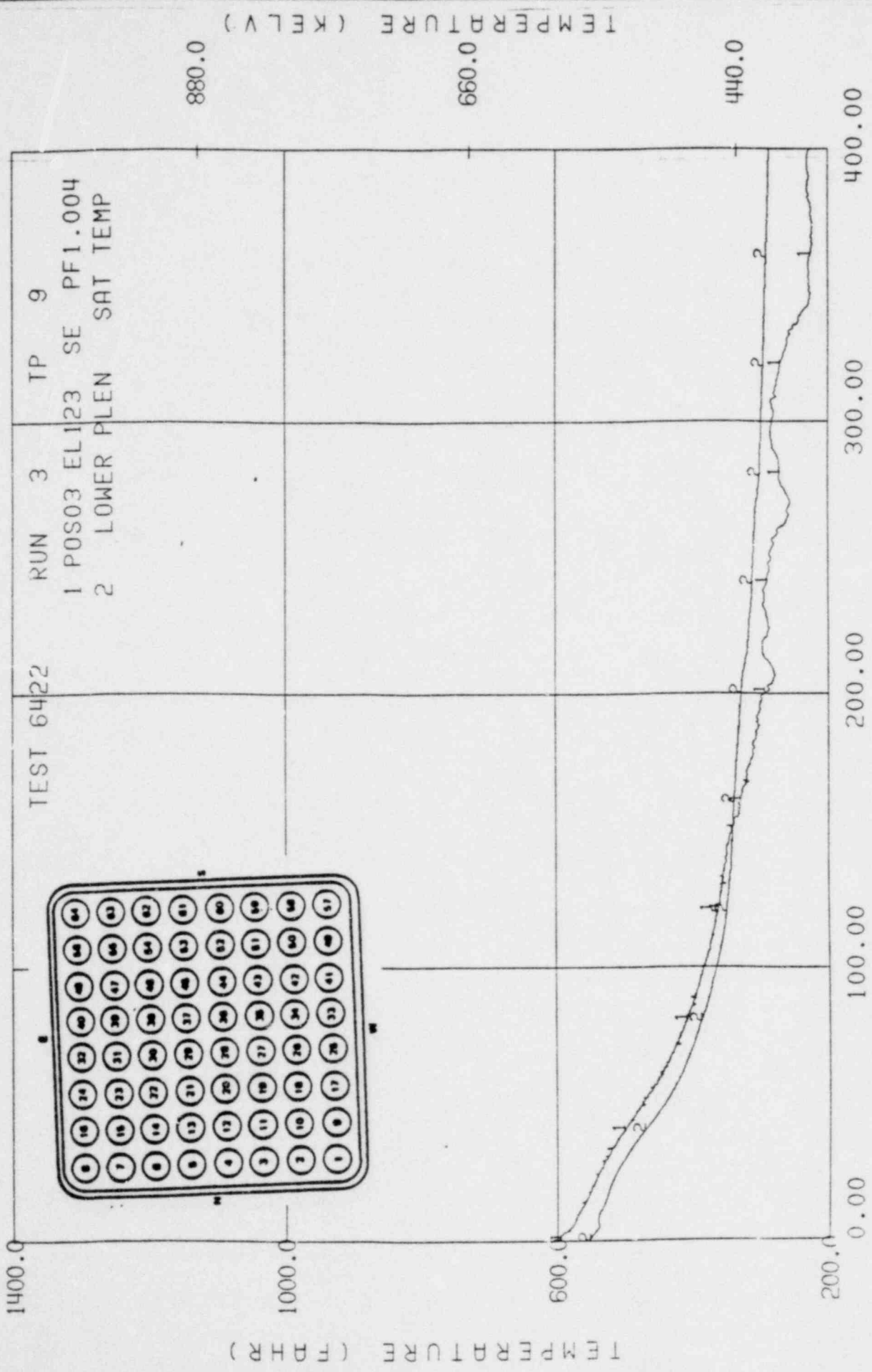


TIME (SECONDS)

Figure 42



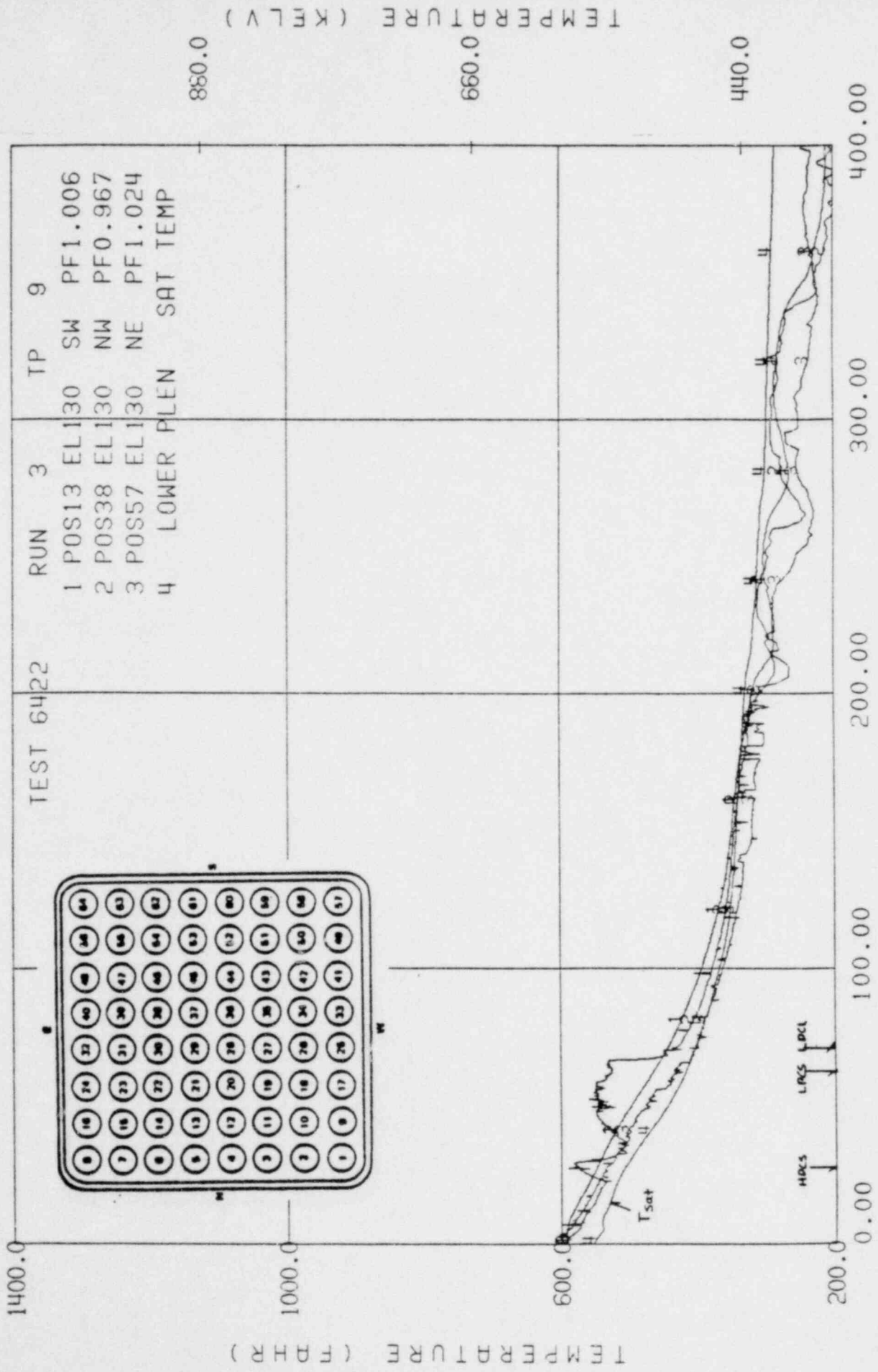
BD/ECC1A 5.05MW TLTA5A



TIME (SECONDS)

Figure 43

BD/ECC1A 5.05MW TLTASA



TIME (SECONDS)

Figure 44

BD/ECC1A 5.05MW TLTA5A

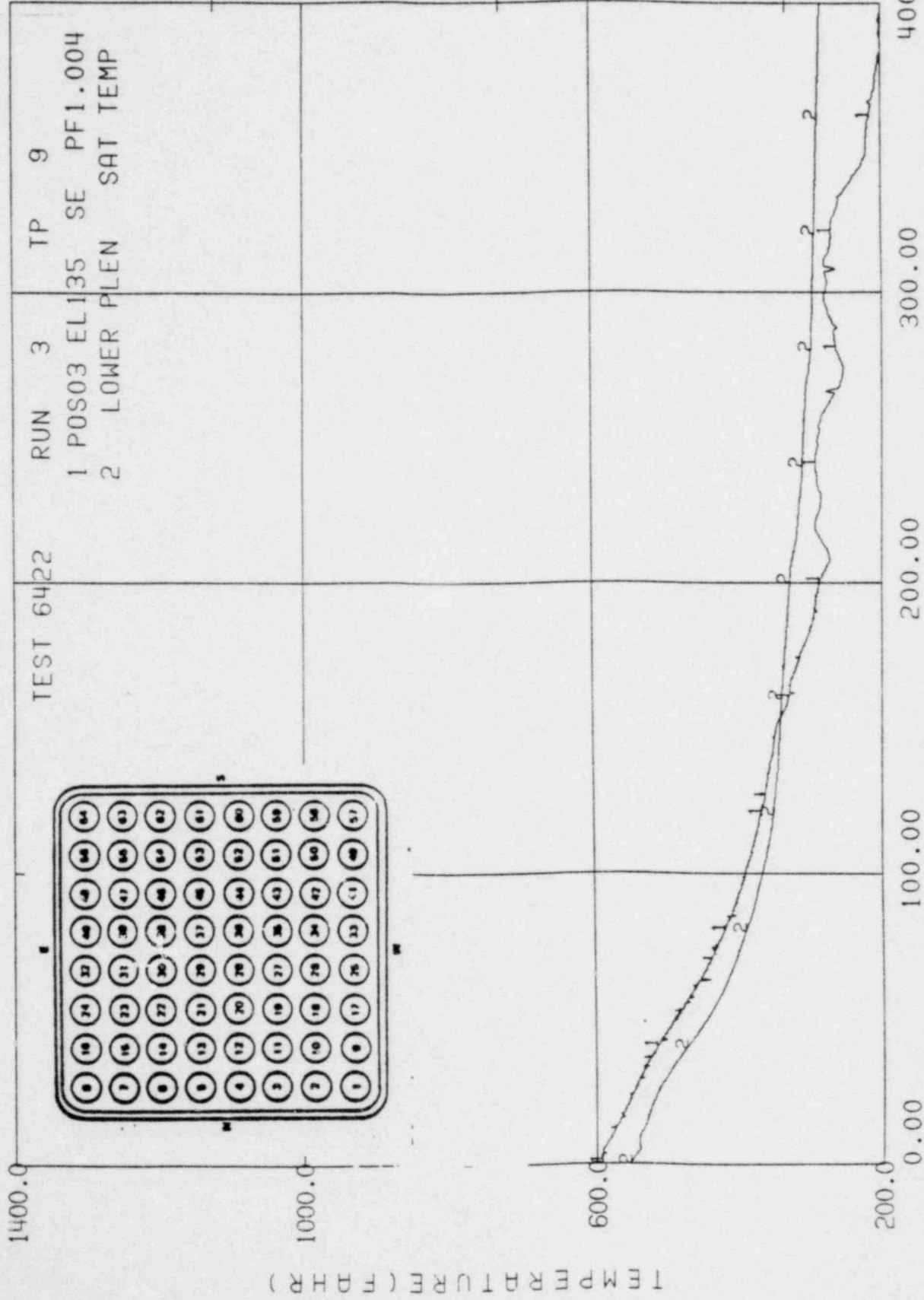


Figure 45

BD/ECC1A 5.05MW TLTA5A

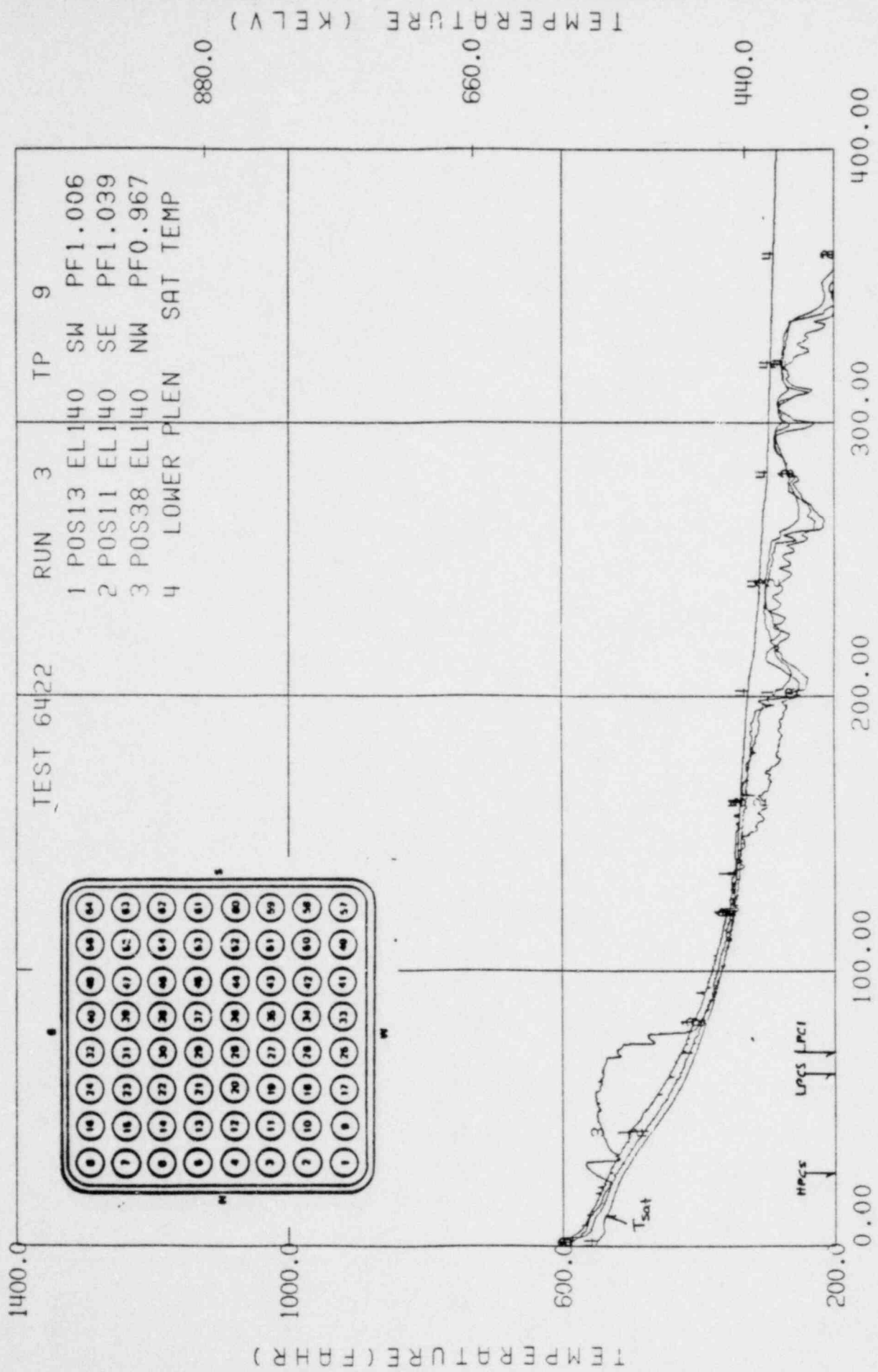


Figure 46

BD/ECC1A 5.05MW TLTA5A

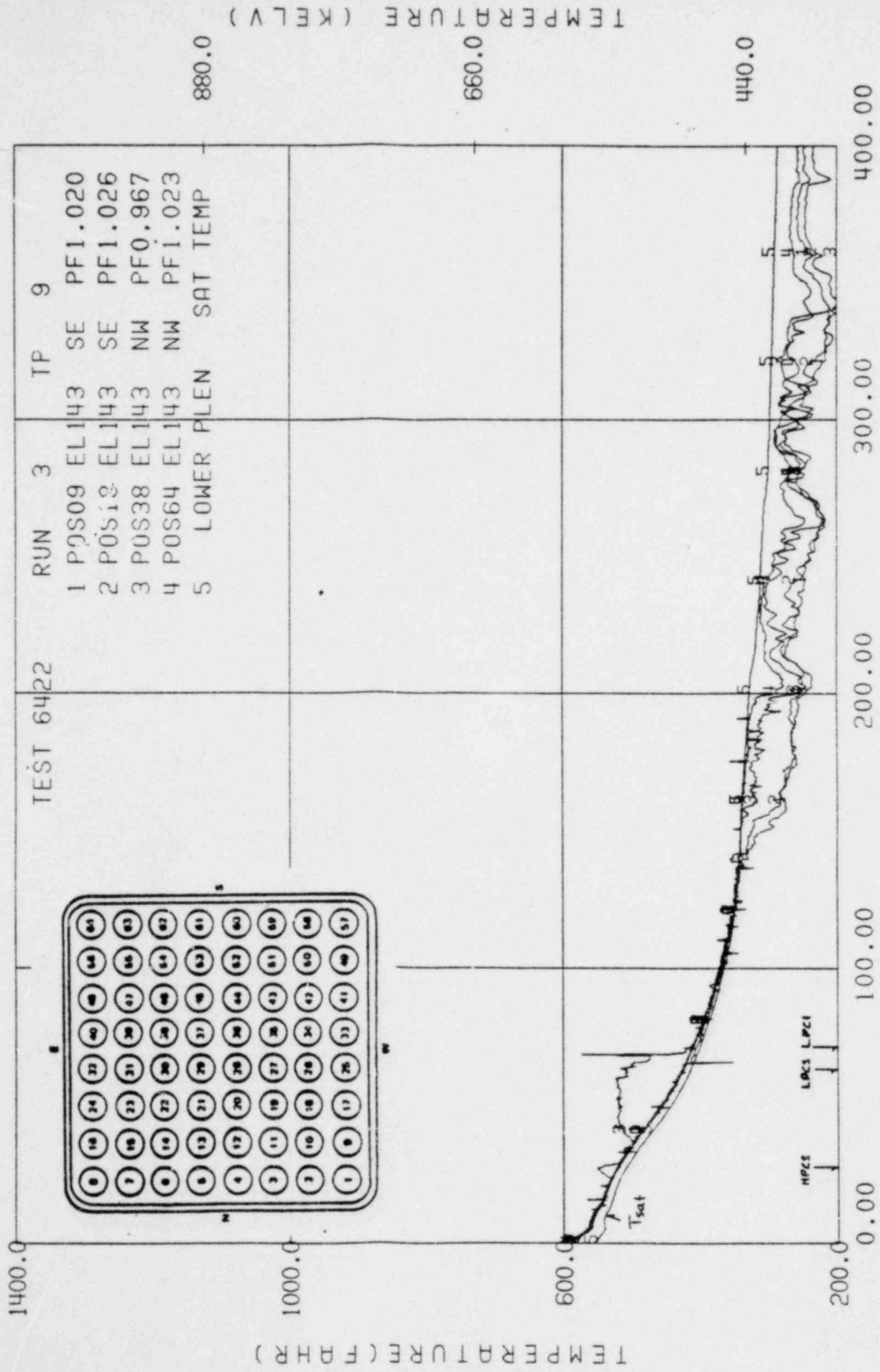
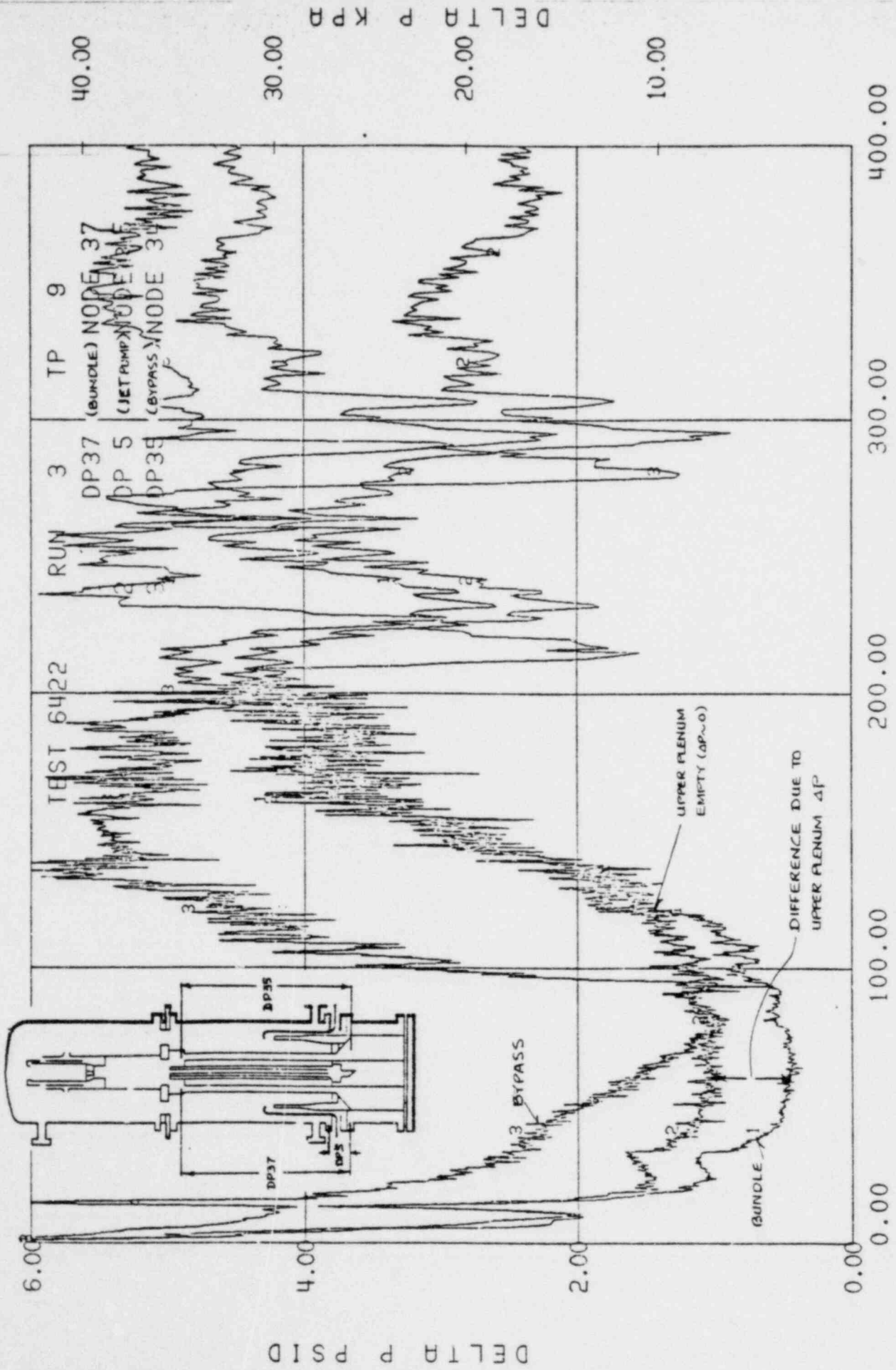


Figure 47

BD/ECC1A 5.05MW TLTA5A



TIME (SECONDS)

Figure A1, Parallel Path  $\Delta P$ 's

BD/ECC1A 5.05MW TLTASA

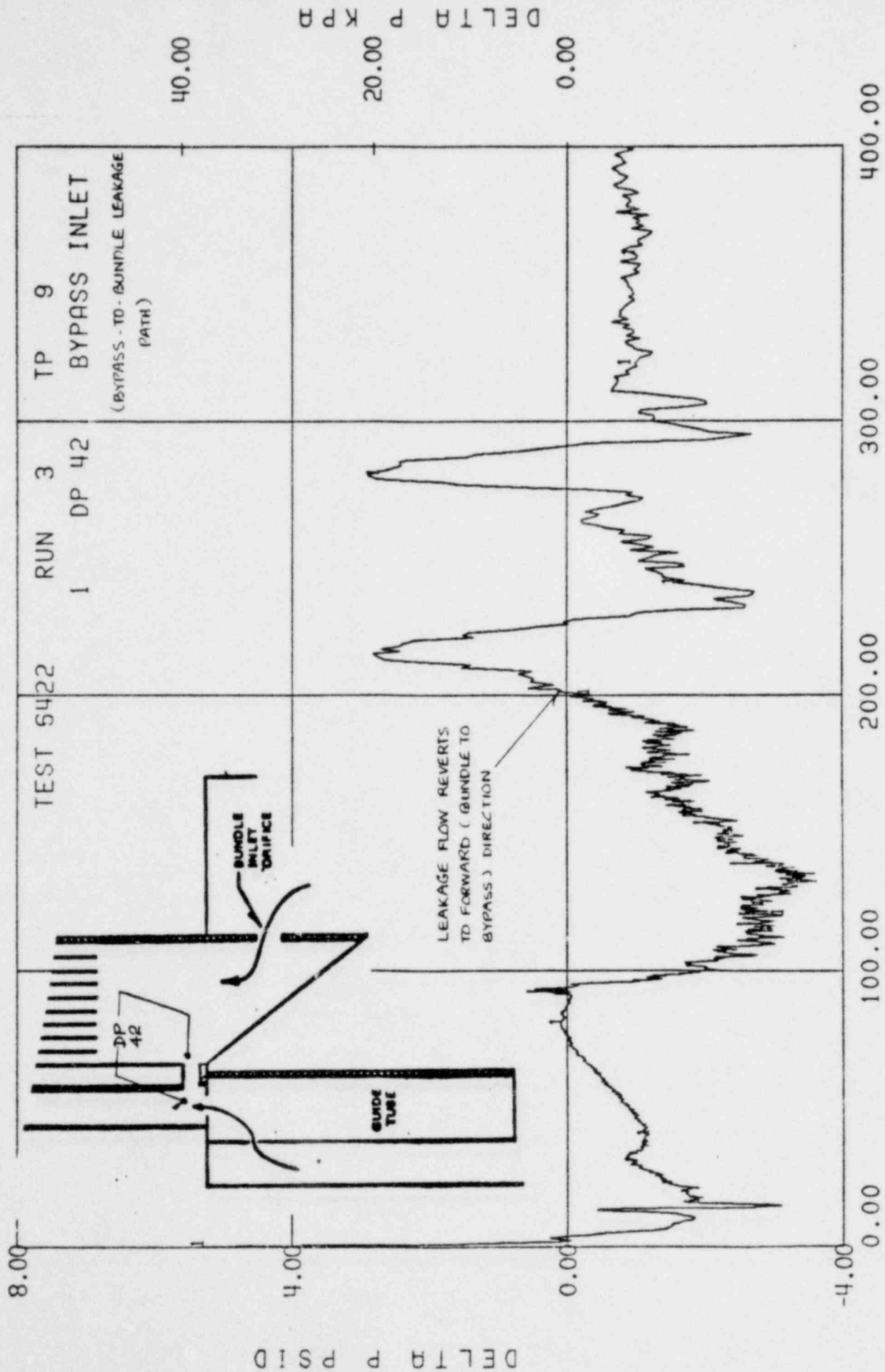
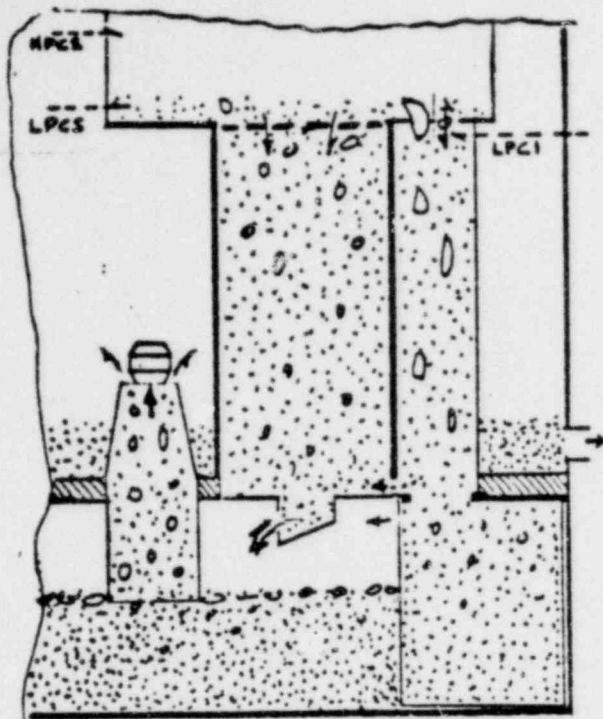
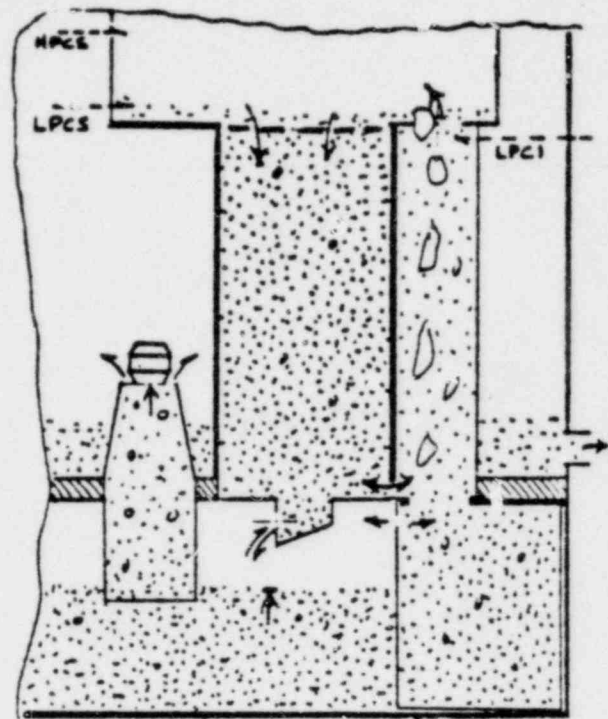


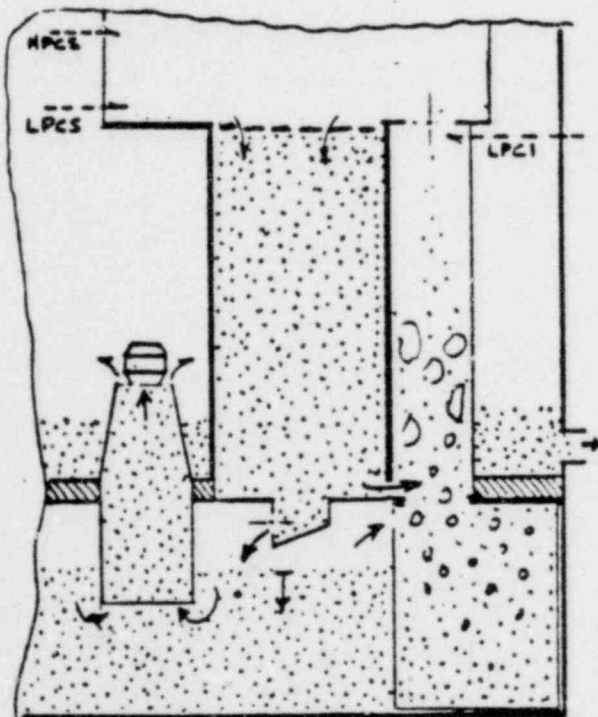
Figure A2, Leakage Flow  $\Delta P$ 's



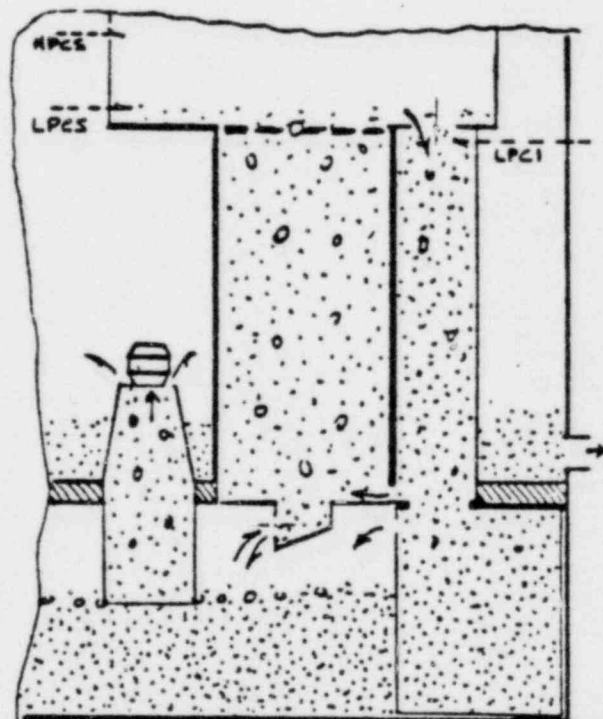
a. REFLOODED BUNDLE DIMINISHES  
LPCI DOWNFLOW



b. VAPOR NOT CONDENSED FLOWS UP  
PUSHING COLD FLUID TO BUNDLE



c. REVERTED LEAKAGE FLOW  
FACILITATES VAPOR VENTING

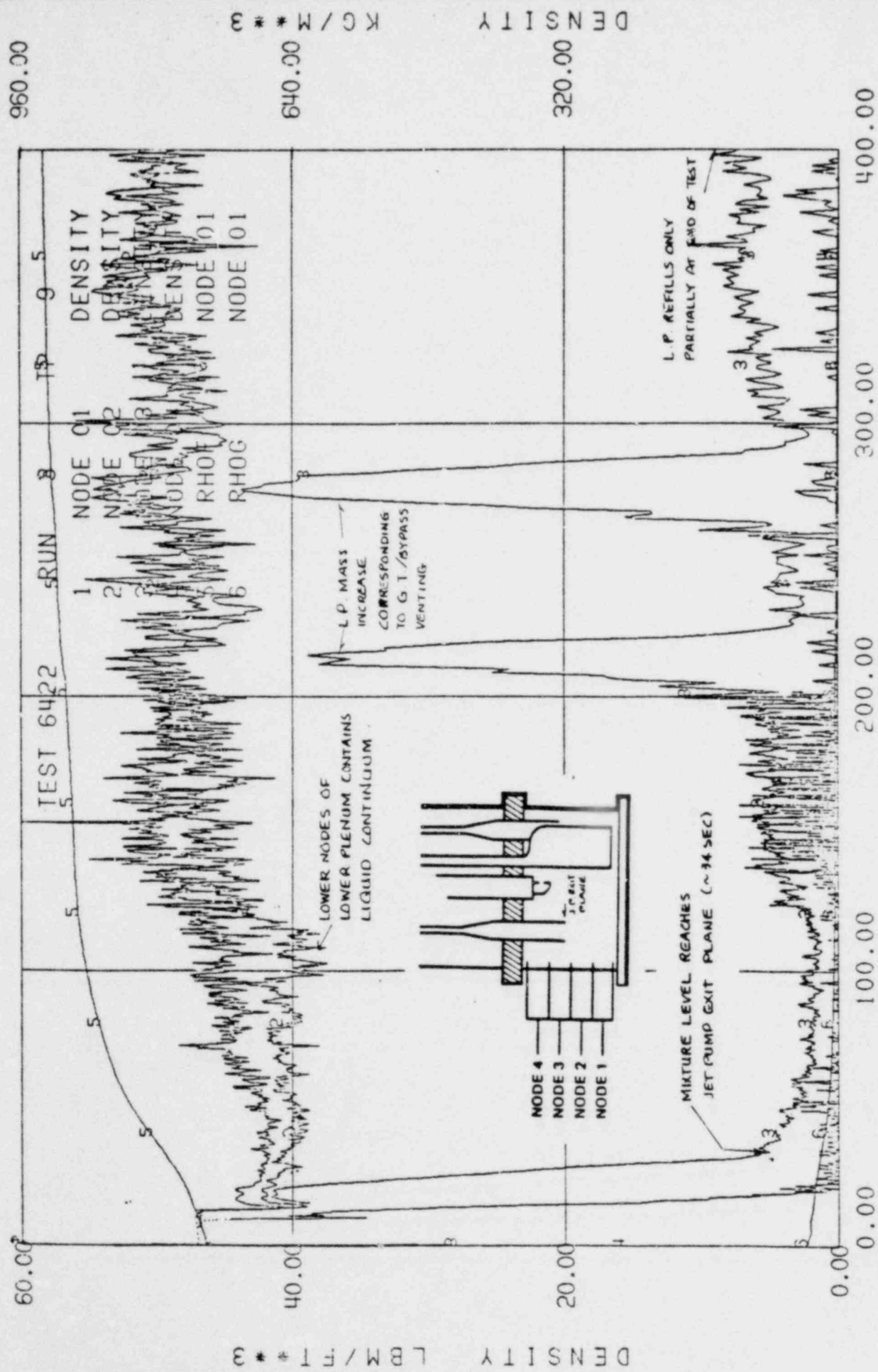


d. BYPASS REFILLS AFTER VAPOR  
VENTING.

Figure A3, Vapor Venting sequence in bypass; TLTA 5A Reference Test  
(6422 Run 3)



BD/ECCIA 5.05MW TLTA5A



TIME (SECONDS)

Figure A4, Lower Menum Nodal Densities

## APPENDIX B

### BUNDLE HEAT TRANSFER COEFFICIENTS & LOCAL CONDITIONS

An evaluation of local rod heat transfer coefficients at several locations in the 8x8 bundle will be completed. These evaluations will be carried out using rod temperature data from both BDHT (without ECC) and BD/ECC 1A tests (Table 1) with the 8x8 bundle. These evaluations will utilize a computational procedure solving transient heat conduction in direct (skin) heater rods with heat transfer to fluid at the outer surface.\*

The corresponding local fluid conditions including steam flow rates will be estimated on the basis of mass and energy conservation in the heater bundle. Such an estimation requires bundle inlet conditions and the latter will be derived from a mass energy balance in the lower plenum, accounting for counter current flow limitation at the core inlet. An upper and lower bound for these estimates will be established. It is anticipated that this work will be completed by the end of July. Table 1 is a list of tests, rod bundle position numbers and elevations at which these calculations will be made.

---

\* Determination of Transient Heat Transfer Coefficients and the Resultant Surface Heat Flux from Internal Temperature Measurements, (GEAP-20731, January, 1975).

TABLE 1  
ROD TEMPERATURE DATA POINTS

<u>TEST</u>	<u>POSITION</u>	<u>ELEVATION</u>
6423	18	71"
6421	18	71"
6423	47	79"
6422	47	79"
6421	47	79"
6423	22	100"
6422	22	100"
6421	22	100"

## APPENDIX C

### TLTA SMALL BREAK TEST NO. II

W.S. HWANG

MAY, 1980

#### Introduction

The second small break test was conducted in the Two Loop Test Apparatus (TLTA). The objectives of the test were to investigate the thermal hydraulic performance of the TLTA with a small break under a degraded ECC systems condition and to provide a data base from which to judge the adequacy of the models and assumptions used in the BWR small break analysis method. Relevant background information related to the test can be found in Reference 1. This report presents a summary of the test results.

#### Test Basis

The scaling basis for the facility and the test is the BWR/6-218. The current TLTA configuration is designated TLTA 5C (Figure 1) and is described in detail in References 2 & 3.

#### Test Execution

The second small break test, 6432/R1, was conducted on March 5, 1980. The major initial conditions for the test were met (Table 1). Based on the comparisons between measured and specified initial test conditions, this test was deemed acceptable.

#### Test Results

The system pressure response is shown in Figure 2. In the early transient the steam line valve was used to automatically control the system pressure at about 970 psia as specified. Flow discharged through the steam line is shown in Figure 3. The system pressure began to increase after the steamline closed completely at 166 seconds and then decreased rapidly due to the large steam discharge (Figure 3) as ADS opened at 286 seconds. The depressurization led to LPCS and !PCI injections at about 435 seconds (Figures 4 & 5).

Figure 6 shows the bundle power applied in the test. Mixture levels measured in various regions are shown in Figures 7 & 8. In the early transient, the upper plenum level remained near the top of the separator, while the annulus

level response was governed mainly by the pressure transient and loss of mass inventory out of the break (Figure 9). The level swell of both inside and outside levels beyond 286 seconds was due to the rapid depressurization as ADS was activated. It can be seen that shortly after ECC injection began the levels began to increase, indicating mass accumulation in the system (Figures 10 through 16).

A mixture level was observed in the lower plenum and bypass after ADS activated (Figure 7), even though the bundle was full of two-phase mixture. Figure 17 shows the fluid density in the bundle. The steam generation that accompanied the large depressurization from ADS initiation led to the occurrence of counter current flow limiting (CCFL) at the side entry orifice (SEO) and the top of the bypass. Figure 18 shows the density distribution in the lower plenum and clearly shows that the two-phase mixture level was well below the core inlet. The density in the bypass (Figure 19) shows that node 14 was only partially filled during the period of 286 to about 465 seconds. The CCFL at the SEO prevented the bundle mass inventory (Figure 12) from draining into the lower plenum (Figure 13) and contributed to the cooling in the bundle. This effect is clearly seen in Figures 20 and 21 which show no bundle heatup with the rod cladding remaining well cooled throughout the transient.

The accumulation of subcooled ECC fluid in the bypass and eventually in the core region led to significant subcooling of the fluid in the bundle as indicated by the subcooled fluid density (Figure 17) and the subcooled temperature (Figures 20 and 21) measured on the bundle cladding at ~600 seconds.

### Conclusion

The second small break test was conducted successfully in the TL1A. The test procedure and approach developed to overcome scaling compromises and facility limitation proved to be adequate.

The test results indicate the CCFL at the side entry orifice at the bundle inlet affects the system behavior particularly after ADS is activated. This CCFL prevents the bundle mass from draining into the lower plenum and hence improves cooling in the bundle. No rod heatup has been observed during the entire test.

## References

1. Letter, R.H. Buchholz (GE), to T.D. Keenan (BWR Owner's Group) to D.F. Ross (NRC), "Verification of Small Break Analysis Model", November 30, 1979.
2. G.W. Burnette to W.D. Beckner (NRC) and P. Kalra (EPRI), "Basis and Conditions for T<sub>1</sub>A Small Break Test No. 2", February 15, 1980.
3. W.J. Letzring et. al, "BWR BD/ECC Program Preliminary Facility Description Report", GEAP 23592, December 1977.
4. "BWR BD/ECC Program, Contract No. NRC-04-76-215, Informal Monthly Progress Report for June 1979", Transmittal, G.W. Burnette (GE) to E.L. Halman (NRC) and C.W. Sullivan (NRC), July 1979.

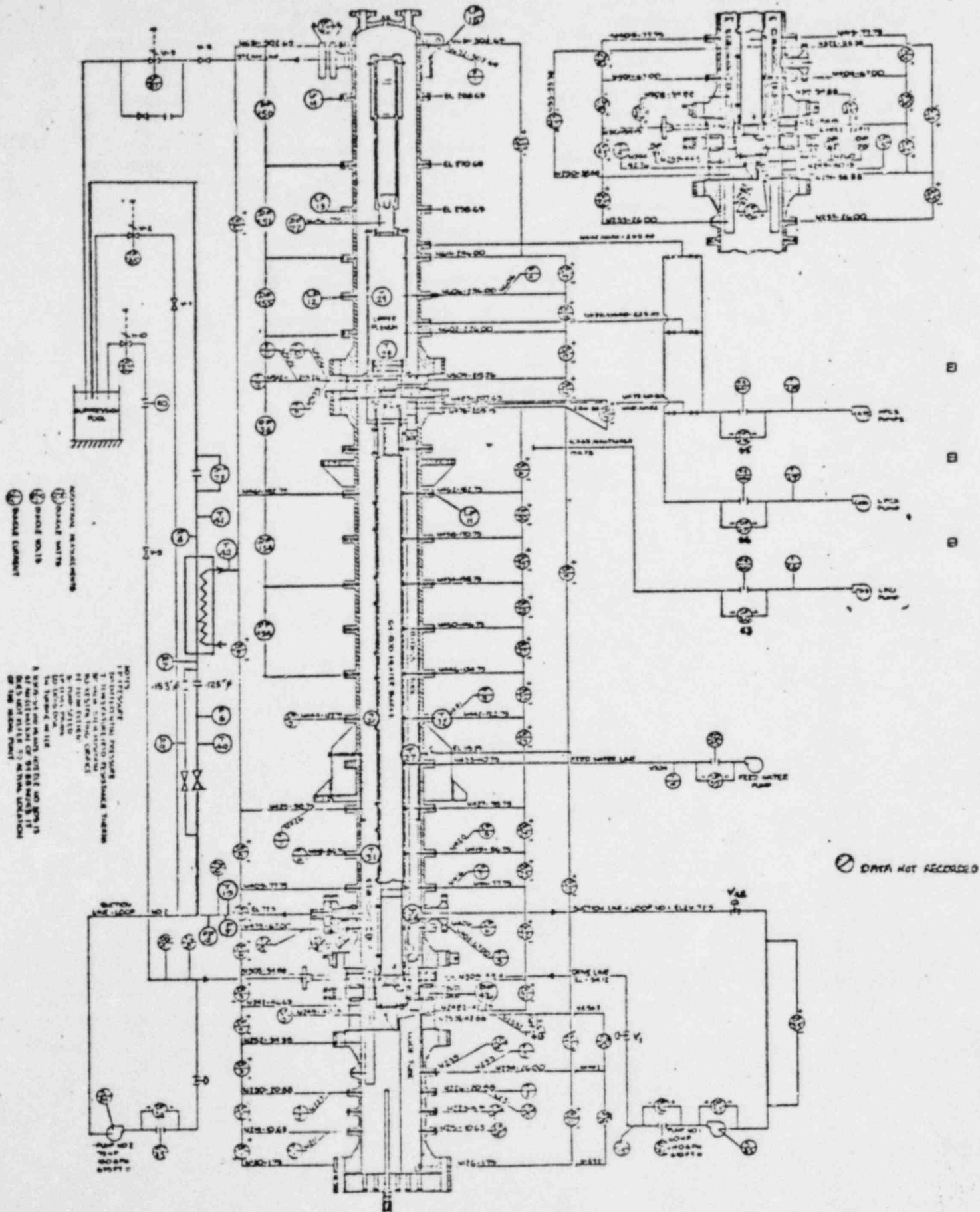


Figure 1 Primary Measurements — Measurement Nodes for TLTA 5C

Table 1 COMPARISON OF TEST CONDITIONS

(TLTA SMALL BREAK TEST #II)

	Specified	Measured
Break Size		
Line #1	0.125 $\pm$ 0.001" diameter	0.125 $\pm$ 0.001" dia.
Line #2	0.153 $\pm$ 0.001" diameter	0.153 $\pm$ 0.001" dia.
ADS Orifice Size	0.677 $\pm$ 0.001" diameter	
ECCS		
Inlet Fluid Temperature	80 $\pm$ 15°F	90°F
HPCS	HPCS deactivated	deactivated
LPCS	activated	activated
LPCI	activated	activated
Initial Condition		
Steam Dome Pressure	1050 $\pm$ 20 psia	1048 psia
Water Level (Outside Shroud)	283 $\pm$ 6" EL	283" EL
Bundle Flow (Core Flow)	34 $\pm$ 5 lbm/sec	34 lbm/sec
Bypass Flow, Total	1.5 $\pm$ 0.5 lbm/sec	2.1 lbm/sec
Steam Flow	1.4 $\pm$ 0.5 lbm/sec	1.6 lbm/sec
Bundle Inlet Subcooling	23 $\pm$ 5°F	21°F
Downcomer Temperature		
Above F.W. Sparger	T sat	553°F
Below F.W. Sparger	(T sat - 23°F) $\pm$ 5°F	532°F
Timings		
Pump #1 Trip	0.0 $\pm$ 0.2 sec	0.0 sec
Pump #2 Trip	4.0 $\pm$ 1.0 sec	4.0 sec
Feed Water Trip	0.0 $\pm$ 0.5 sec	0.1 sec
Break Open Line #1	t $\geq$ 140 sec $\pm$ 1 sec	t $\geq$ 138 sec
Break Open Line #2	140 $\leq$ t $\leq$ 286 sec	138 $\leq$ t $\leq$ 286 sec
ADS Opening	286 $\pm$ 2 sec	286 sec
MSIV (Steam Valve) Closure	166 $\pm$ 2 sec	165 sec
ECCS Activated	37 $\pm$ 1 sec	37 sec
Intact Recirculation Loop	20 $\pm$ 1 sec	20 sec
(#1) Isolated		



Figure 2 SYSTEM PRESSURE

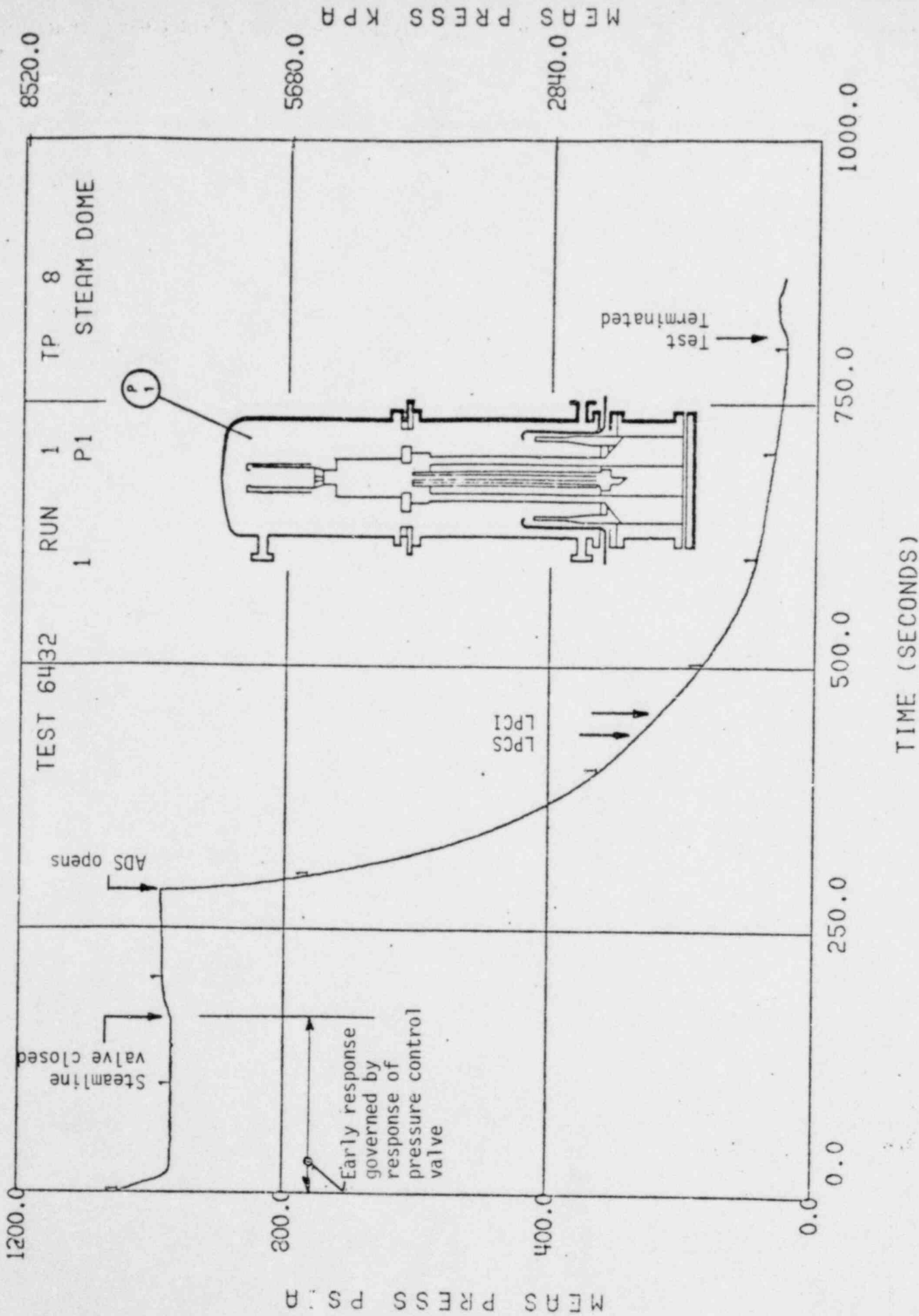


Figure 3 STEAM LINE FLOW

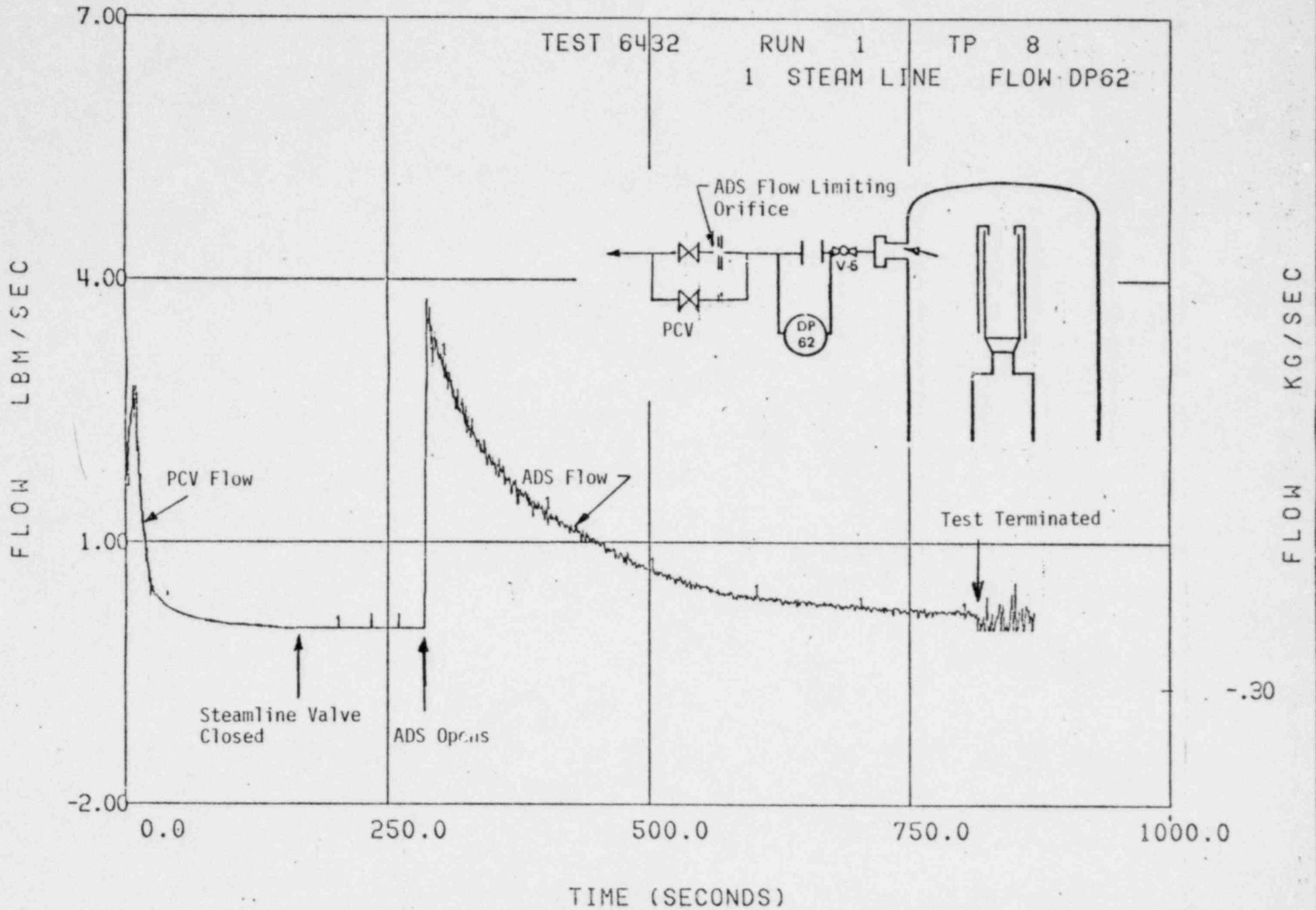


Figure 4 LPCS FLOW

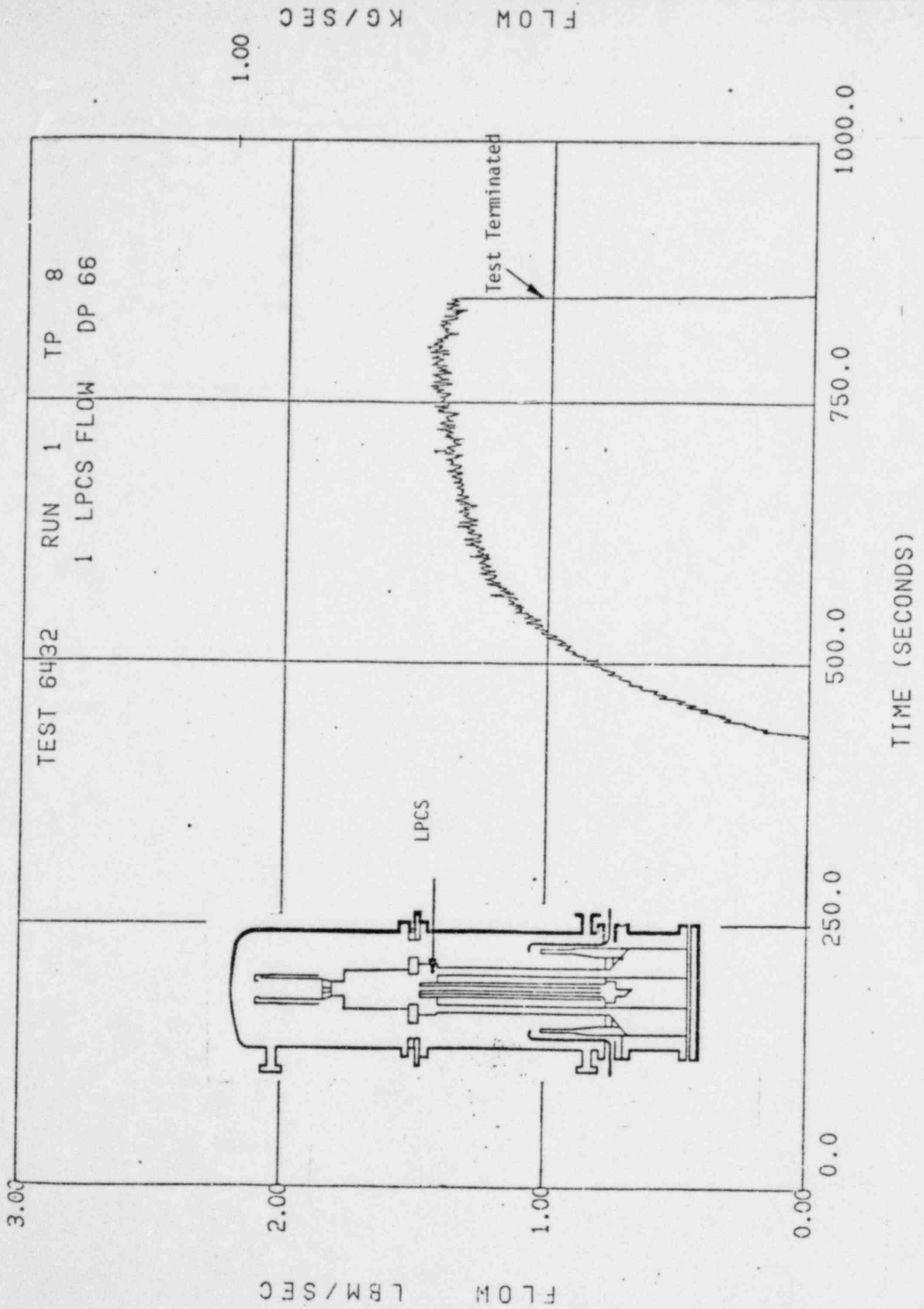


Figure 5 LPCI FLOW

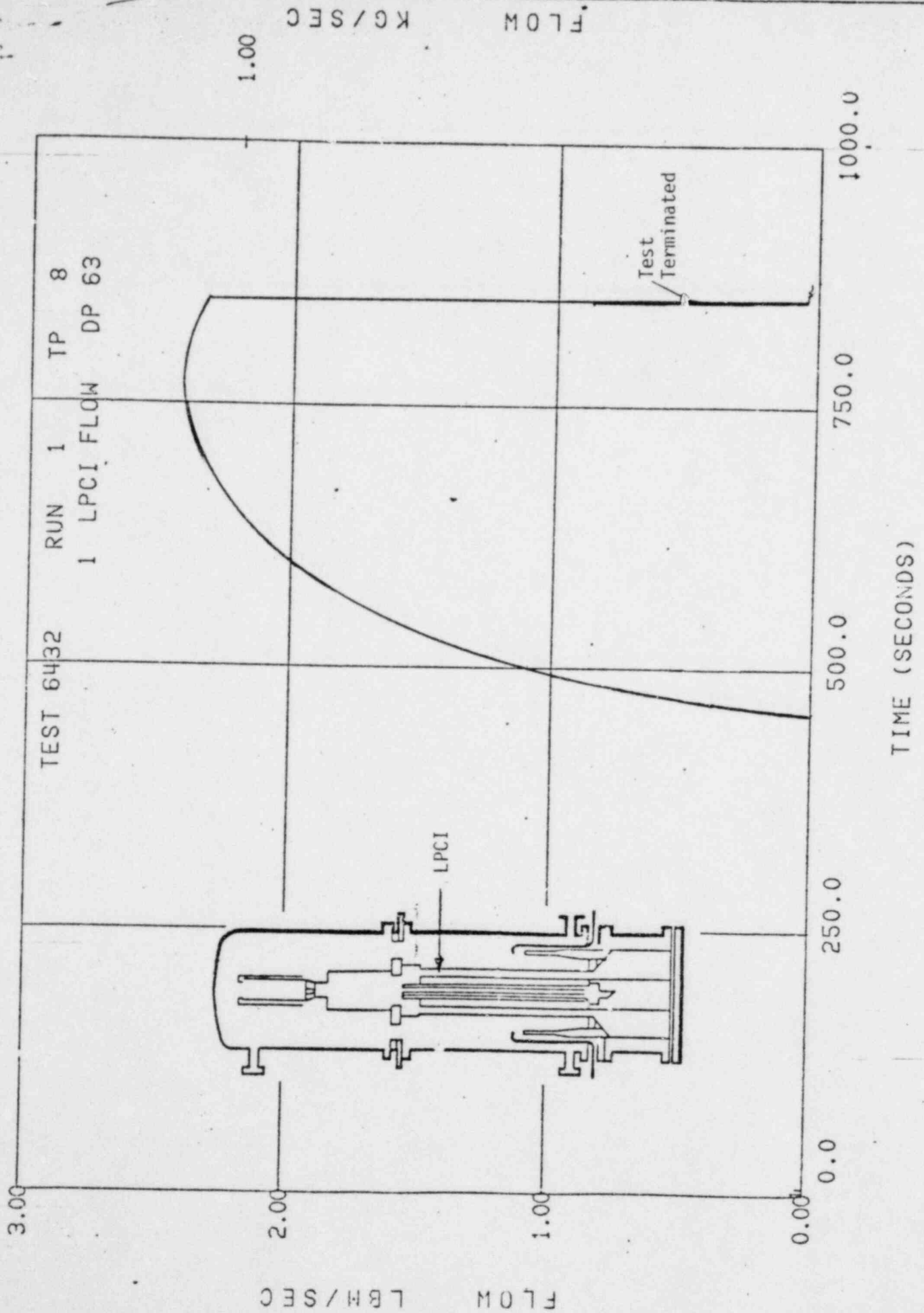


Figure 6 BUNDLE POWER

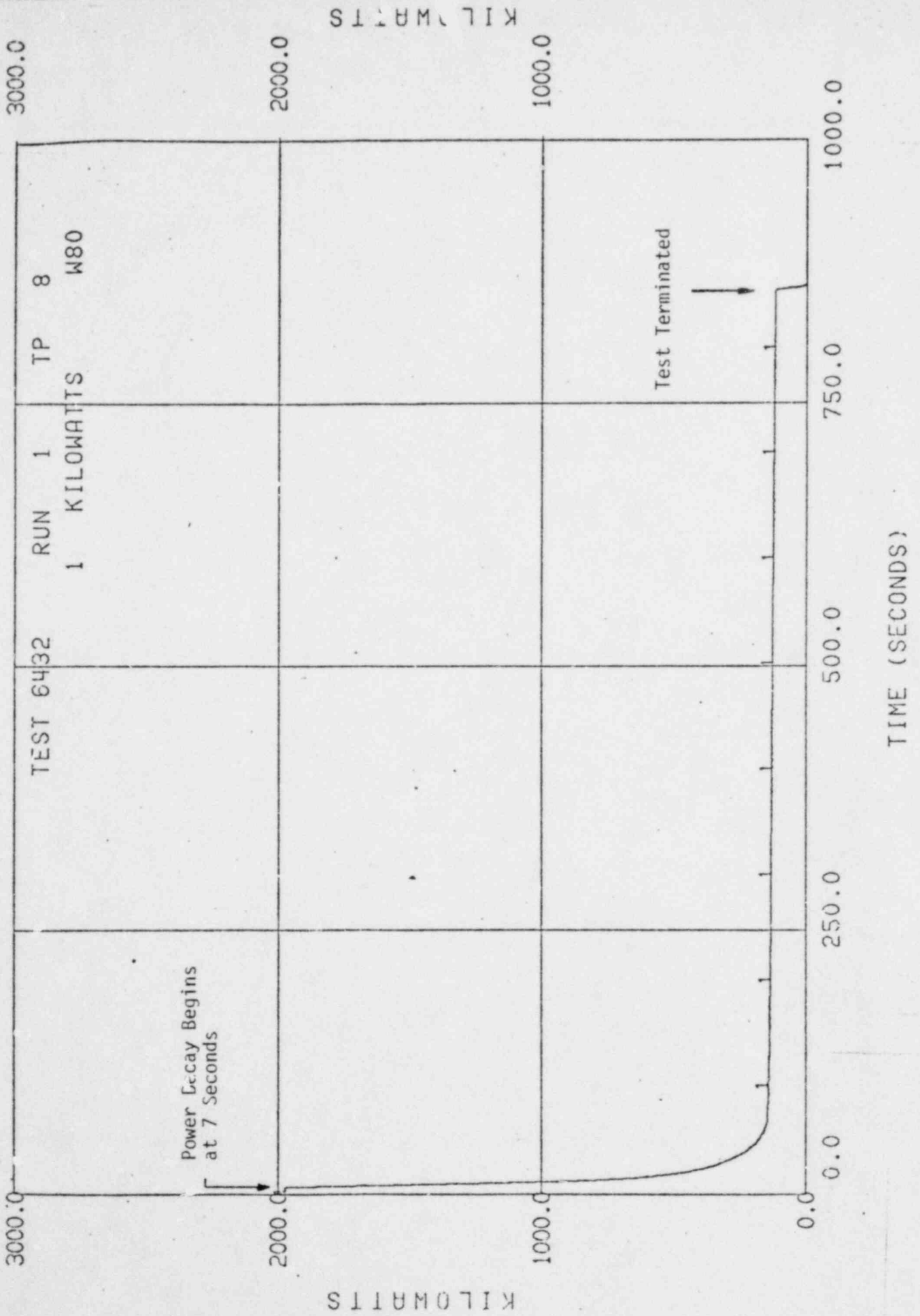


Figure 7 TWO-PHASE MIXTURE LEVEL (INSIDE THE SHROUD)

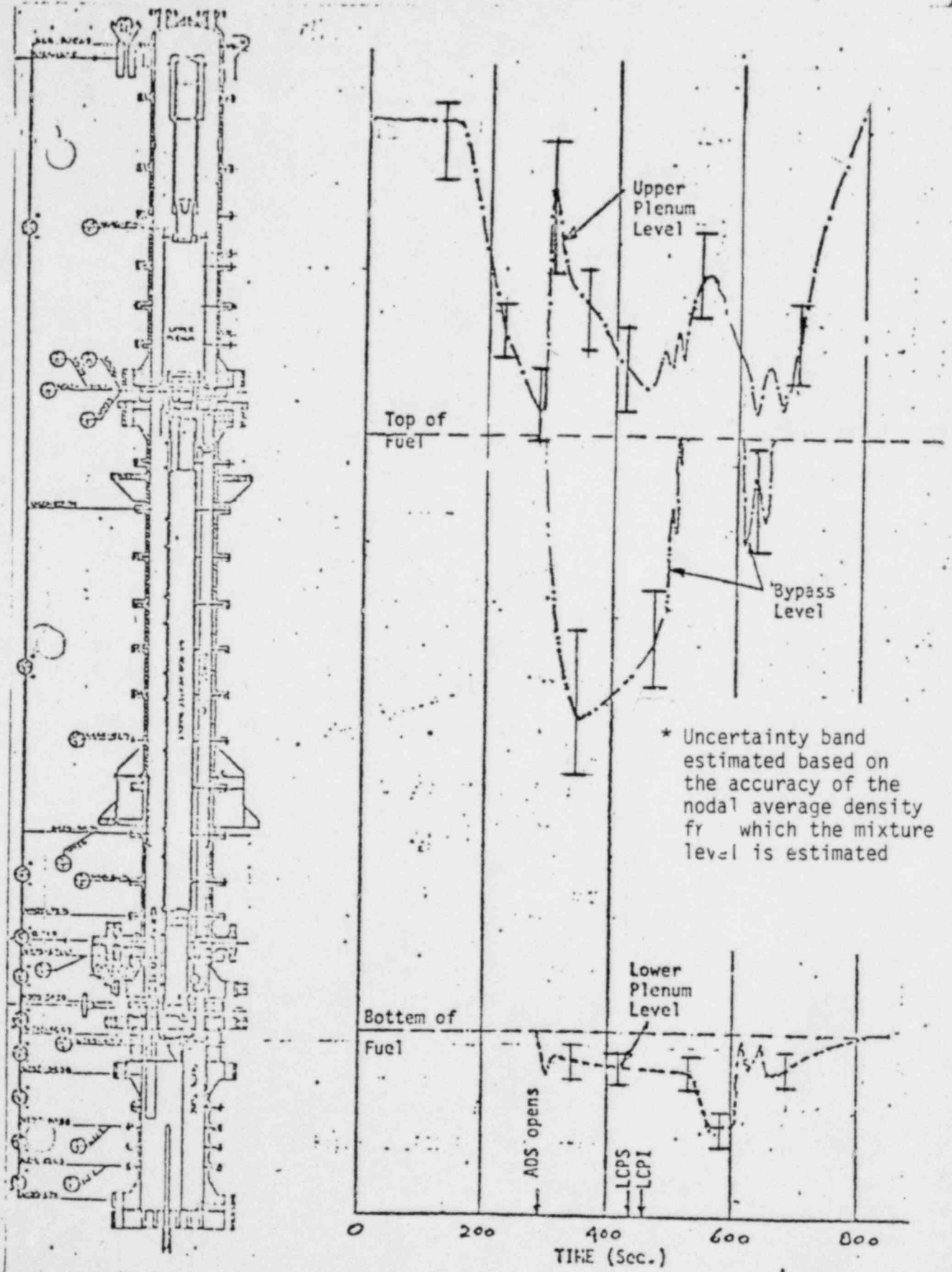
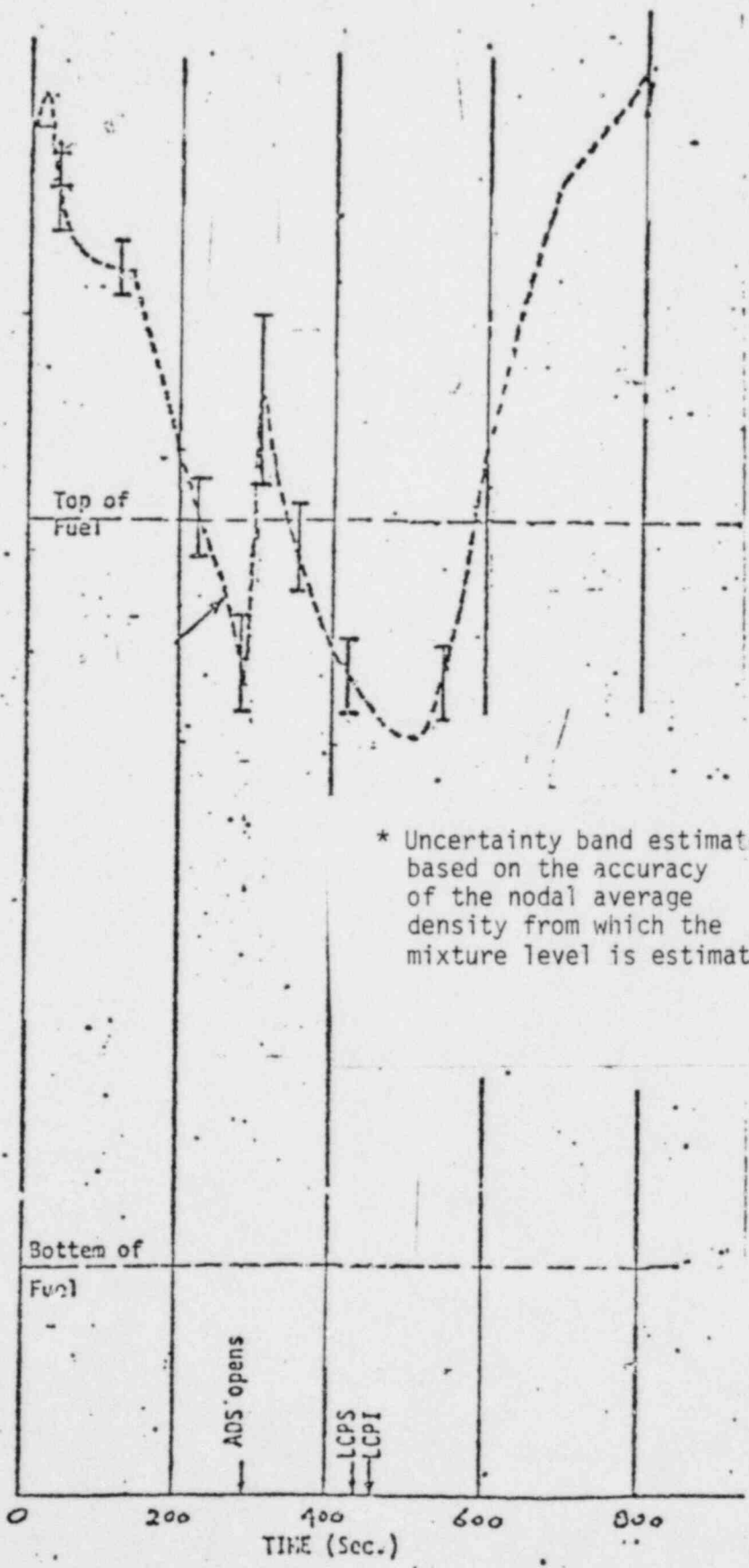
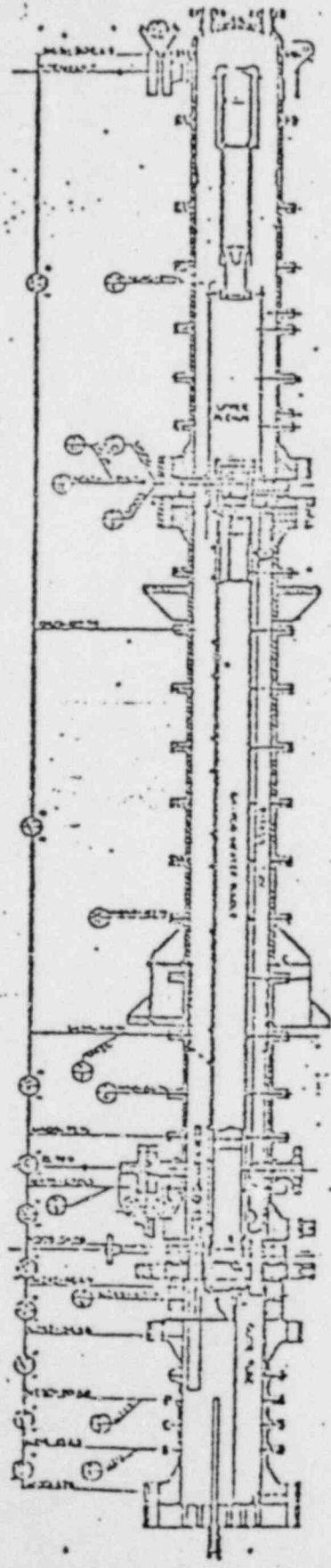


Figure 8 TWO-PHASE MIXTURE LEVEL OUTSIDE THE SHROUD



\* Uncertainty band estimated based on the accuracy of the nodal average density from which the mixture level is estimated

Figure 9 BREAK FLOW

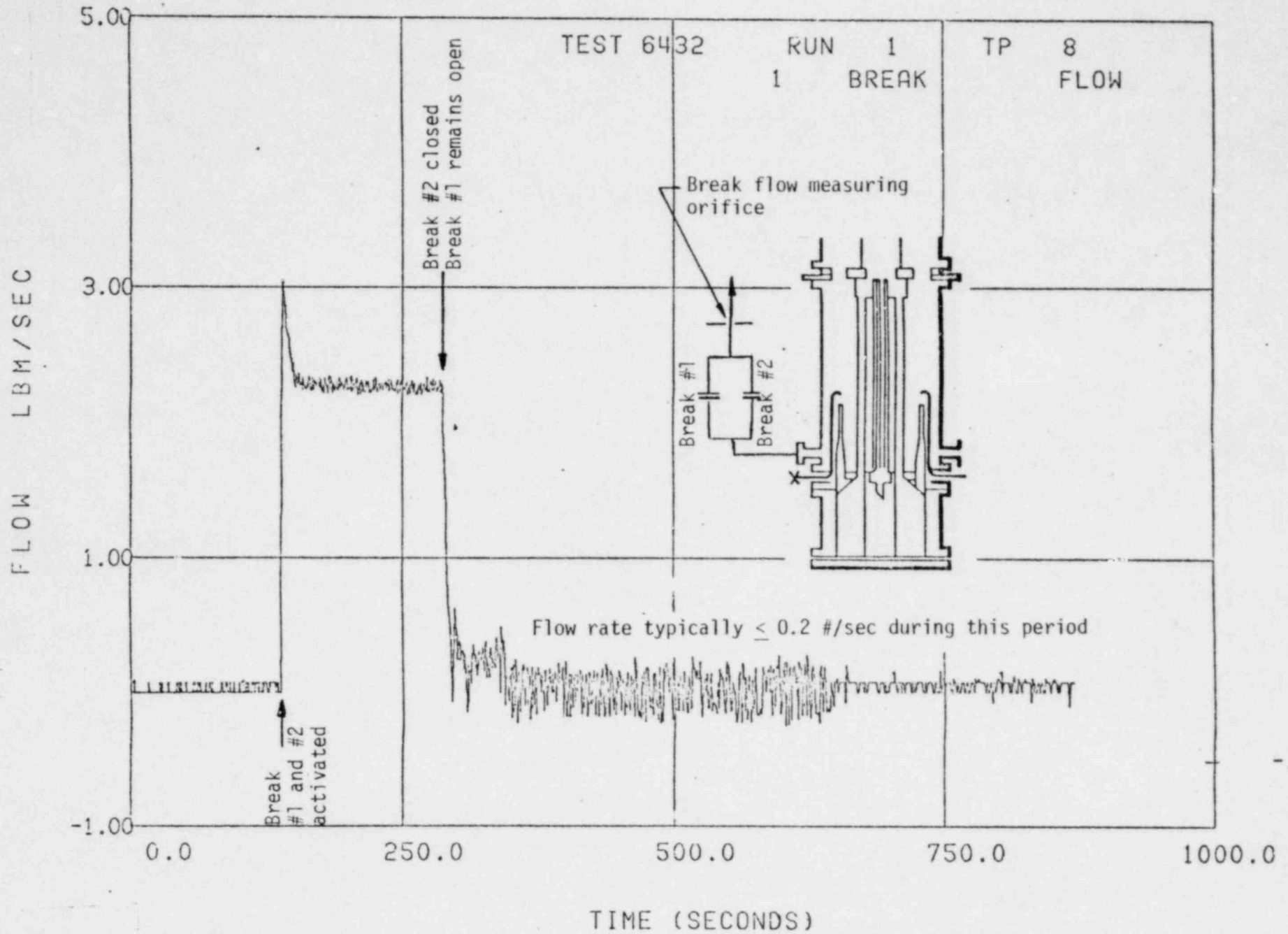




Figure 10 UPPER PLENUM MASS

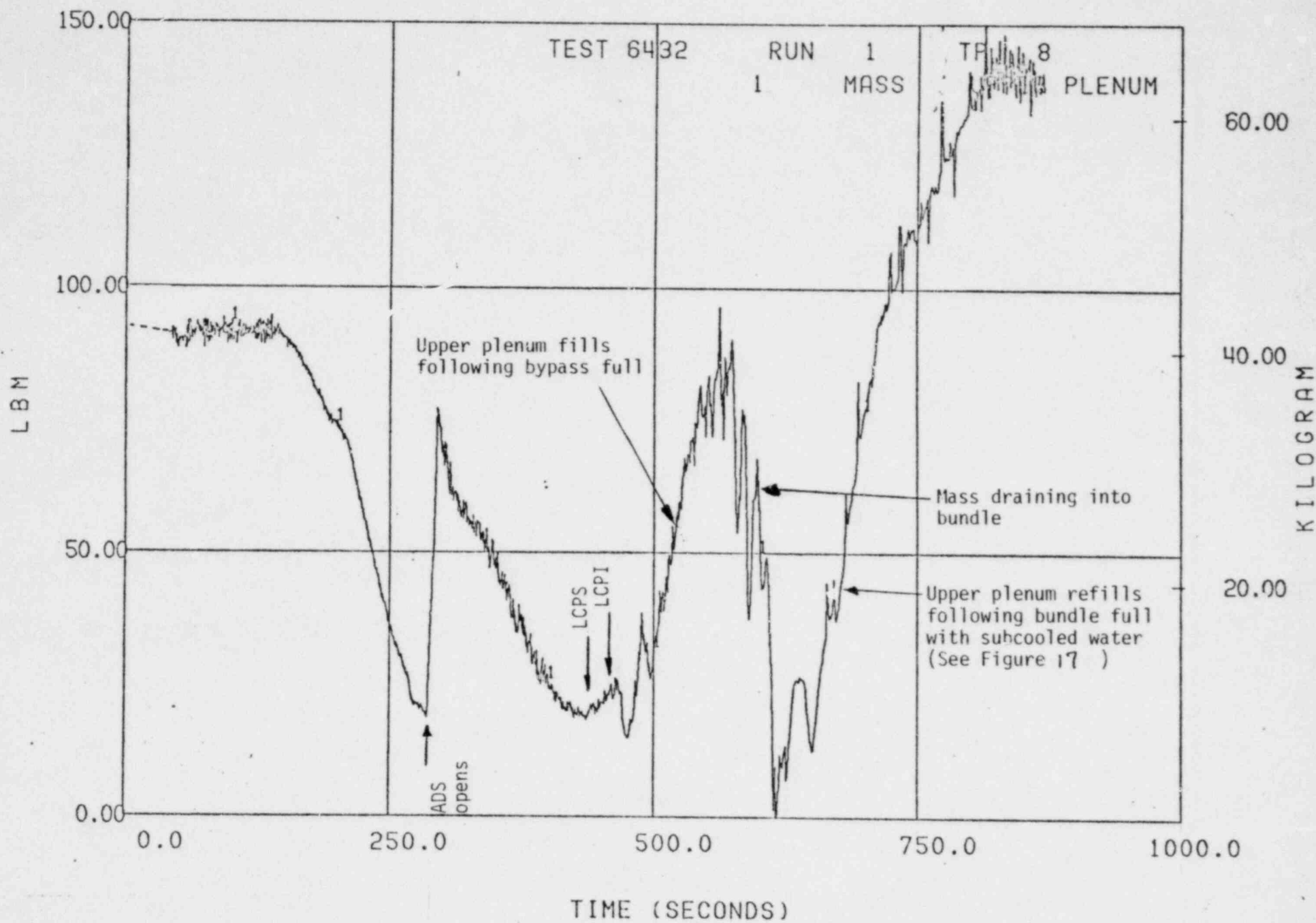


Figure 11 BYPASS MASS

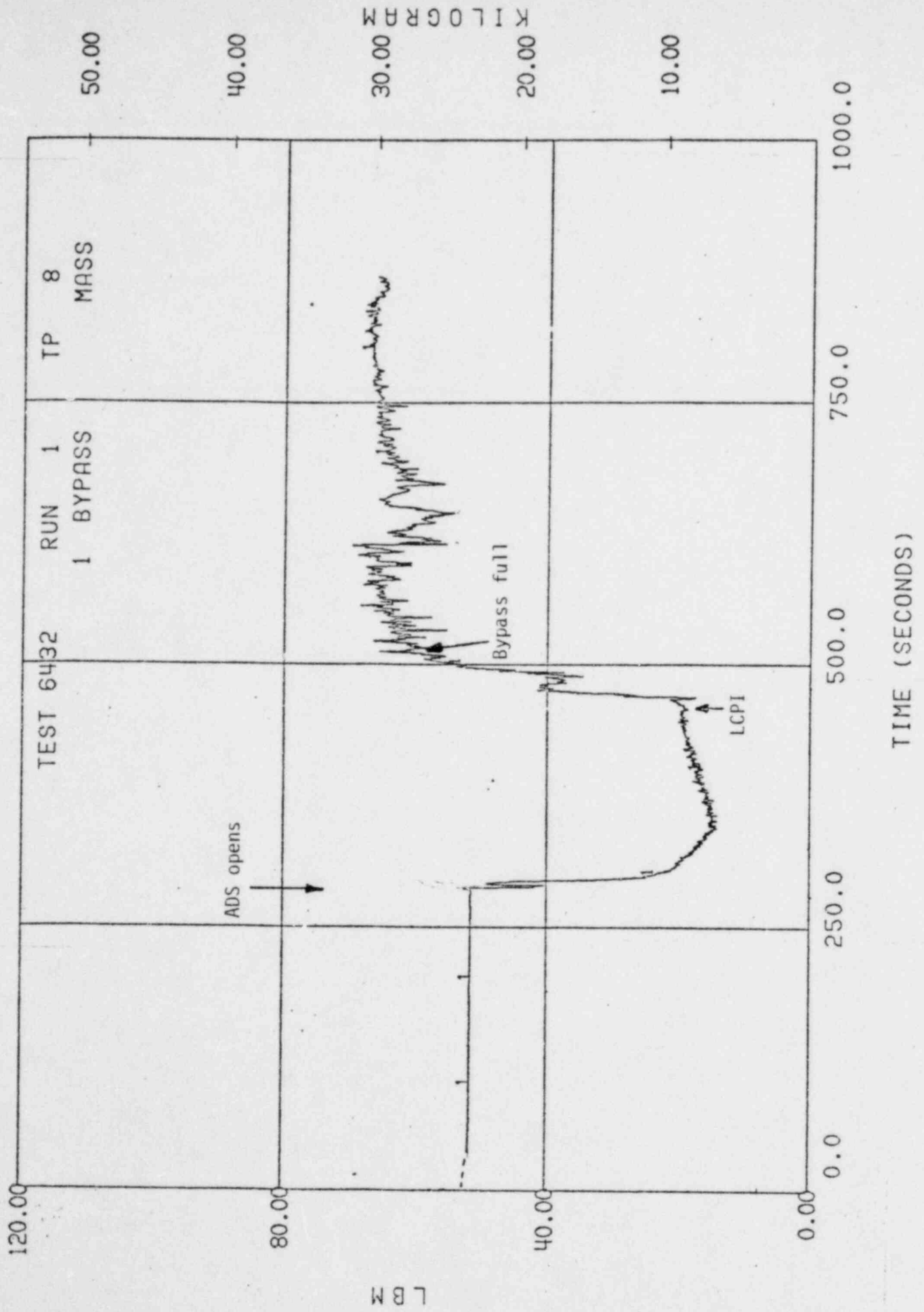


Figure 12 BUNDLE MASS

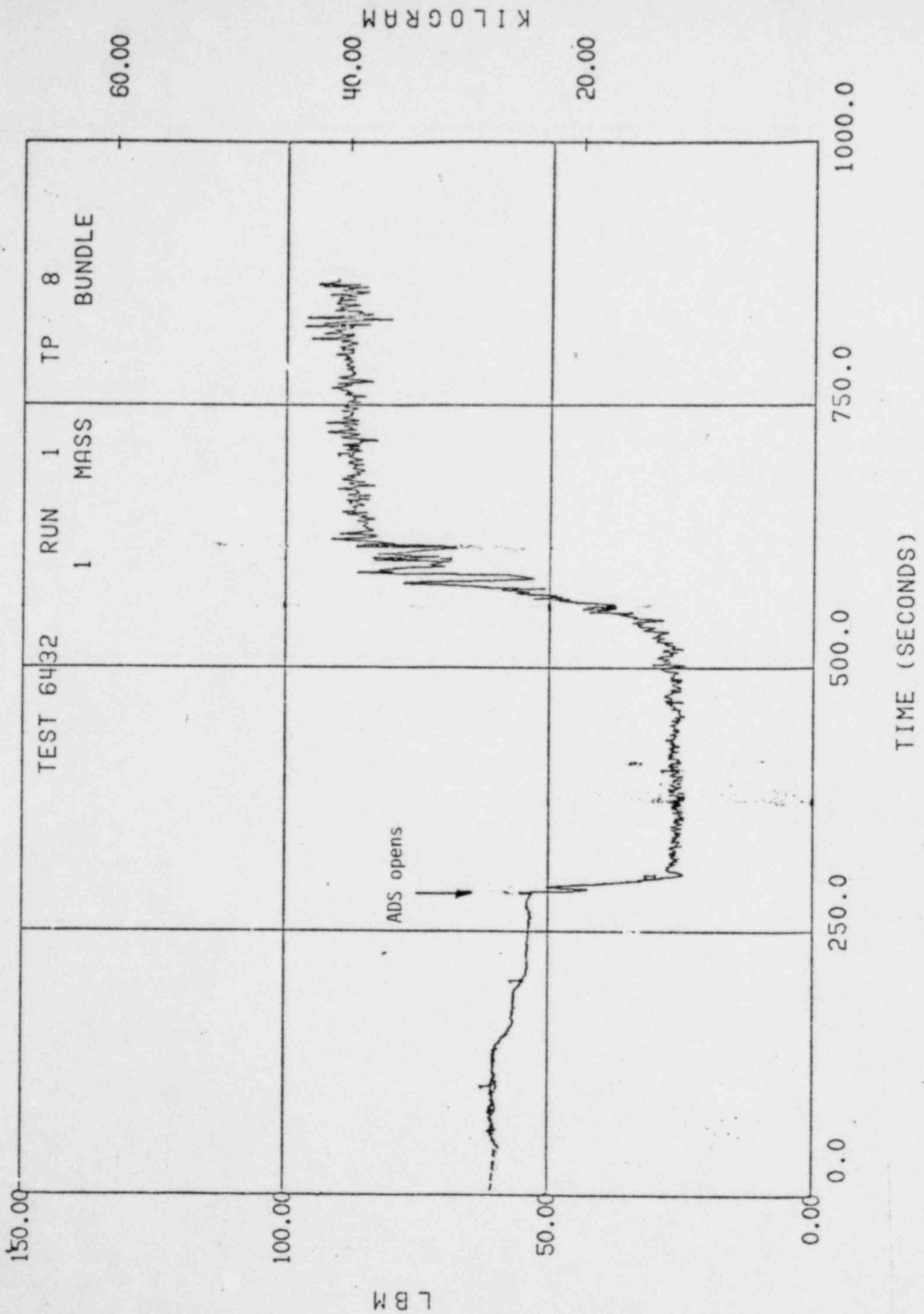


Figure 13 LOWER PLENUM MASS

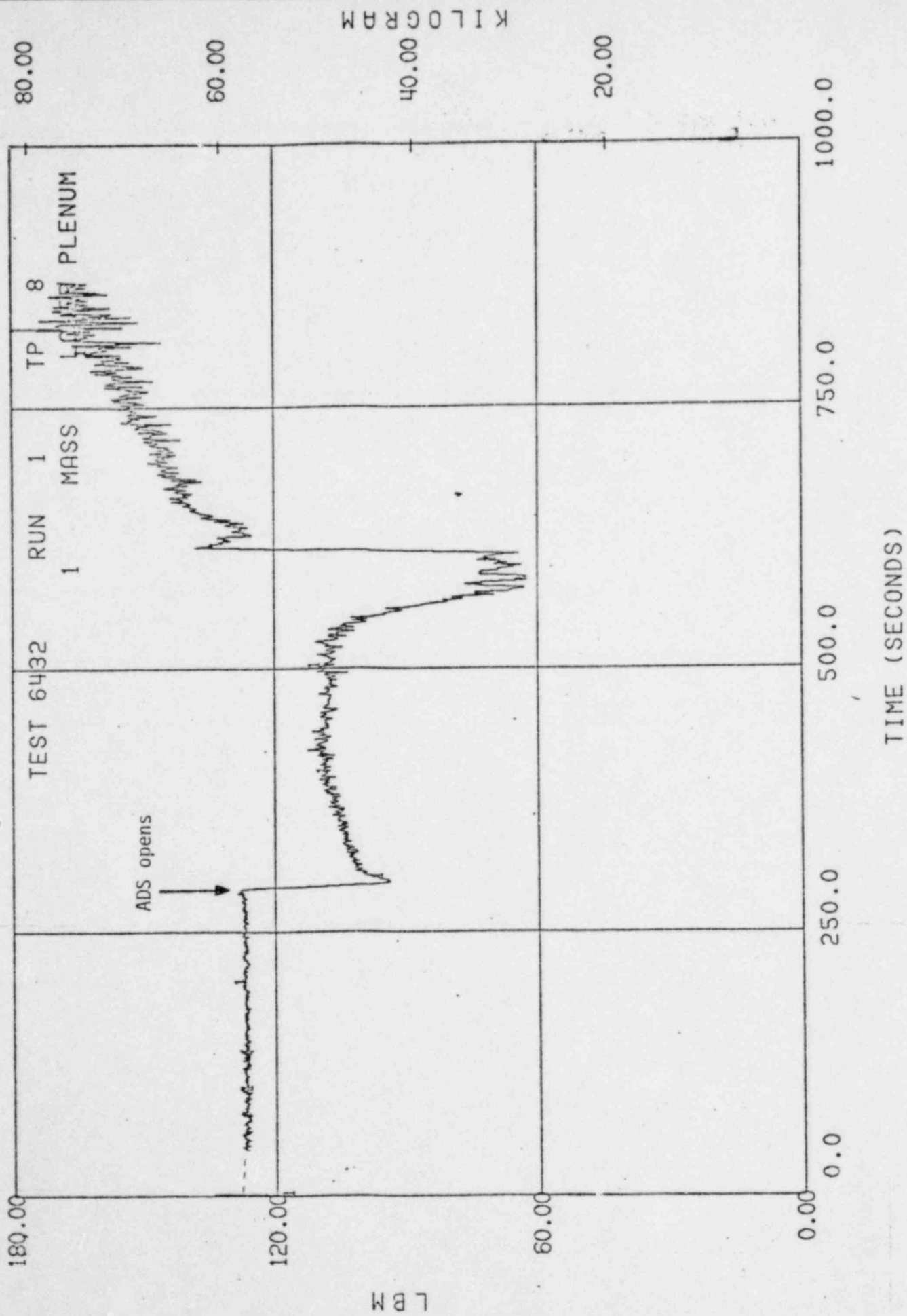


Figure 14 GUIDE TUBE MASS

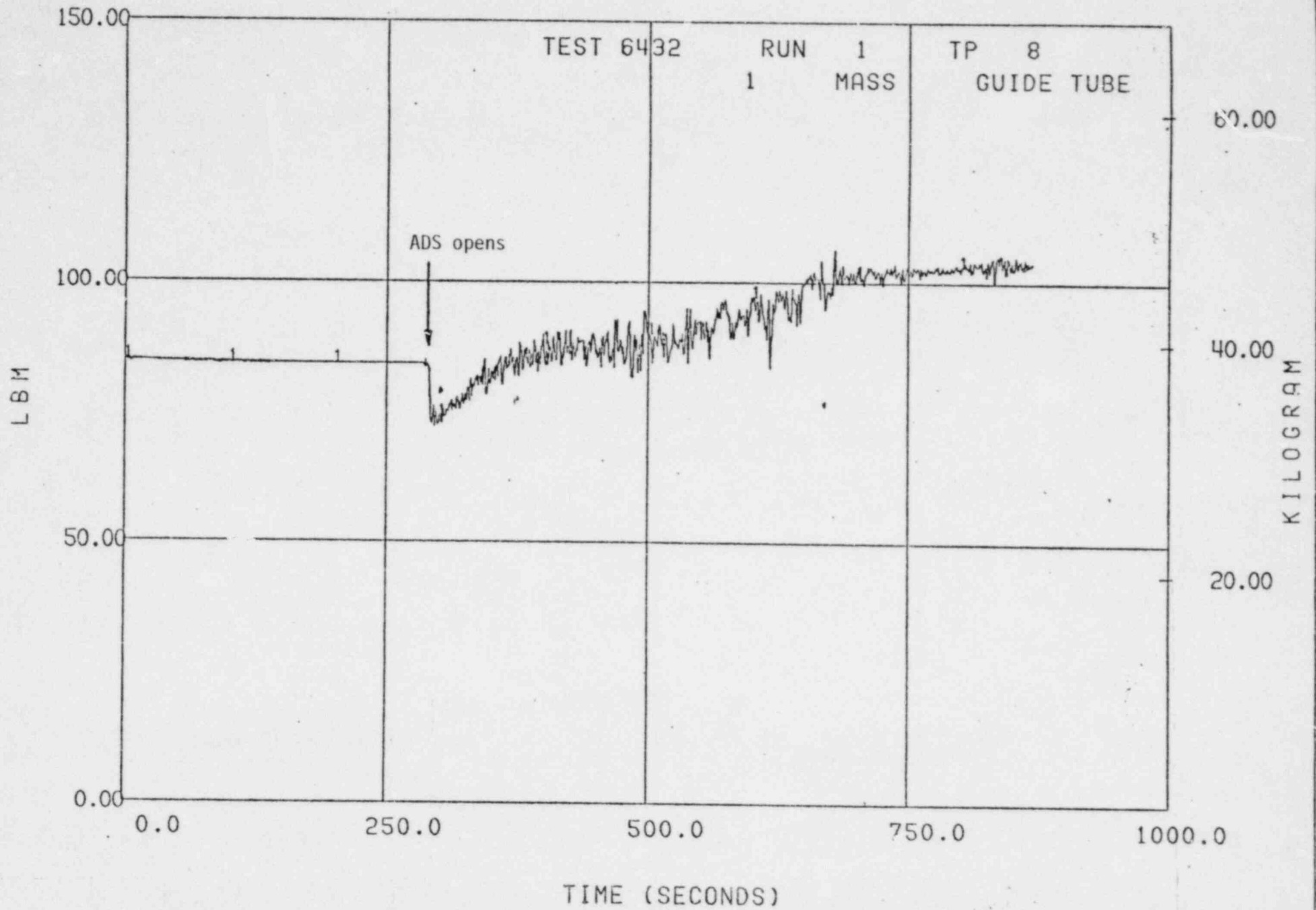


Figure 15 ANNULUS MASS

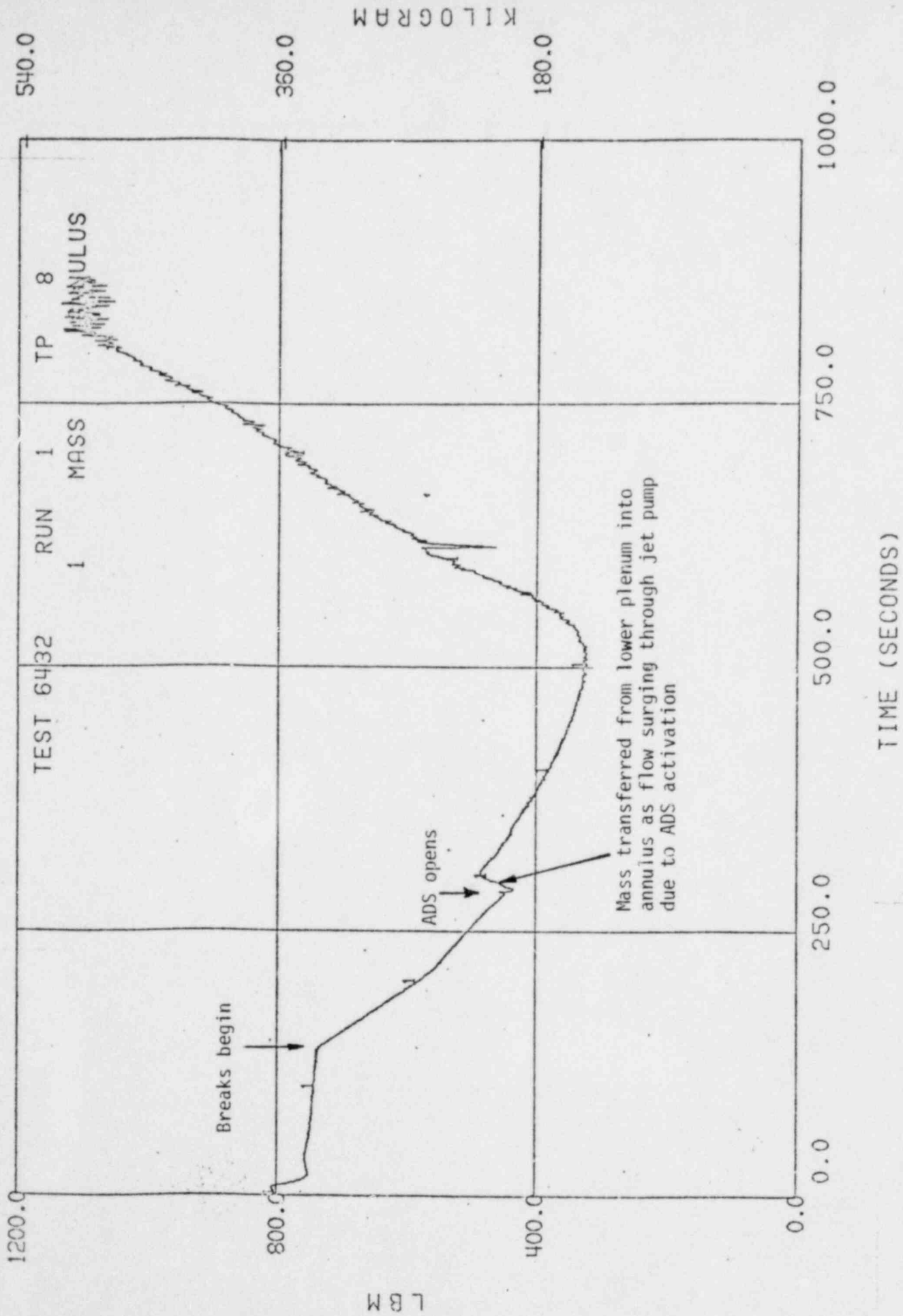


Figure 16 SYSTEM MASS

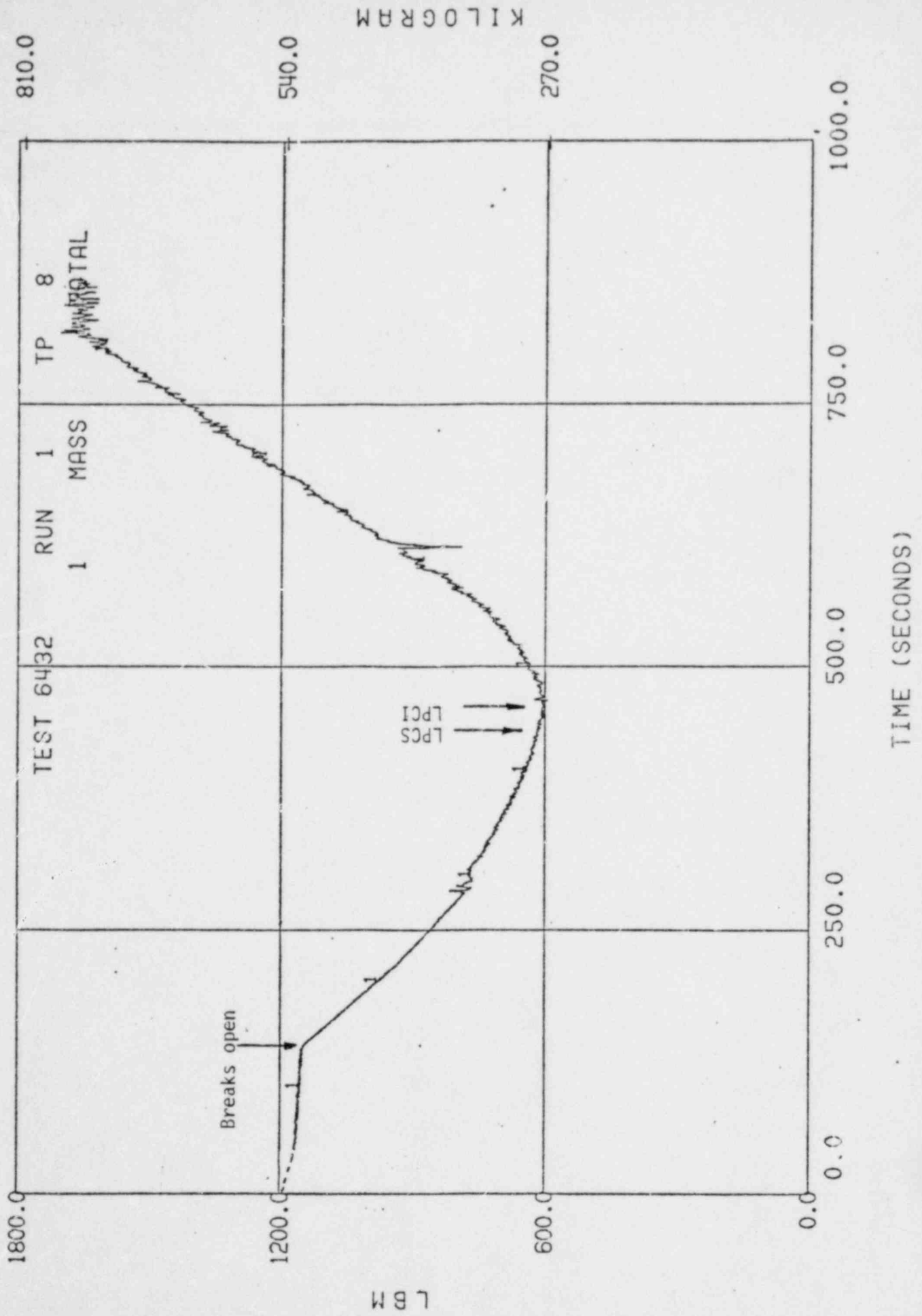
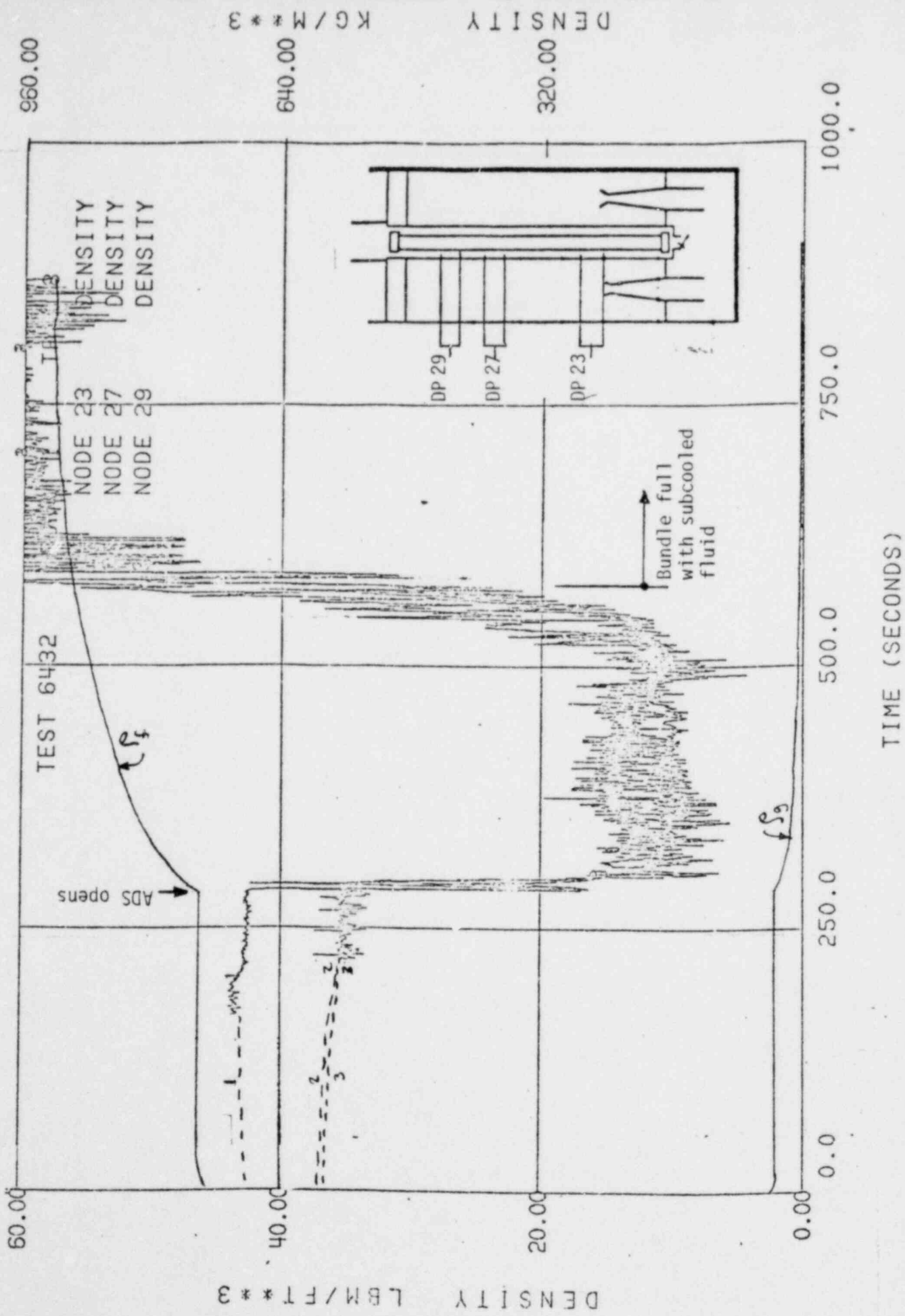
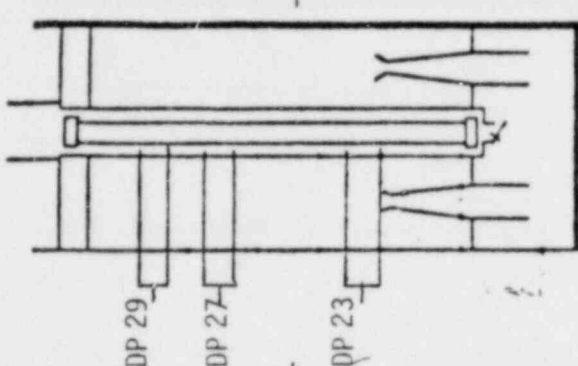


Figure 17 BUNDLE FLUID DENSITY



DENSITY  
 DENSITY  
 DENSITY  
 NODE 23  
 NODE 27  
 NODE 29



Bundle full with subcooled fluid

TEST 6432

ADS opens

DENSITY LBM/FT\*\*3

DENSITY KG/M\*\*3

TIME (SECONDS)



Figure 18 LOWER PLENUM PLENUM DENSITY

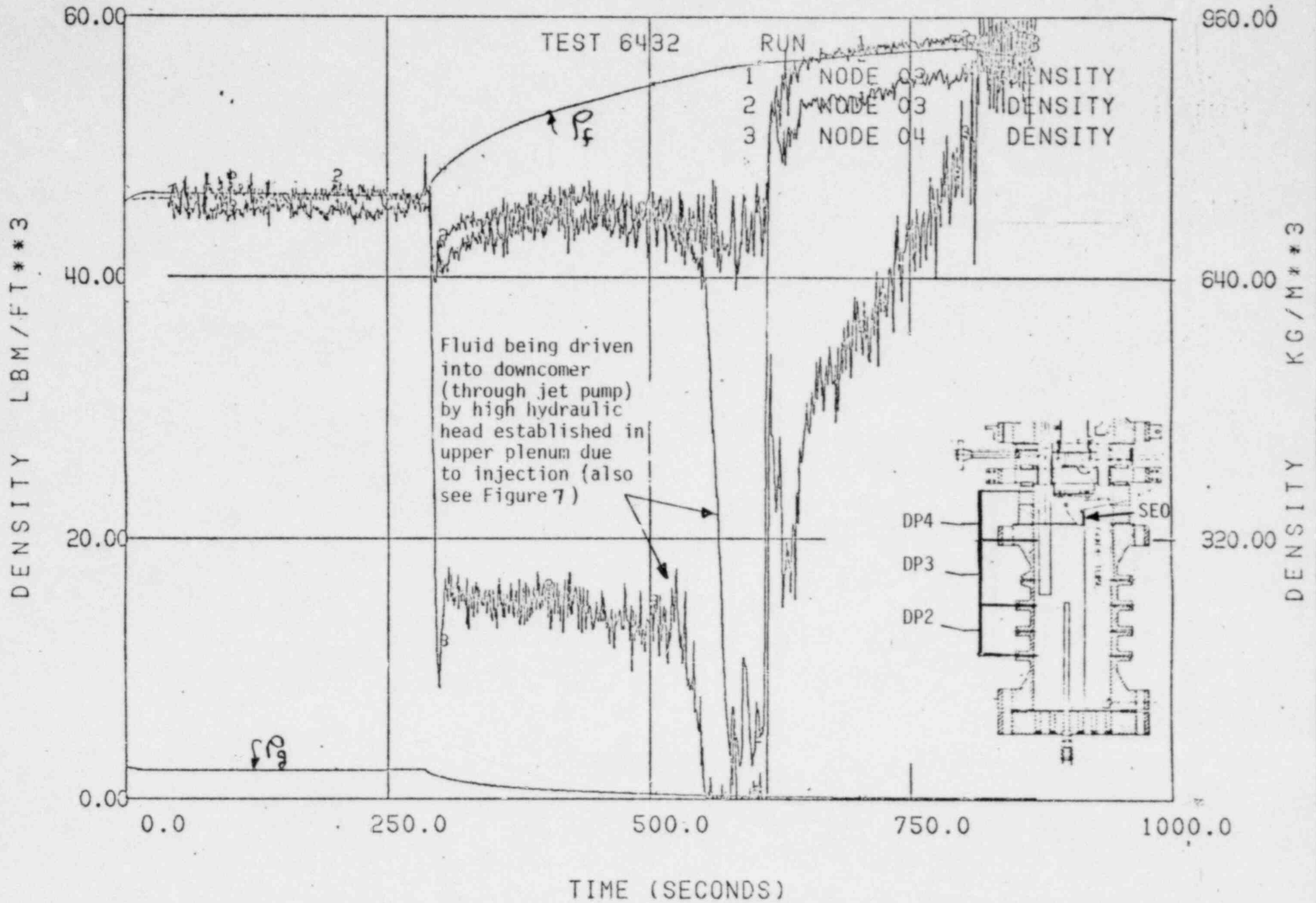


Figure 19 BYPASS DENSITY

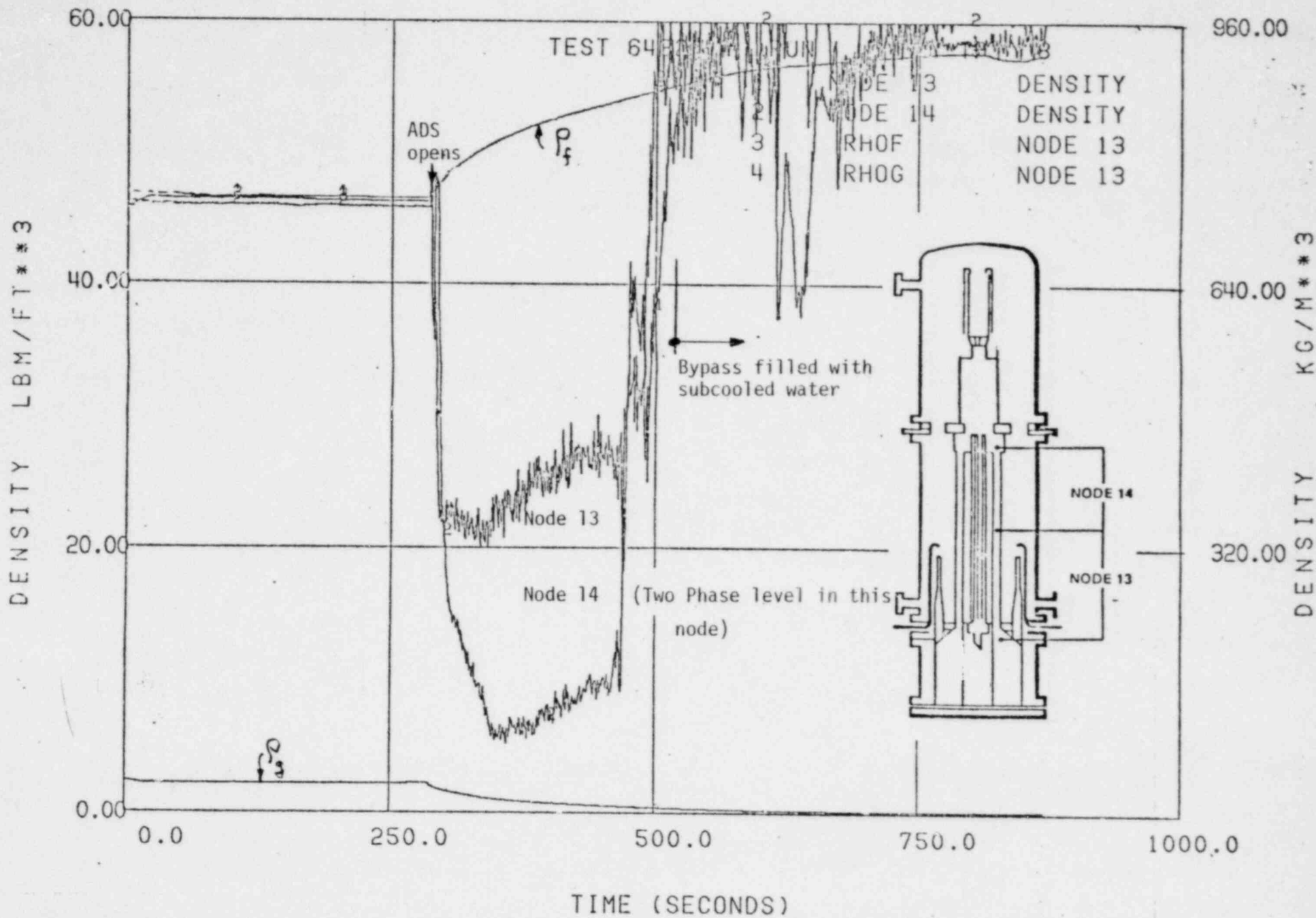


Figure 20

Rod Cladding Temperature (TLTA Small Break Test No. 2)

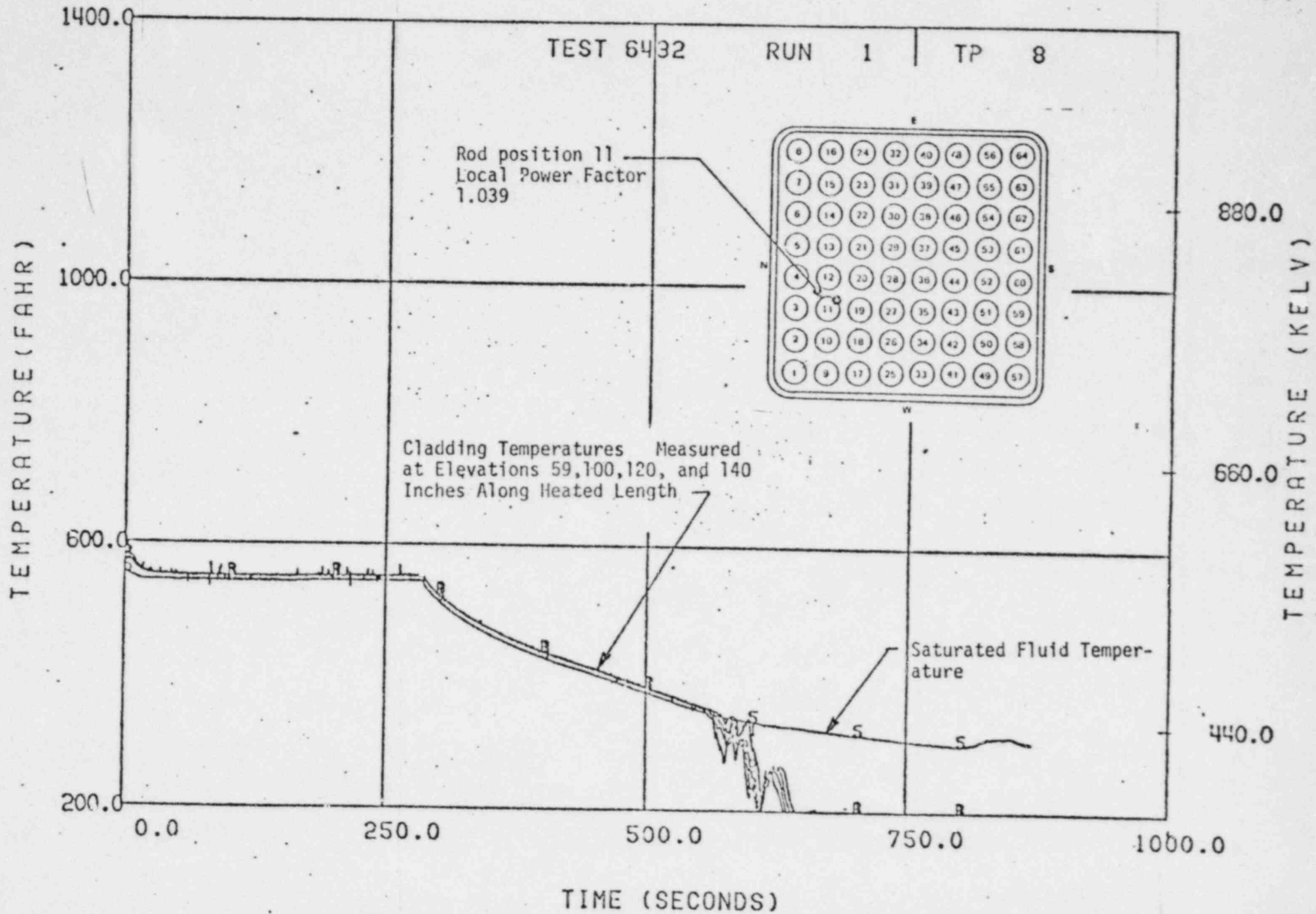


Figure 21

Rod Cladding Temperatures (TLTA Small Break Test No. 2)

